ANNALS OF MICROSCOPY

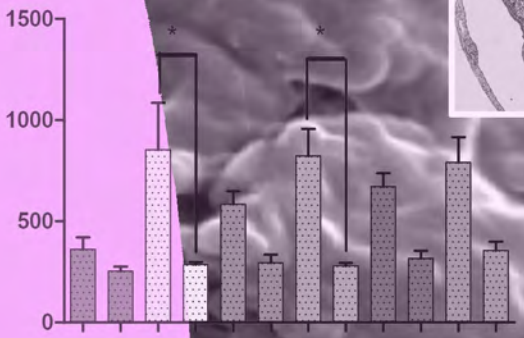

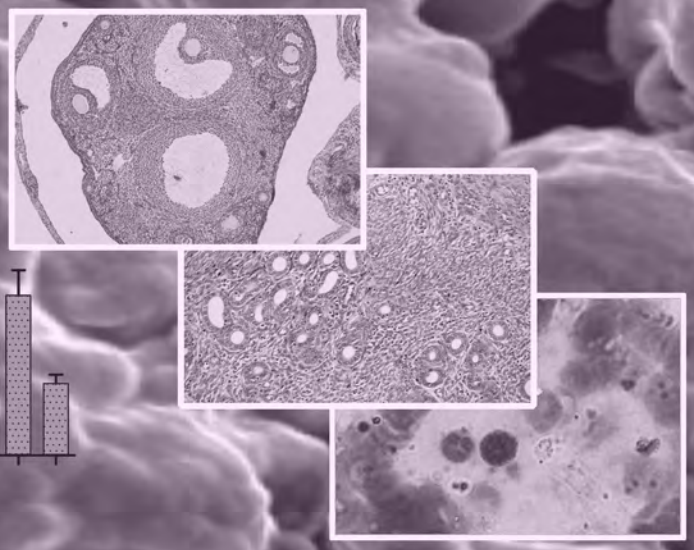

Vol 14, April 2014

Microscopy Society (Singapore)

Published under the auspices of
Microscopy Society (Singapore)

SCOPE OF THE JOURNAL

The "Annals of Microscopy" provides an international forum for researchers in biological, physical and materials sciences to present and discuss new research on microscopy.

Fields of interest include: all forms of microscopy. Image acquisition and improvement techniques, along with computer-aided microscopy and analysis are included.

The journal publishes short communications, technical or scientific articles and reviews. Regular articles feature reports of new instrumentation, new theoretical methods and their applications to microstructural analysis in a broad range of fields in biological, physical and material sciences.

The journal also publishes selected news and commentaries of interest to members of microscopy societies and others working in the field of microscopy and microanalysis.

EDITORIAL BOARD

ISSN: 0219-2209

Contents

A Simple Scanning Electron Microscope Method for the Preparation of Rat Red Blood Cells

Santhana Raj L.[1], Mohd Fuad Rahmat S.[3], Izan Shahrina A.[1], Siti Aminah N. [1] Paramasvaran S[2] and Balkis B[3].

[1] Electron Microscopy Unit, , Institute for Medical Research, Kuala Lumpur, Malaysia.
[2] Medical Research Resource Center, Institute for Medical Research, Kuala Lumpur, Malaysia.
[3] School of Diagnostic & Applied Health Sciences, Faculty of Health Sciences, Universiti Kebangsaan Malaysia, Kuala Lumpur

ABSTRACT

A simple, fast and safe method to prepare a scanning electron (SEM) micrograph of rat red blood cells sample is described. This method allows a good ultrastructure to be maintained and facilitates an even distribution of the rat red blood cells. The preparation method developed provides detailed images for fast investigation.

INTRODUCTION

In electron microscopy, images are really no more than magnified projections of the various densities proportionate to the components of the section. To achieve this, a method must be developed to accommodate the detail of the sample and at the same time it must be simple and fast. In this study, we developed a simple SEM method in preparing the red blood cells. The method requires a shorter fixation process compared to the standard SEM method (Hyatt, 2000)

MATERIALS AND METHODS

Red blood cells sample (with concentration of 10^7) was washed with saline (3X) and then fixed in 1.25 % Gutaraldehyde in Phosphate Buffer Saline (137 mM Sodium Chloride, 2 mM Potassium Chloride and 10 mM Phosphate Buffer) for 5 minutes. The fixed sample was then spread evenly on a poly-L-lysine cover slip and allowed to settle for 5 minutes. A fibreless paper was place on the poly-L-lysine cover slip and dehydrated in 100% ethanol for 10 seconds (X3). The sample is then dried using the critical point dryer and subsequently spurted with 45 nm gold and viewed under SEM.

RESULTS AND DISCUSSION

Observations made mainly focus on the biconcave shape of the rat red blood cells. The electron micrographs show the intact biconcave shape of the rat red blood cells (Fig. 1). No shrinkage or distortion of the specimen was observed.

Preparation of SEM specimen without undergoing the tedious and time-consuming fixation process shortens the time required for specimen investigation. The method developed eliminates the use of osmium tetroxide, and therefore reduces the health risks to researchers due to exposure to the toxic chemical (McLaughlin *et al*. 1946).

CONCLUSION

This study describes a method which retains the ultrastructure of the specimen for scanning electron microscope examination. This fast and simple method offers a safe alternative method of preparing rat red blood cells for electron microscopy analysis.

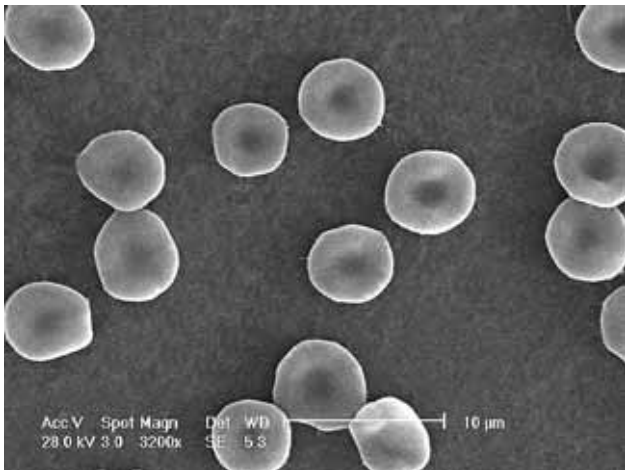

Fig. 1. Shows biconcave shape of the rat red blood cells.

ACKNOWLEDGEMENTS

We would like to express our gratitude to the Director General of Health Malaysia for the permission to publish this paper. We extend our sincere appreciation to the Director of Institute for Medical Research, Malaysia for the support in this project.

REFERENCES

Hayat M.A., editor. (2000). Principles and techniques of electron microscopy: Biological applications. 4th ed. Cambridge: Cambridge University Press, pp 24-96.

McLaughlin, A.I.G., Milton, R., & Perry, K.M.A. (1946) Toxic manifestations of Osmium Tetroxide. *British Journal of Industrial Medicine*. 182-186.

Morphological Characterizations of Selected Brown Rice Commercially Available in East Coast of Peninsular Malaysia

W.I. Wan Rosli* and I. Nurul Ain
School of Health Sciences, Health Campus, Universiti Sains Malaysia, 16150 Kubang Kerian, Kelantan, Malaysia.

ABSTRACT

Presently, the intake of brown rice has becomes more popular for people who are very conscious about their health. The present study was conducted to examine the morphological characteristics of different sources of brown rice commercially available in Kelantan state of Peninsular Malaysia. Macroscopic observation was done on fresh brown rice samples and white rice sample. Longitudinal and horizontal section shows the present of both aleuron and bran layers obviously for all brown rice samples. Long grain and wholegrain mix brown rice had the longest and the thickest values compared to control (white rice). The brown rice samples consist of the pericarp, aleuron layer, endosperm, starch, parenchyma cells and parenchyma cells wall. All brown rice samples also had different thickness of aleuron layer. The cross sectional diameters of the brown rice samples were in the range from 847.2 to 1000 μm. These observations are vital in selecting the best cooking techniques for brown rice so that it is most palatable for human consumption.

Keywords : Brown rice, Scanning Electron Microscope (SEM), morphological characterization

INTRODUCTION

Rice is among the most important staple food for half of world's population (Heinemann *et al.* 2005) including Malaysia. Approximately 97% of the Malaysian population consumed rice twice a day and on average, 2½ plates of rice per day (Norimah *et al*., 2008). Rice can be consumed either as milled or non-milled. The former is commonly known as white rice while the latter known as brown rice. There are thousands of rice varities available around the world. Today, brown rice is suggested as whole grain rice to provide more nutrients and health benefits than the more common white rice. Brown rice is the unmilled rice containing the pericarp, the seed coat and nucellus, the germ or embryo and the endosperm (Deepa *et al.* 2008). The difference between the brown rice and white rice is not only the color but also its bran layer, whereas white rice has had its bran layer removed by a polishing process.

Before white rice has been milled, brown rice is produced as the milling process only removes the outermost layer, the hull, of the rice kernel and is the least damaging to its nutritional value. The outer layer of rice grains are covered with an oily layer of the brown rice or also known as rice bran which is composed of some botanical entities, including sub layers within the pericarp and aleuron layer.

Brown rice is considered healthier than white rice as many nutrients are contained in the bran layer, however brown rice has a different taste and texture, takes longer time to cook, and does not store as well as white rice. Abas *et al.* (2011) stated that, rice bran has 20–30% total dietary fibre which most of it are insoluble fibre. The endosperm cells are thin-walled and packed with amyloplasts containing compound starch granules.

MATERIALS AND METHODS

Sample preparation

The brown rice samples were purchased from a local hypermarket in Kota Bahru District, Kelantan state of Malaysia. There were three different commercially available brands of brown rice for experimentation and one brand of white rice was purchased for control purpose. Three

brown rice sample from each variety were selected, cleaned and one of them was cut into half for cross sectional view. The samples were subjected to morphological characterization.

Scanning Electron Microscopy

Scanning electron micrographs of the native brown rice samples were obtained by viewing with a scanning electron microscope (Quanta FEG 450, FEI Electron Microscopy). The brown rice samples was mounted on round aluminum stubs with the aid of double-sided adhesive tape. The samples were coated with gold (~22.7 μm) by means of a SCD 005 high vacuum evaporator and scanned. Cross-sections and longitudinal sections of brown rice samples were made and characteristics were studied using a Scanning Electron Microscope (SEM). The selected regions were then captured for futher characterization of the morphological properties.

RESULTS AND DISCUSSION

The physical characteristics like grain length, width and thickness of grain varied significantly among the different commercially available brown rice varieties used in this study. Table 1.1 shows physical characteristics of some selected brown rice commercially available in Kelantan state of Malaysia.

Generally, when brown rice is observed under SEM, it shows similar morphological characteristics to white rice with husk colour varying from golden yellow to brownish black. Each of the brown rice samples have different length, width and thickness which are attributed to the biological origin of the rice (Babu *et al.* 2009). Long grain rice (S1) had the longest grain length and significantly longer than other unpolished rice samples. In other characteristic, S3 (wholegrain rice mix) had the widest and thickest values. The thickness of this brown rice could be due to the thicker pericarp and aleuron layer surrounding the endosperm of brown rice. The outer coating bran layer of brown rice accounted for the reason why it needs a longer time to cook compared to white rice.

Table 1.1: Tabulation of the physical characteristics of some selected brown rice commercially available in Kelantan state of Malaysia

Sample	Characteristics/ features			
	Rice length (mm)	Rice width (mm)	Rice thickness (mm)	Length to width ratio
S1	7.406 ± 0.081	2.069 ± 0.011	1.769 ± 0.032	3.570
S2	7.412 ± 0.085	2.076 ± 0.037	1.688 ± 0.053	3.570
S3	7.034 ± 0.199	2.245 ± 0.124	1.771 ± 0.021	3.130
S4	6.728 ± 0.184	2.156 ± 0.035	1.748 ± 0.028	3.070

Data are tabulated based on means of 10 grains rice ± standard error of brown rice from each sample. S1 = long grain rice; S2 = Unpolished Thai fragrant rice, S3 = Wholegrain rice mixture, S4 = White rice (control)

Fig. 1.1a shows the rough external surface of long grain rice (S1) under 100x magnification. The photomicrographs show some facture of layer present signify the long grain rice (S1), it have two distinct layer which the outermost layer known as pericarp (p) and aleuron layer. For determination of shape, length-width ratio for long grain rice (S1) is 3.57 which have same slender shape like Thai fragrant brown (S2). Close view photomicrographs (to the uncovered layer under 1000x magnification in Fig. 1.1b) show the presence of aleuron grains (ag).

At higher magnification (5000x), the parenchyma cells (pc), aleuron grains (ag) and parenchyma cell wall were clearly shown in Fig. 1.1c. The clear globular shape of aleuron grains can be observed which is slightly larger than Thai fragrant brown (S2) and the arrangement of aleuron grains (ag) is closely packed together with parenchyma cells (pc). The broad surface which

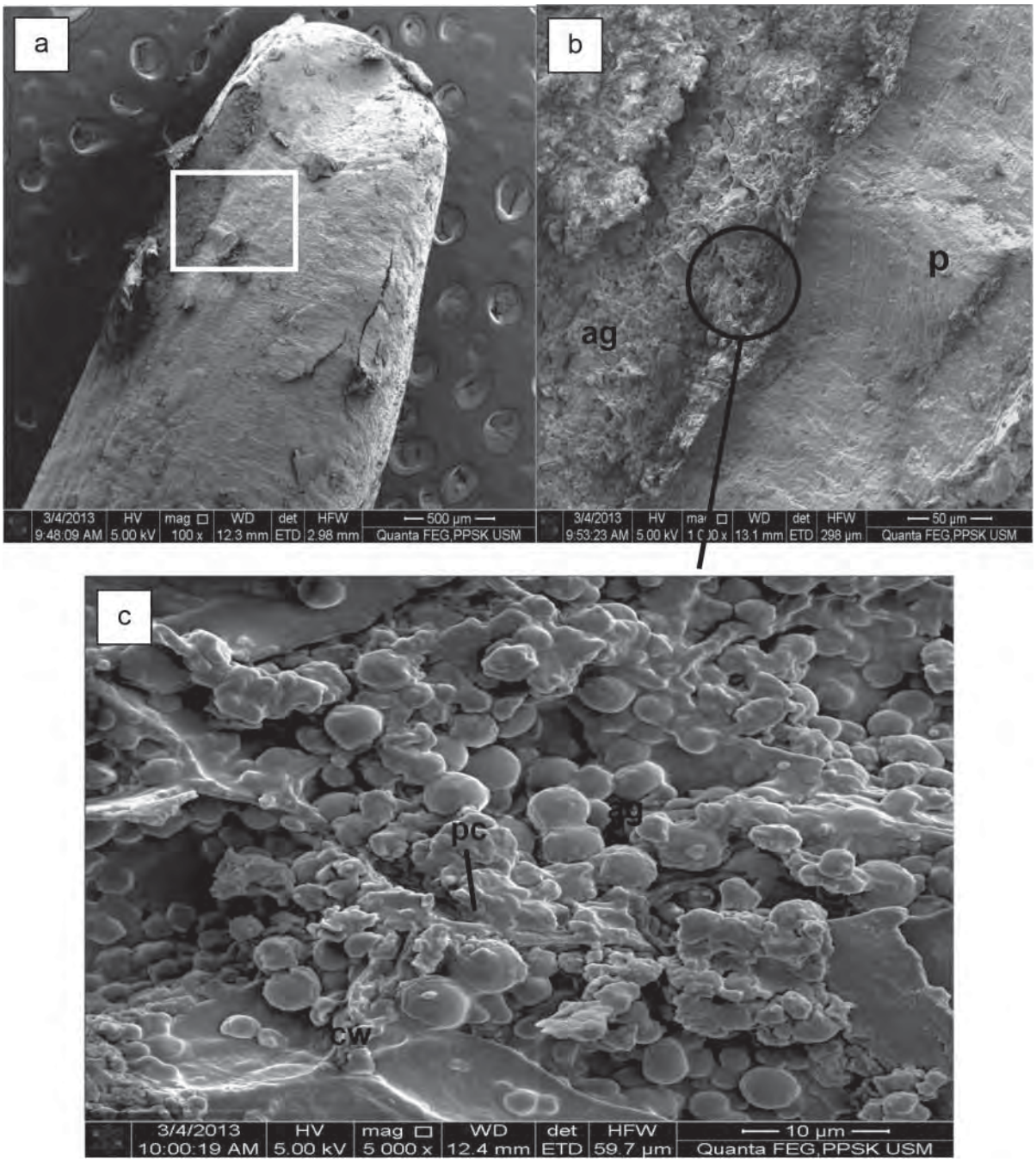

Fig. 1.1 (a, b, c) show scanning electron photomicrographs (100x-5000x magnification) of the long grain rice (S1). Photomicrograph 1.1a is the overall view structure of long grain rice (S1). Photomicrograph 1.1b shows the fissure between the two distinct layers of long grain rice (S1) which consist of pericarp (p) as outer layer. Photograph 1.1c shows the presence of aleuron grains (ag), parenchyma cells (pc) and parenchyma cells wall under 5000x magnification.

covers aleuron grains is the parenchyma cells wall (wc).

Fig. 1.1d shows scanning electron photomicrographs of representative transverse cross section (under 100x magnification) of sample 1 (long grain rice). From the photomicrographs, two distinct layers were observed where these slightly contact with each other connecting between the pericarp (p) and endosperm (en). The diameter of the cross section is approximately 862.7 µm and

endosperm (en) is located centrally right after the pericarp (p) layer which cover outermost layer of brown rice.

The spatial distance was observed in Fig. 1.1e between aleuron layer and endosperm (en) was lesser compared to Thai fragrant brown rice (S2). The thickness of aleuron layer of rice grains where aleuron grains (ag) and parenchyma cells (pc) present is approximately 20.2 μm. Compound of starch (c) was present on the endosperm (en) area in polygonal like-shape. Fig. 1.1f show the aleuron grains (ag) and parenchyma cells wall (cw) under 5000x magnification with average diameter around 0.5 to 3.6 μm.

Fig. 1.2a show the whole external structure of the Thai fragrant brown rice (S2). It shows rough surface and some fissure which reveal two distinct layers on the surface. According to Rice Knowledge Bank, the shape of brown rice (BrS) depends on the length-width ratio which the ratio

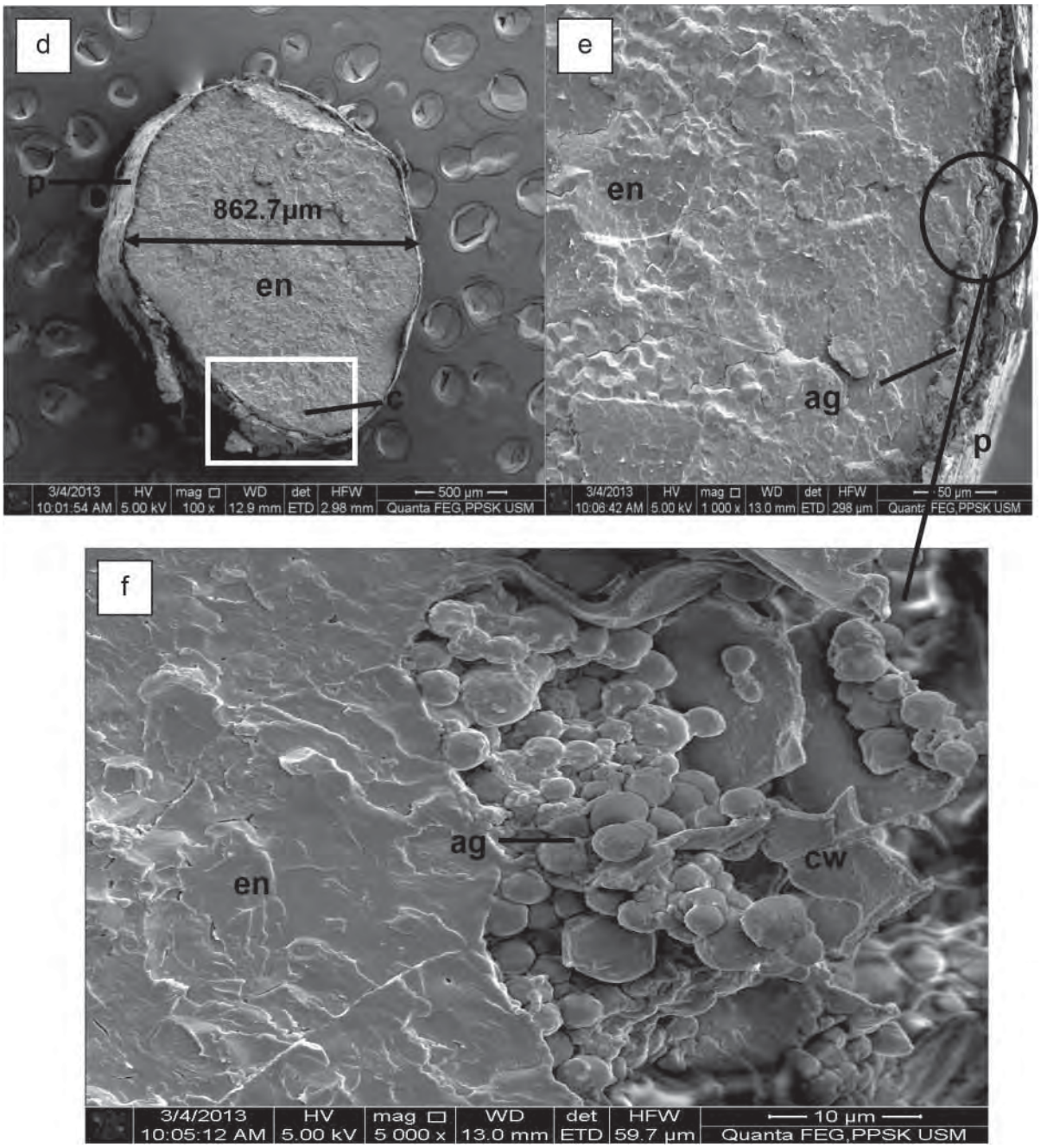

Fig. 1.1 (d, e, f) are scanning electron photomicrographs (100x-5000x magnification) of transverse cross section of long grain rice (S1). Photomicrograph 1.1d is representative rice grain which has been cut to view the cross section. Close view of the space between the pericarp (p) and aleuron layer with endosperm (en) in Fig. 1.1e under 1000x magnification. Scanning electron photomicrograph 1.1f shows the parenchyma cells (pc) which surrounded by aleuron grains (ag) under 5000x magnification.

for Thai fragrant brown (S2) grains rice is 3.57, over 3.0 have a slender shape. The outer layer of brown rice is covered by pericarp layer (p) as shown in Fig. 1.2b and the presence of aleuron grains (ag) as well as parenchyma cell (pc) underneath the pericarp layer.

The shape of aleuron grains (ag) under 5000 magnification (Fig. 1.2c) showns the small globular like shape and the arrangement is slightly in contact with each other. Juliana (1972) stated that the aleuron grains (ag) in parenchyma cells (pc) contain protein richly surrounded by fat- staining substances.

Fig. 1.2 (d, e, f) show scanning electron photomicrographs of representative transverse cross section from the Thai fragrant brown rice (S2) which consists of two loosely distinct layers. The diameter of the cross section is approximately 847.2 μm and endosperm (en) is located centrally right after the pericarp (p) layer which covers outermost layer of brown rice.

In addition, Fig. 1.2e shows the presence of space between aleuron layer and endosperm, which in endosperm consists of a compound of starch (c) in polygonal like-shape. The thickness of aleuron layer of rice grains depend on the number of parenchyma cells present. The diameters of aleuron grains were estimated (0.25 - 3.5μm) under high magnification 5000x as shown in Fig. 1.2f.

Fig. 1.3a shows the end part of brown rice to view the external morphology structure of wholegrain rice mix (S3) which have slightly smooth surface compared to the Thai fragrant brown rice (S2). The actual colour of this type of sample is dark brown compared to the other sample. The difference in colour intensity may due to the degree of milling process of each sample. The presence of fracture or fissure as indicator of two distinct layer is lesser. Watson and Dikeman (1977) stated that there are several polyhedral starch granules in a single amyloplast of rice sample.

Fig. 1.3b shows that compound starch granule (c) have a polygonal shape similar to the shape of other cereals as reported by Parengam *et al*. (2010). The shape of polyhedral compound starch granule (c) might be due to the compression of starch granule during development (Juliana 1972). The shape of aleuron grains (ag) present is irregular globular shape compared to the long grain rice (S1) as show in Fig. 1.3c under 5000x magnification.

Fig. 1.3d shows scanning electron photomicrographs of representative transverse cross section under 100x magnification of the wholegrain rice mix (S3). The two distinct layers were clearly observed where they tightly contact with each other. The diameter of the cross section is approximately 1000 μm and endosperm (en) is located centrally right after the pericarp (p) layer which cover outermost layer of brown rice. There is no space precent between the pericarp (p) and endosperm (en) was observed in Fig. 1.3e.

The thickness of aleuron layer of rice grains where aleuron grains (ag) and parenchyma cells (pc) are present is approximately 23.3 μm. Compound of starch (c) was present in small size on the endosperm (en) area in polygonal like-shape. Fig. 1.3f shows the close view of aleuron grains (ag) which has irregular globular shape and differ from other sample. The estimated diameter for aleuron grains (ag) is approximately 0.5 to 3.8 μm and the parenchyma cells wall (cw) is surrounded around the aleuron grains (ag) at 5000x magnification.

Fig. 1.4a show the end part of white rice (S4) as a control to view the external morphological surface structure which differs from all brown rice samples. The surface area of white rice is smooth without any fracture of layer. The colour of this type of sample is whitish because of milling process removes almost completely bran layer. The close view of the surface of white rice (S4) in Fig. 1.4b under 1000x magnification shows the surface cover with aleuron grains (ag) as outermost layer which totally differ from brown rice sample.

Fig. 1.4c shows the aleuron grains (ag) with parenchyma cells (pc) under 5000x magnification. The shape of aleuron grains (ag) present is in irregular globular shape while parenchyma cells (pc) also present as shown in Fig. 1.4c under 5000x magnification. Fig. 1.4 (d, e, f) shows photomicrographs of representative transverse cross section from the white rice of sample 4 which do not consist any aleuron layer covering the endosperm (en). The diameter of the cross sectional of white rice (S4) sample is approximately 826.6 μm. The endosperm (en) is located centrally and

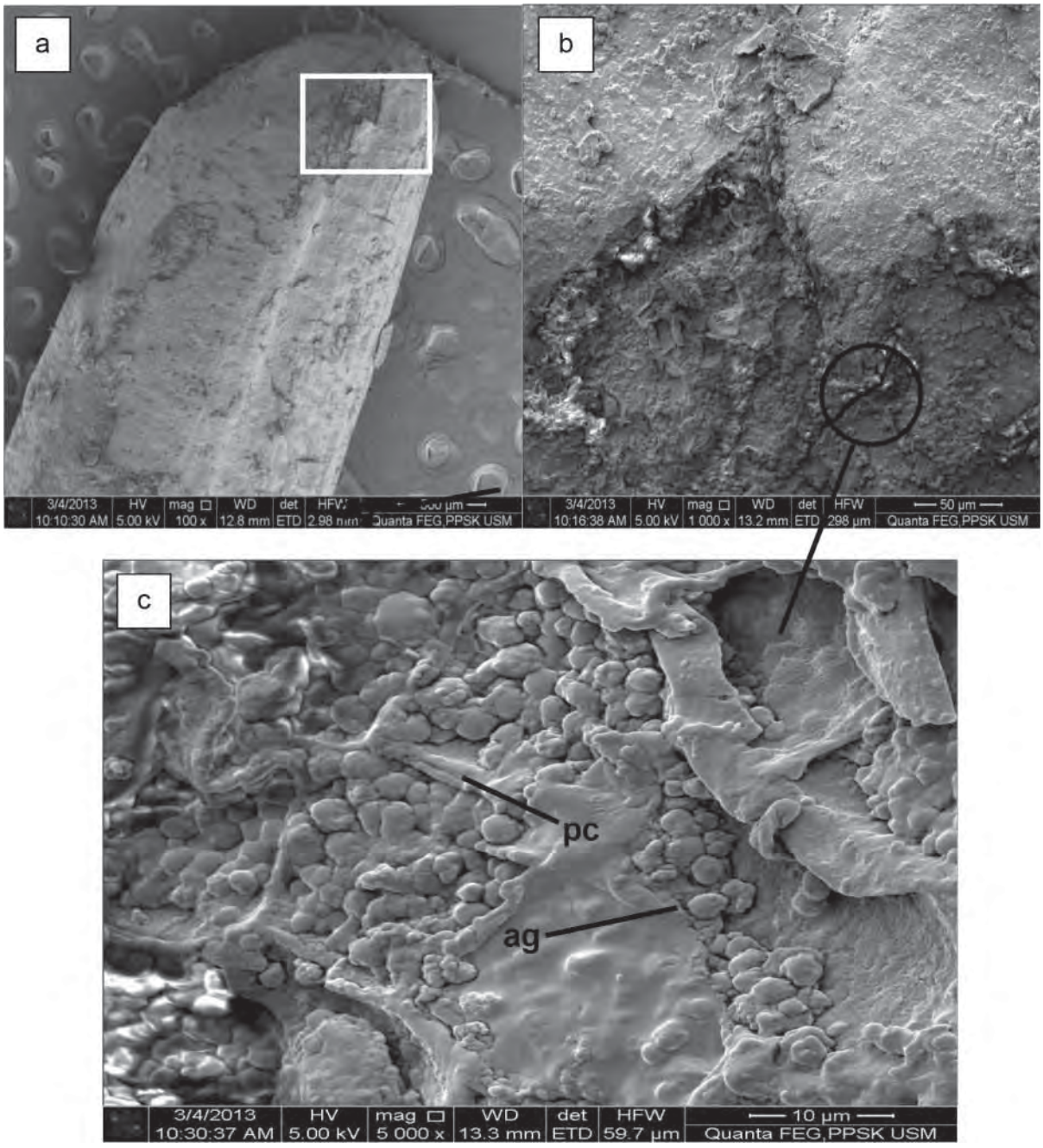

Fig. 1.2 (a, b ,c) are the scanning electron photomicrographs in high magnification (100x-5000x) of the sample 2 (Thai fragrant brown rice). Photomicrograph 1.2a is the overall view structure of sample 2 (Thai fragrant brown). Photomicrograph 1.2b shows the fissure between the two distinct layer of sample 2 (Thai fragrant brown) which consist pericarp (p) as outer layer. Photomicrograph 1.2c shows the presence of aleuron grains (ag) and parenchyma cells (pc) at 5000x magnification.

there is no pericarp (p) or bran layer observed at the outermost layer. Fig. 1.4e shows the close view (under 1000x magnification) of peripheral side which the most outer layer of white rice contain only endosperm (en) with some of aleuron grains (ag).

The starch compound (c) is also present and has polygonal like-shape at endosperm. The thickness between the aleuron grains and parenchyma cells presenting as the outer layer of white rice is approximately 8.97 µm. The diameter of aleuron grains was estimated to be between 0.25 – 1.8 µm under high magnification (5000x) shown in Fig. 1.4f.

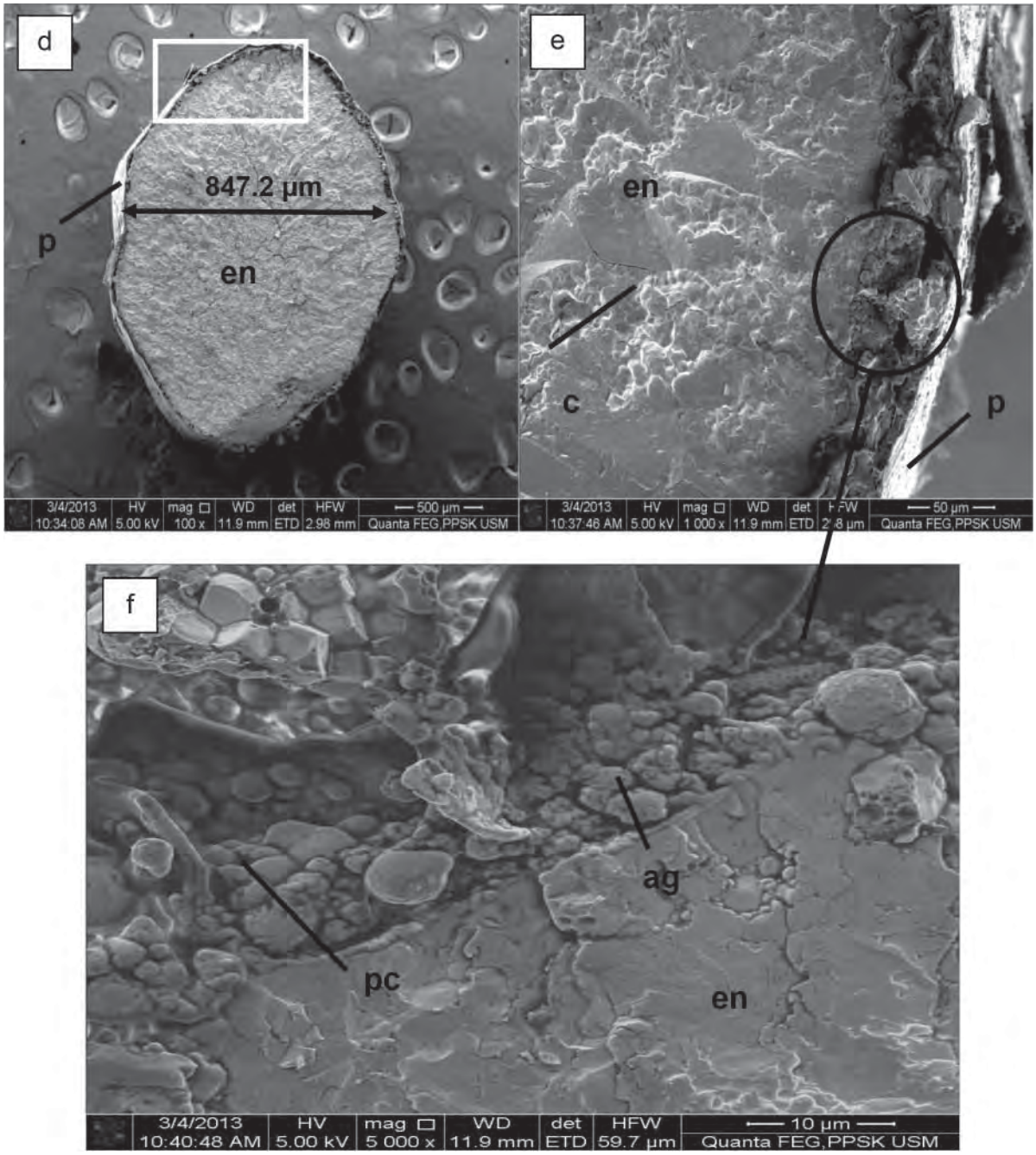

Fig. 1.2 (d, e, f) are scanning electron photomicrographs in high magnification (100x-5000x) of transverse cross section of sample 2 (Thai fragrant brown rice). Photomicrograph 1.2d is a representative rice grain which has been cut to view the transverse cross section. Close view of the space between the pericarp (p) and aleuron layer with endosperm (en) in Fig. 1.2e under 1000x magnification. Scanning electron photomicrograph 1.2f shows the parenchyma cells (pc) which surrounded by aleuron grains (ag) under 5000x magnification.

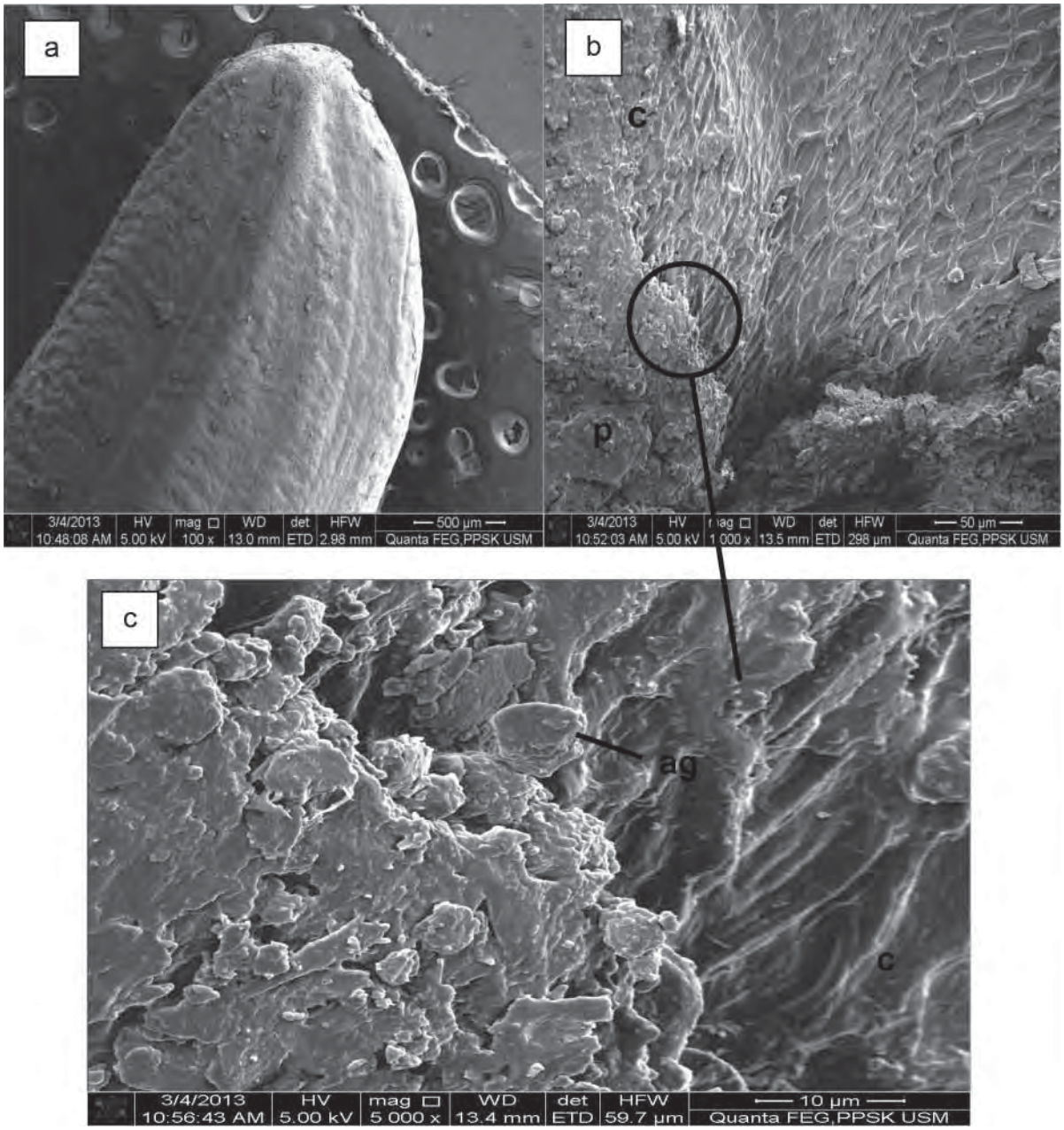

Fig. 1.3 (a,b,c) are the scanning electron photomicrographs in high magnification (100x-5000x) of the whole grain rice mix (S3). Photomicrograph 1.3a is the overall view structure of the wholegrain rice mix (S3). Photomicrograph 1.3b shows the fissure between the two distinct layer of the wholegrain rice mix (S3) which consist pericarp (p) as outer layer and the presence of plygonal compound starch granules (c). Photomicrograph 1.3c shows the presence of aleuron grains (ag) under 5000x magnification.

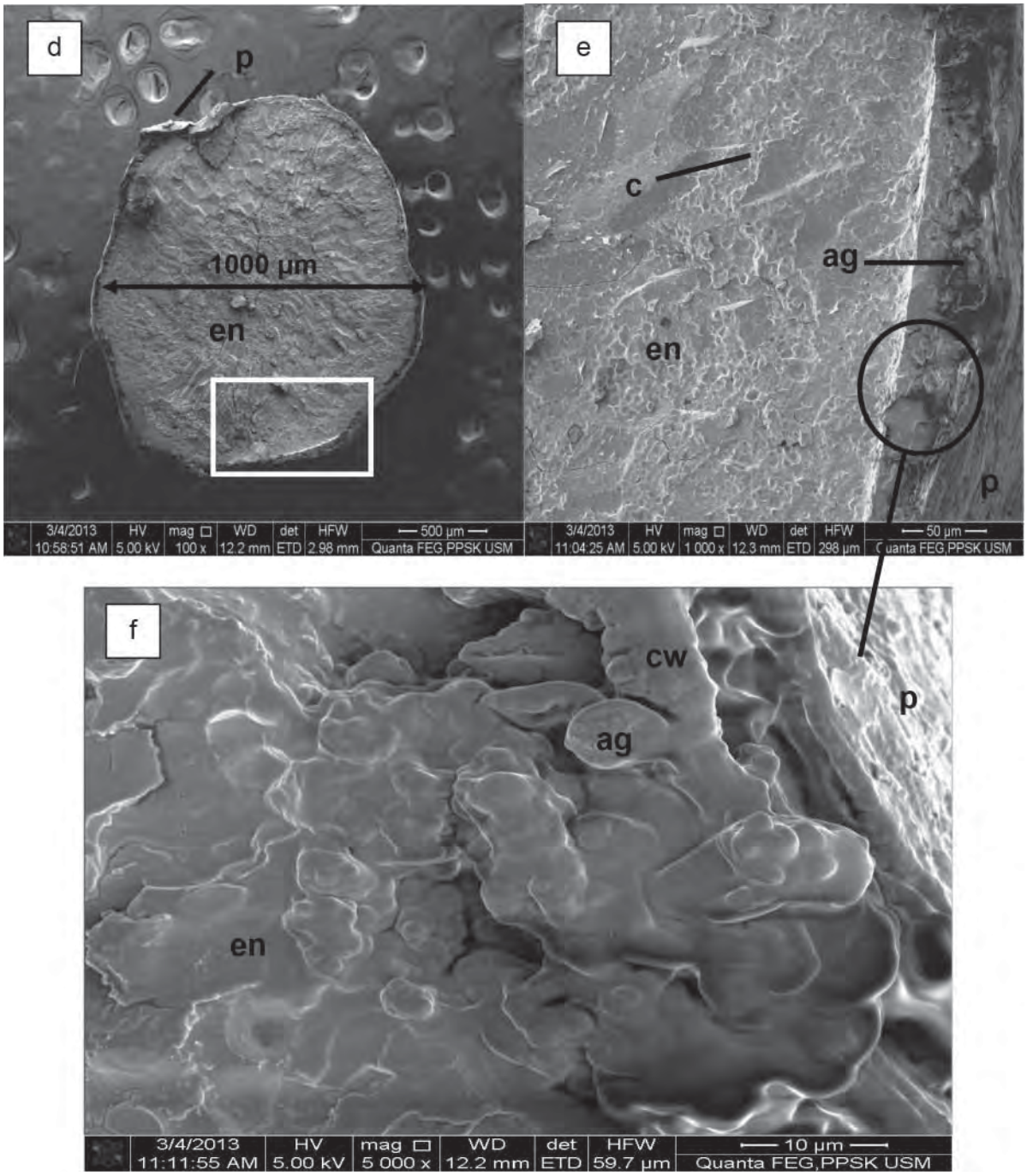

Fig. 1.3(d, e, f) are scanning electron photomicrographs at high magnification (100x-5000x) of transverse cross section of the whole grain rice mix (S3). Photomicrograph 1.3d is a representative rice grain which has been cut to view the transverse cross section. Close view of the space between the pericarp (p) and aleuron layer with endosperm (en) in Fig. 1.3e under 1000x magnification. Scanning electron photomicrograph 1.3f shows the parenchyma cells wall (cw), which is surrounded by aleuron grains (ag) under 5000x magnification.

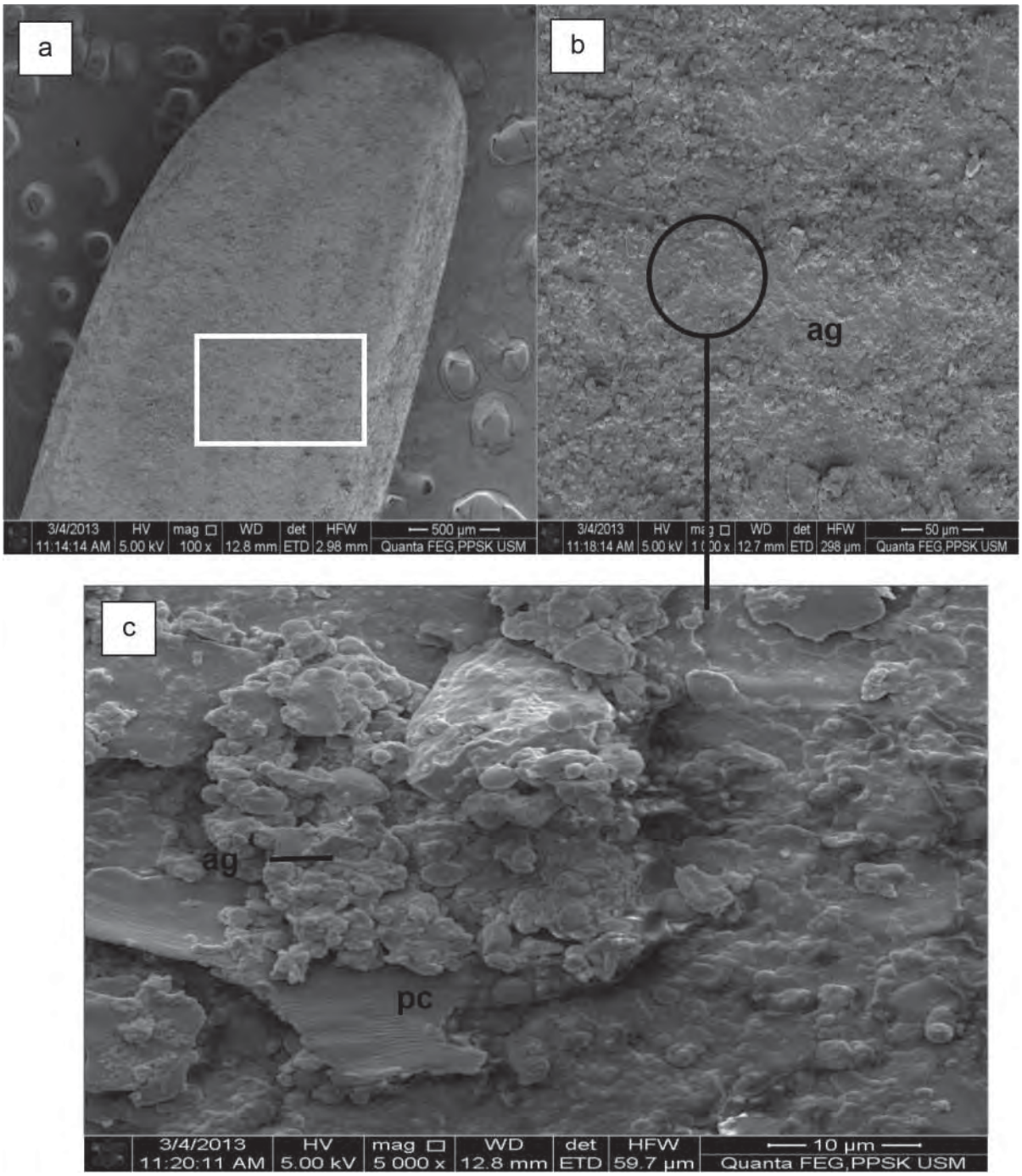

Fig. 1.4 (a,b,c) are the scanning electron photomicrographs at high magnification (100x-5000x) of the white rice (S4) as a control. Photomicrograph 1.4a is the overall view structure of white rice (S4). Photomicrograph 1.4b shows the smooth surface without fracture which consists of endosperm (en) with aleuron layer as outer layer. Photomicrograph 1.4c shows the presence of aleuron grains (ag) and parenchyma cells (pc) at 5000x magnification.

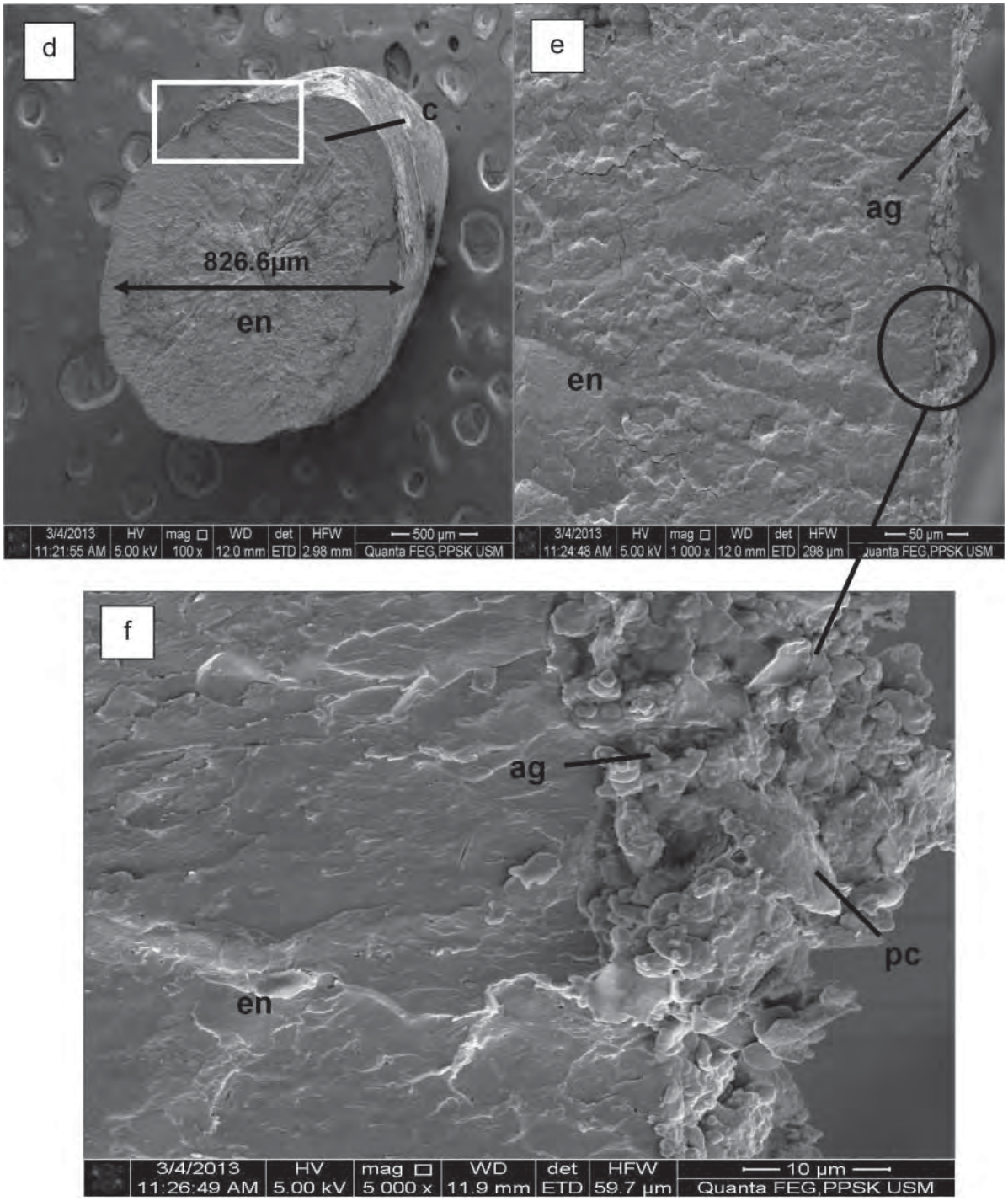

Fig. 1.4 (d, e, f) are scanning electron photomicrographs in high magnification (100x-5000x) of transverse cross section of white rice (S4). Photomicrograph 1.4d is a representative rice grain which has been cut to view the transverse cross section. Close view of sample without any aleuron layer but only aleuron grains (ag) with endosperm (en) present in Fig. 1.4e under 1000x magnification. Scanning electron photomicrograph 1.4f shows the parenchyma cells (pc) which are surrounded by aleuron grains (ag) under 5000x magnification.

CONCLUSION

The external morphology of brown rice is dissimilar for different varieties and depends on the degree of milling process. The brown rice has a layer which known as aleuron and bran layer which cover the outermost layer while it is absent in white rice sample. These layers are thought to store many essential nutrients such as minerals, essential oils and other functional phytochemicals that provide various health benefits to the consumer.

AKNOWLEDGEMENTS

The authors acknowledge the Universiti Sains Malaysia's grant funding for this research undertaking.

REFERENCES

Abas A, Murtaza S, Aslam F, Khawar A, Rafique S, Naheed S (2011) Effect of Processing on Nutritional Value of Rice (*Oryza Sativa*). World Journal of Medical Sceinces. 6 (2): 68-73.

Babu P D, Subhasree R, Bhakyaraj R, Vidhyalakshmi R (2009) Brown Rice-Beyond the Color Reviving a Lost Health Food. A Review: American-Eurasian Journal of Agronomy. 2: 67-72.

Deepa G, Singh V, Naidu K A (2008). Nutrient composition and physicochemical properties of Indian medicinal rice – Njavara. Food Chemistry. 106: 165–171.

Norimah A K, Safiah M, Jamal K, Haslinda S, Zuhaida H, Rohida S, Fatimah S, Norazlin S, Poh B K, Kandiah M, Zalilah M S, Manan, W M, Fatimah S, Azmi Y (2008) Food Consumption Patterns: Findings from the Malaysian Adult Nutrition Survey (Mans). Malaysian Journal of Nutrition. 14: 25-39.

Heinemann R, Fagundes P, Penteado M, Lanfer-Marquez U (2005) Comparative study of nutrient composition of commercial brown, parboiled and milled rice from Brazil. Journal of Food Composition and Analysis. 18: 287-296.

Hoseney R, Davis A, Harbers L (1974) Pericarp and endosprem structure of sorghum grain shown by scanning electron microscopy. Cereal Chemistry. 51: 552.

Juliana B (1972). The rice caryopsis and its composition. In D. Houston, Rice: Chemistry and Technology. pp 16.

Parengam M, Judprasong K, Srianujata S, Jittinandana S, Laoharojanaph S (2010) Study of nutrients and toxic minerals in rice and legumes by instrumental neutron activation analysis and graphite furnace atomic spectroscopy. Journal of Food Composition and Analysis. 23: 340-345.

Rosniyana A, Rukunudin I, Shariffah Norin S (2006). Effects of milling degree on the chemical composition, physicochemical properties and cooking characteristics of brown rice. Journal of Tropical Agriculture and Food Science. Trop. Agric. and Fd. Sc. 34(1): 37–44A.

Watson C, Dikeman E (1977) Structure of The Rice Grains Shown by Scanning Electron Microscope. Cereal Chemistry. 54(1): 120-130.

Does Extract of *Pleurotus sajor-caju* affect Liver Enzymes and Histological Integrity?

Nik Norliza, N. H., T. A. Tengku Farah Adilah, M. Siti Hajar, W. A. Wan Amir Nizam and W. I. Wan Rosli*

School of Health Sciences,Universiti Sains Malaysia Health Campus, 16150 Kelantan, Malaysia

**rosliishak@gmail.com, wrosli@kck.usm.my*

ABSTRACT

Pleurotus sajor-caju (PSC) is believed to have both antihyperlipidemic and hepatoprotective activities. The present study aimed to investigate the effect of PSC on liver enzymes and histological integrity. This study used five groups of rats fed with ghee, in the ratio 32g ghee per 68g pellet, to induce hypercholesterolemia and one group was fed on cholesterol free basal diet. Rats treated with 100 mg/kg of PSC for a month was found to have an effect on the liver enzymes activities since plasma alkaline phosphatase (ALP) concentration in this group showed a significant reduction ($P<0.05$) and a higher percentage reduction (66.01%) as compared to 20 mg/kg-PSC and 200 mg/kg-PSC treatment groups. The plasma aspartate aminotransferase (AST) and alanine aminotransferase (ALT) only showed a mild increased by 35.04% and 15.00% respectively in 100 mg/kg-PSC treatment group and there was no significant increased ($P>0.05$) found in these both AST and ALT concentrations. Atorvastatin treatment also showed reduction in ALP enzymes but no significant reduction ($P>0.05$) as compared to 100 mg/kg-PSC treatment group. On the other hand, plasma AST and ALT in 20 mg/kg of atorvastatin treatment were increased in percentage by 275.97% and 112.50% respectively indicated the adverse effects of statin in term of elevation of plasma enzymes activities. Histologically, there was no significant finding in the micrograph study between treatment and hypercholesterolemic (HPC) liver rat. The micrograph of rat liver treated with 100 mg/kg PSC showed smooth and clear surface of hepatocytes compared to HPC group.

Key words: antihyperlipidemic, hepatoprotective, *Pleurotus sajor-caju*, plasma enzymes

INTRODUCTION

Edible mushrooms have been world widely cultivated mainly for food, health and medicinal purposes. These fungi are commonly cultivated on decayed organic material while producing edible portion on the surface of the substrate. *Pleurotus sajor-caju* (PSC), also known as oyster mushrooms, is easily cultivated and is done so widely in the tropical regions and many other parts of the world. It is reported to possess distinctive aroma and highly palatable.

In South East Asian countries, oyster mushroom is widely used in the preparation of vegetable, soup, stew and other culinary products. This edible fungus is suggested to possess considerable importance in the human diet as its rich in non-starchy carbohydrates, dietary fibre, β-glucans, minerals, vitamin B while having low in fat. β-glucans, also a components of soluble or insoluble dietary fibre (SDF, IDF) is present in appreciable amounts in mushrooms and are linked to the ability to lower blood cholesterol levels and glycaemic response *in vivo* (Manzi *et al*. 2004), hypercholesterolemic properties and other therapeutic functions. The present study was conducted to investigate whether *Pleurotus sajor-caju* extract affect liver enzymes and histological integrity.

METHODS AND MATERIALS

Pleurotus sajor-caju

Oyster mushroom (*Pleurotus sajor-caju*, PSC) was supplied by Anjaad Industries Sdn Bhd (Serkam, Malacca State of Malaysia). PSC mushroom was already in the ground dried form. Aqueous extract of PSC was extracted using Soxhlet apparatus.

Animals

The procedure and protocol described below were approved by Animal Ethics Committee USM (USM/Animal Ethics Approval/ 2013/ (83) (446))**.** Eighteen male Wistar rats weighing 250-370 g were obtained from Animal Research and Service Centre of Universiti Sains Malaysia (ARASC). For adaptation, the rats were fed with a basal diet for one week before treatment begins. They were housed in rat cages at room temperature of 22 ± 1°C under a 12-h light-dark cycle. Rats were divided randomly into six feed groups (3 rats/group): control group was fed a basal diet; while the remaining five groups were given 32 g ghee per 68 g pellet (high-cholesterol diet). Rats were fed for two weeks and were allowed free access to water. After two weeks of high-cholesterol diet, blood was withdrawn from the rats through saphenous vein. Blood samples were then sent to BP Laboratory Pte Ltd for total cholesterol levels determination. Plasma total cholesterol was determined using automated Abbott Ci8200 Biochemistry analyzer based on enzymatic kits methods. Rat with serum cholesterol level > 2.3 mmol/L was considered hypercholesterolemic and included in this study. Group I was served as normal control (NC) rats, whereas Group II was left as a hypecholesterolemic (HPC) control rats. Meanwhile Group III, IV, V and VI were treated with 20 mg/kg PSC, 100 mg/kg PSC, 200 mg/kg PSC and 20 mg/kg atorvastatin respectively.

Plasma enzymes analysis

At the end of experiment, the rats were anaesthetized with 6% pentobarbital and blood was collected through cardiac puncture and sent to the BP Laboratory for liver function tests (LFTs) analysis. Plasma liver enzymes were determined using automated Abbott Ci8200 Biochemistry analyzer based on photometric IFCC (Intrenational Federation of Chemistry) methods.

Histological analysis of liver by using scanning electron microscope (SEM)

Liver tissues were rapidly dissected, removed and fixed in McDowel-Trump Fixative at 4°C for 24 hours. The fixed tissues were then cut, washed, post-fixed and dehydrated. The samples was then processed with critical point drying step, coated with gold and lastly viewed under Quanta FEG 450 Scanning Electron Microscope (SEM) by using XTm Product Version 4.1.7.2095 viewer software.

Statistical analysis

All values used in analysis are presented as means ± SEM. Comparisons among the different groups were performed by one-way analysis of variance (ANOVA), followed by Bonferroni multiple comparisons test and differences were considered significant when $P < 0.05$.

RESULTS AND DISCUSSION

Effects of PSC on plasma liver enzyme profile

Table 1 summarizes the values for all liver enzyme analysis before and after treatments. There were no significant differences found in total protein, albumin, globulin, and albumin/ globulin (A/G) ratio for all experimental groups. AST level in 20mg/kg-PSC, 200mg/kg-PSC and HPC group was increased by 127.50%, 85.39% and 147.22% respectively. Like AST, there was an increased in ALT by 65.79%, 23.40% and 53.49% respectively for 20mg/kg-PSC, 200 mg/kg-PSC treatment and HPC group of rats. The least amount of increase in AST and ALT were found in 100 mg/kg-PSC treatment group (35.04% and 15.00% respectively). In contrast, the highest increased in AST and ALT were found in atorvastatin treatment group (275.97% and 112.5% respectively). ALP level in 20mg/kg-PSC, 200mg/kg-PSC and 20mg/kg-atorvastatin treatment group was increased in percentage changes by 49.40%, 52.95% and 54.97% respectively. A significant reduction by 66.47% and 66.01% was found in HPC and 100mg/kg-PSC treatment groups respectively. There were no changes observed in both total bilirubin and GGT enzymes before and after treatment.

Lower plasma ALP concentration in hypercholesterolemic rats was assessed to be significantly

($P < 0.05$) reduced by the supplementation of diet with 100 mg/kg PSC (Fig. 1). Treatment with 20 mg/kg and 200 mg/kg of PSC was not significantly different ($P > 0.05$) in their impact on ALP enzyme. Thus, by comparing to other treatment groups, dose of 100 mg/kg of PSC was the effective dose of PSC to lower the plasma ALP. However, this finding was not significant as HPC group was also found to have significant reduction in plasma ALP ($P > 0.05$). The reason for such result may be due to the modulation of mechanism or physiological functions in hypercholesterolemic rats which cannot be controlled. ALP is a marker enzyme of the plasma membrane and can be found mainly in liver and bone origin. The underlying mechanism for reduction of plasma ALP enzymes by mushroom is not clearly understood. However, study by Mishra and Singh (2010), had shown that mushroom (*Pleurotus* sp.) restores the changes in ALP, AST and ALT activities due to antioxidant effects and their ability as a radical scavenger, thus, protecting membrane permeability.

Plasma AST and ALT were found to be elevated in all groups. However, there was no significant increased ($P > 0.05$) found for both enzymes (Fig. 2 and 3). Increase in plasma AST and ALT was more prominent in 20mg/kg PSC-treatment, atorvastatin treatment and hypercholesterolemic control groups. From the result, we found that 20mg/kg of PSC-treatment was the least effective treatment compared to the other two PSC-treatment groups. On the other hand, plasma AST and ALT concentrations for 100mg/kg PSC treatment was increased by 35.04% and 15.00% respectively which is the smallest percentage of increased in concentration as compared to HPC and other PSC-treatment groups.

In this study, atorvastatin treatment served as positive control group, thus, the results should be almost similar with PSC treatment group. However, by comparing with HPC and PSC treatment groups, we found that AST and ALT levels in 20 mg/kg atorvastatin treatment group showed a significant increased by 275.97% and 112.50% respectively. Thus, we can postulate that increase in these two liver enzyme parameters may be due to statin adverse effects. There is a correlation that exists between statin treatment and hepatic adverse effects. However, the underlying mechanism of this effect is still not clearly understood. A previous study had postulated that statin causes changes in the lipid components of the hepatocyte membrane and this will leads to an increase in its permeability and result in an increased of liver enzymes (Rossana *et al.* 2010).

Fig. 3 - 7 shows no significant difference ($P > 0.05$) in plasma total protein, albumin, globulin and A/G ratio respectively for all treatments. There were also no changes in concentration of pre- and post-study for total bilirubin and GGT concentration (Table 1). In addition, there were also no significant differences of total protein within groups ($P > 0.05$) in both pre and post-treatment of PSC and atorvastatin on total protein level of HPC rats (Fig. 4). On the other hand, the effect of pre and post-treatment of PSC and atorvastatin on plasma albumin of HPC rats resulted reduction in albumin values for all groups, however there were no significant decreased of albumin (Fig. 5) within groups ($P>0.05$). In addition, globulin level was decreased for 20 mg/kg and 100 mg/kg-PSC treatment groups, but increased for other groups. However, there were no significant differences of globulin levels (Fig. 6) within groups ($P > 0.05$). In addition, albumin/globulin ratio (A/G) of HPC rats' ratio was reduced in normal, HPC, 200 mg/kg-PSC and 20 mg/kg atorvastatin treatment groups, whereas other groups showed no changes in values (Fig. 7). There were no significant differences of A/G ratio within groups ($P > 0.05$).

Histological study

Scanning electron microscope (SEM) study indicated three-dimensional features of intrahepatic structures in liver of the rat, especially the surface characteristics of hepatocytes and sinusoidal endothelial cells. At 4000 x magnification, HPC rat liver treated with 100 mg/kg-PSC (Fig. 8a) showed smooth surface of hepatocytes with bile canaliculi as compared to HPC rat (Fig. 8c). Hepatocytes seen were polyhedral and sharply angulated shape. However, the surface seen was not so clear due to the presence of some artifact. Fig. 8b shows micrograph of HPC rat liver treated with atorvastatin in which the morphological features of liver surface resembled those of the PSC-treatment group (Fig. 8a) to some extent. However, the surface of hepatocytes seen in

Table 1 Effect of *Pleurotus sajor-caju* on liver enzymes of hypercholesterolemic rats

Group	Treatment	TP (g/L)	Alb (g/L)	Glo (g/L)	A/G	TB (μmol/L)	SGOT/AST (U/L)	SGPT/ALT (U/L)	ALP (U/L)	GGT (U/L)
I (Normal control, NC)	Before	61.5±1.5	24.0±2.0	37.5±0.5	0.70±0.05	1.7	129.0±7.0	40.0±1.5	362.0 ± 58.0	4
	After	61.5±2.5	23.0±0.5	39.0±2.0	0.60±0.0	1.7	215.0±80.0	61.0±15.5	254.0±23.0	4
	% changes	-	-4.17	+4.00	-14.29	-	+66.67	+52.50	-29.83	-
II (HPC)	Before	60.0±1.5	24±1.0	35.5±0.5	0.70±0.05	1.7	126.0±17.0	43.0± 2.0	854.5±23.5	4
	After	57.5±0.7	22±0.5	36.0±1.0	0.6±0.0	1.7	311.5±169.5	66±18.5	286.5±12.5	4
	% changes	-4.17	-8.33	+1.41	-14.29	-	+147.22	+53.49	-66.47*	-
III (20 mg/kg-PSC)	Before	62.0±2.0	25±0.9	36.7±1.5	0.7± 0.03	1.7	120.0±7.4	38±1.8	585.0±62.6	4
	After	58.3±2.3	23.0±1.2	35.3±1.5	0.7±0.03	1.7	273.0±65.2	63.0±10.2	296.0±39.5	4
	% changes	-5.97	-8.00	-3.81	-	-	+127.50	+65.79	-49.40	-
IV (100 mg/kg-PSC)	Before	62.0±0.3	25± 0.9	37.0±1.0	0.70±0.06	1.7	122.7±11.2	40.0±2.3	823.7±133.4	4
	After	58.3±1.2	24.0±0.0	34.3±1.2	0.7±0.03	1.7	165.7±38.1	46.0±4.4	280.0±14.1	4
	% changes	-5.97	-4.00	-7.30	-	-	+35.04	+15.00	-66.01*	-
V (200 mg/kg-PSC)	Before	58.0±3.2	24.0±1.0	34.0±2.3	0.8±0.1	1.7	130.7±22.8	47.0±7.0	672.3±65.9	4
	After	61.0±1.2	24.0±0.6	37.0±1.0	0.6± 0.03	1.7	242.3±84.4	58.0±13.3	316.3±37.9	4
	% changes	+5.17	-	+8.82	-25.00	-	+85.39	+23.40	-52.95	-
VI (20 mg/kg-Atorvastatin)	Before	63.7±0.9	25.0±0.6	38.7±0.7	0.5±0.1	1.7	115.7±6.2	40.0 ±1.8	791.3±124.7	4
	After	60.7±0.7	22.0±0.9	39.0±0.6	0.6± 0.03	1.7	435.0±243.4	85.0±30.8	356.3±43.2	4
	% changes	-4.71	-12.00	+0.78	+20.00	-	+275.97	+112.50	-54.97	-

Values are expressed as means ± SEM for each group; * indicates significantly different at $P < 0.05$. TP: total protein (g/L); Alb: albumin (g/L); Glo: Globulin (g/L); A/G: albumin/globulin ratio; TB: total bilirubin (μmol/L); SGOT/AST: serum glutamic oxaloacetic transaminase/aspartate transaminase (U/L); SGPT/ALT: serum glutamic pyruvate transaminase/alanine aminotransferase (U/L); ALP: alkaline phosphatase (U/L); GGT: gamma-glutamyl transpeptidase (U/L).

atorvastatin treatment was not as smooth as those after PSC-treatment. This may be due to the incorrectly applied technique in the process of cutting the liver.

In addition, at 12 000 X magnification, rat liver after 100 mg/kg PSC treatment and atorvastatin treatment demonstrated smooth surface of hepatocytes as compared to those of the HPC control rat (Fig. 9a-9d). Round structure with whitish color may be assumed as fat storing cells or fatty infiltration but were not clearly seen. Normal control rat showed the whitish round structures but not as prominent as HPC rat. At higher magnification (30 000 X), round structures with whitish color may be assumed as fat storing cells or fatty infiltration but were not clearly seen (Fig. 10a-10d). Normal control rat (Fig. 10d) showed these whitish round structures measuring about 0.8 μm but not as prominent as HPC (Fig. 10c) rat. A small amount of fat storing cells or fatty infiltration may be present in the 100 mg/kg PSC and 20mg/kg atorvastatin treatment rat liver but are not clearly seen and not prominent in HPC rat.

CONCLUSION

This preliminary study demonstrated that feeding 100 mg/kg of PSC significantly reduced plasma ALP concentration. However, this finding was not significant as HPC group also showed significant reduction in ALP enzymes. Atorvastatin drug was proven to have clinically significant adverse effects as an elevated ALT and AST enzymes were prominent in 20 mg/kg atorvastatin-

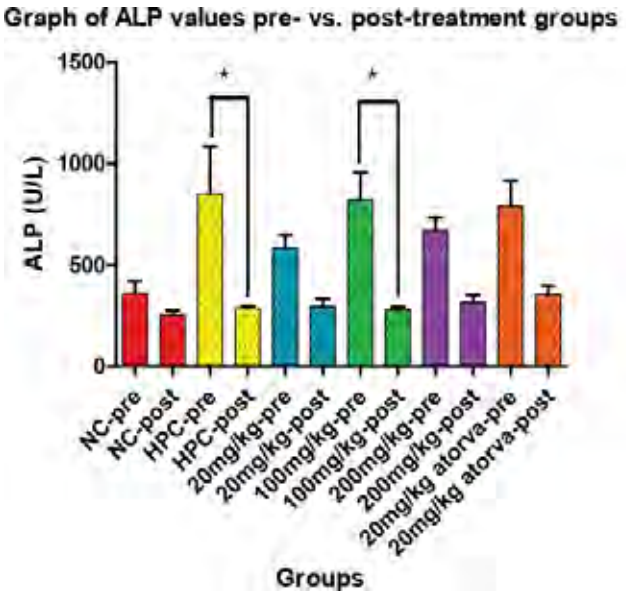

Fig 1 Effect of pre- and post-treatment of PSC and atorvastatin on plasma alkaline phosphatase (ALP) of HPC rats. Values are in means ± SEM.
*indicates significantly different at $P < 0.05$.
NC = normal control, HPC = hypercholesterolemic

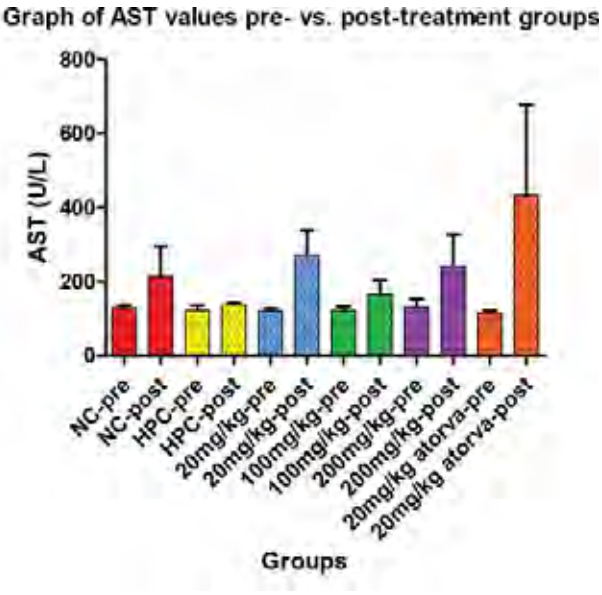

Fig 2 Effect of pre and post-treatment of PSC and atorvastatin on plasma aspartate aminotransferase (AST) of HPC rats. Values are in means ± SEM.
NC = normal control, HPC = hypercholesterolemic

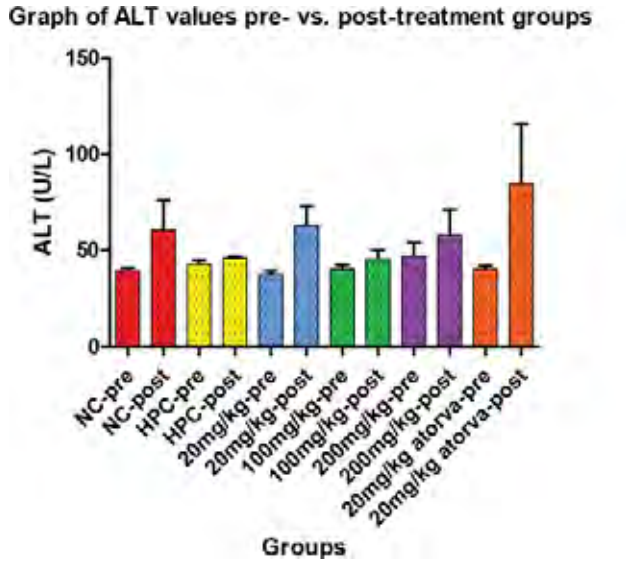

Fig 3 Effect of pre and post-treatment of PSC and atorvastatin on plasma alanine aminotransferase (ALT) of HPC rats. Values are in means ± SEM.
NC = normal control, HPC = hypercholesterolemic

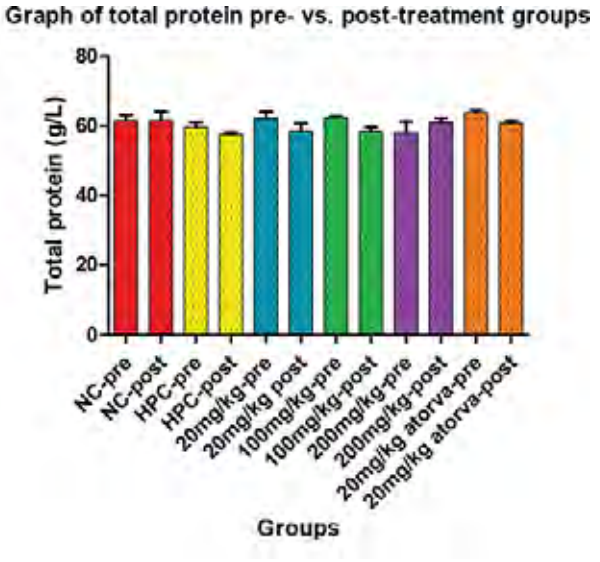

Fig 4 Effect of pre and post-treatment of PSC and atorvastatin on total protein level of HPC rats. Values are in means ± SEM.
NC = normal control, HPC = hypercholesterolemic

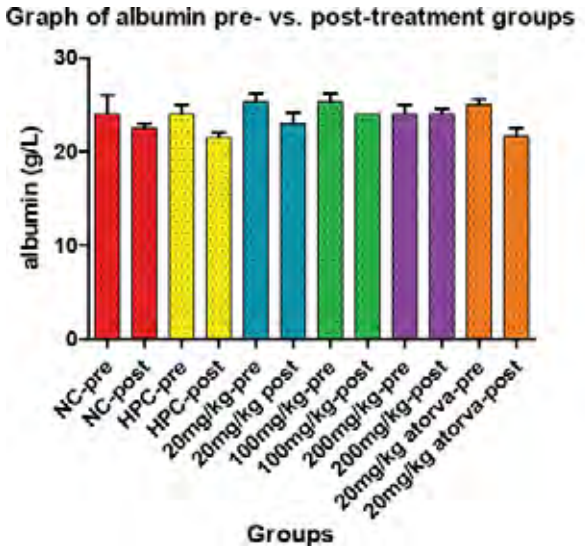

Fig 5 Effect of pre and post-treatment of PSC and atorvastatin on plasma albumin of HPC rats. Values are in means ± SEM.
NC = normal control, HPC = hypercholesterolemic

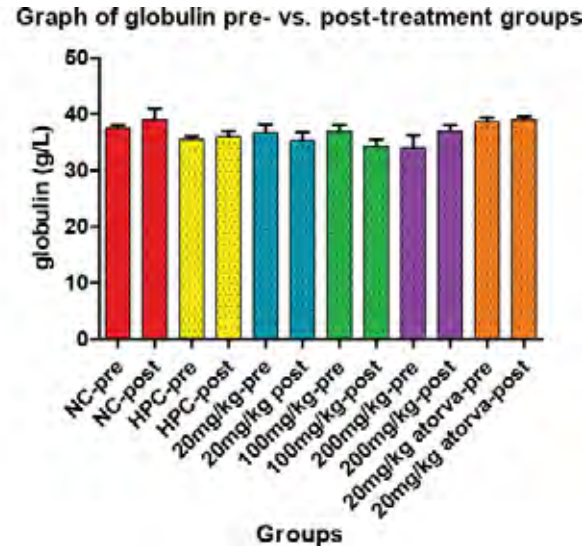

Fig 6 Effect of pre and post-treatment of PSC and atorvastatin on globulin level of HPC rats. Values are in means ± SEM.
NC = normal control, HPC = hypercholesterolemic

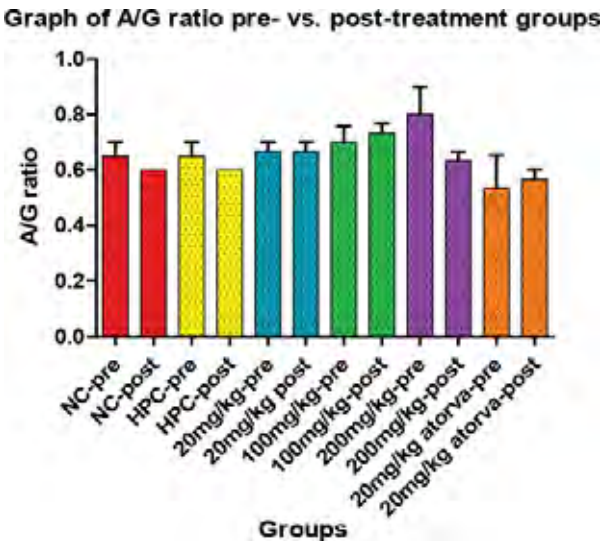

Fig 7 Effect of pre and post-treatment of PSC and atorvastatin on albumin/globulin ratio (A/G) of HPC rats. Values are in means ± SEM.
NC = normal control, HPC = hypercholesterolemic

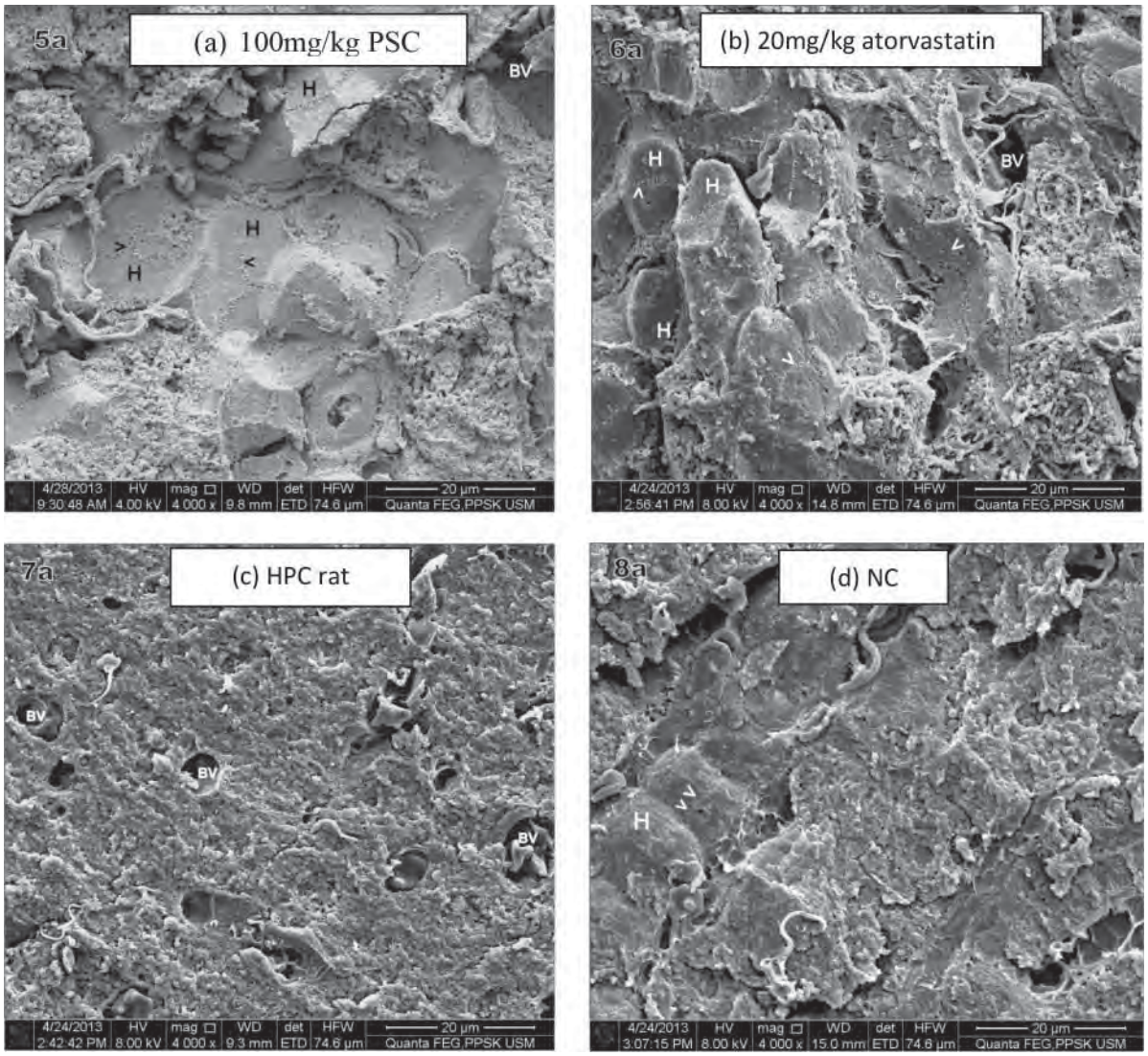

Fig 8 (a): Micrographs of rat liver after 100 mg/kg PSC treatment; **(b):** atorvastatin treatment; **(c):** HPC control; **(d):** normal control. (H: hepatocytes; arrowhead: bile canaliculi; BV: blood vessel) (4 000 x magnification)

treatment group as compared to PSC-treatment groups. However, there was no significant finding in the electron microscopic study on the liver of HPC- and PSC-treatment rat. The only different in this histological study is the surface of hepatocyte in PSC- and atorvastatin treatment rat was smooth as compared to HPC rat. For future work, it is suggested to use normal light microscopic staining (Haematoxylin and Eosin, H&E and Oil-Red staining) or TEM to study for any fatty infiltration and fatty changes in HPC- and PSC-treated rats.

ACKNOWLEDGEMENTS

The study was funded by Universiti Sains Malaysia (1001/PPSK/813057). Special thanks to all staffs who assist this preliminary investigation (Roslina, Shazwan) including Mr Fakurudin for his technical assistance and support when viewed samples using SEM.

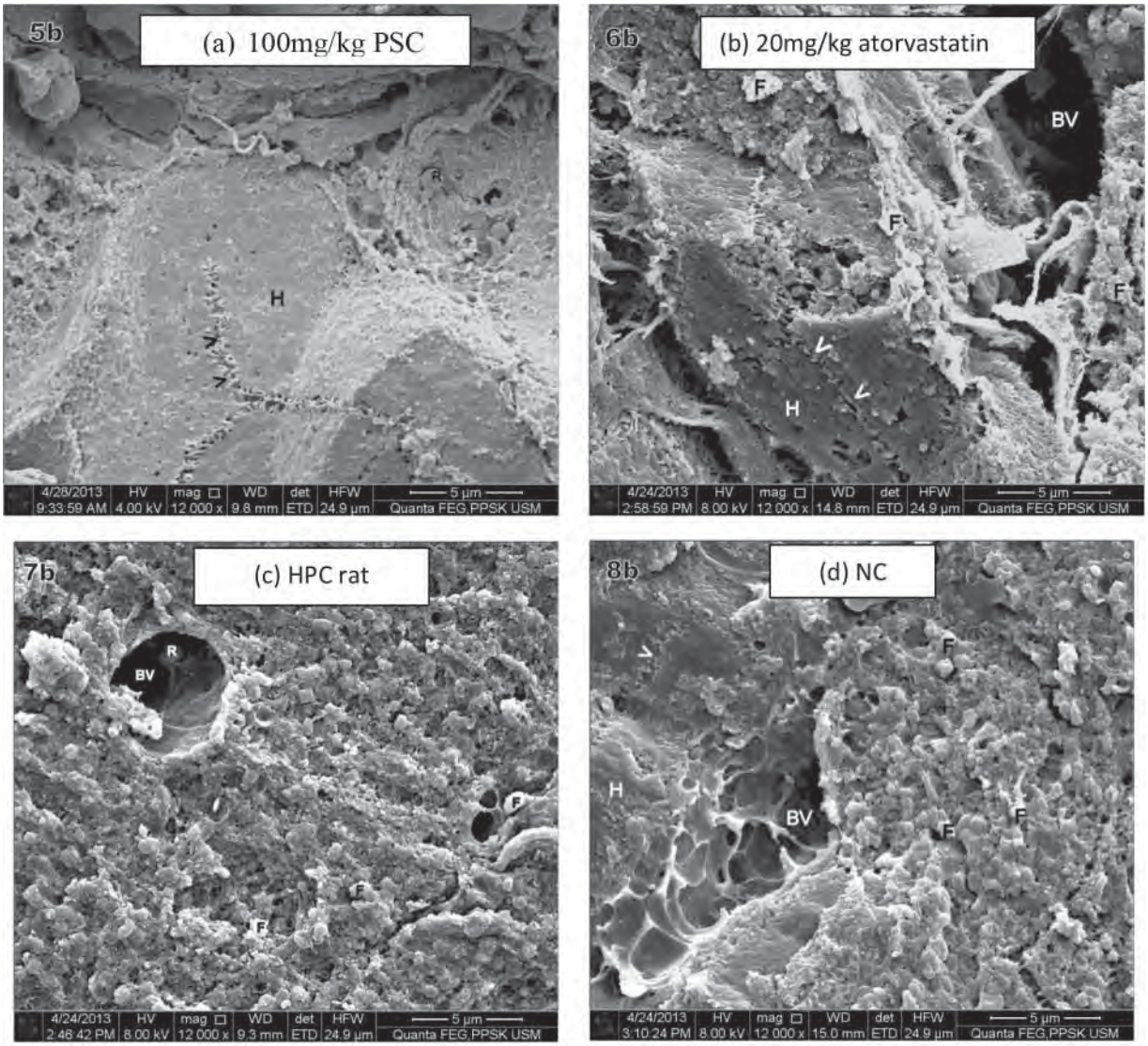

Fig 9 (a): Micrographs of rat liver after 100 mg/kg PSC treatment; **(b):** atorvastatin treatment; **(c):** HPC control; **(d):** normal control. (H: hepatocytes; arrowhead: bile canaliculi; BV: blood vessel; R: red blood cell) (12 000 x magnification)

REFERENCES

Adams, L. A., Angulo, P. and Lindor, K. D. (2005) Nonalcoholic fatty liver disease. *Canadian Medical Association Journal*, **172**(7), 899-905.

Agrawal, R., Chopra, A., Lavekar, G., Padhi, M., Srikanth, N. and Ota, S. (2010) Effect of oyster mushroom on glycemia, lipid profile and quality of life in type 2 diabetic patients. *Australian J Med Herbalism* **22**, 50-54.

Alam, N., Amin, R., Khan, A., Ara, I., Shim, M. J. and Lee, M. W. (2009) Comparative Effects of Oyster Mushrooms on Lipid Profile, Liver, Kidney Function in Hypercholesterolemic Rats. *The Korean Society of Mycology* **1**, 37-42.

Alam, N., Amin, R., Khan, A., Ara, I., Shim, M. J. and Lee, M. W. (2009) Comparative effects of oyster mushrooms on lipid profile, liver and kidney function in hypercholesterolemic rats. *Mycobiology* **37**(1), 37-42.

Alam, N., Yoon, K. N., Lee, J. S., Cho, H. J., Shim, M. J. and Lee, T. S. (2011) Dietary effect of Pleurotus eryngii on biochemical function and histology in hypercholesterolemic rats. *Saudi Journal of Biological Sciences* **18**(4), 403-409.

Alam, N., Yoon, K. N. and Lee, T. S. (2011) Antihyperlipidemic activities of Pleurotus ferulae

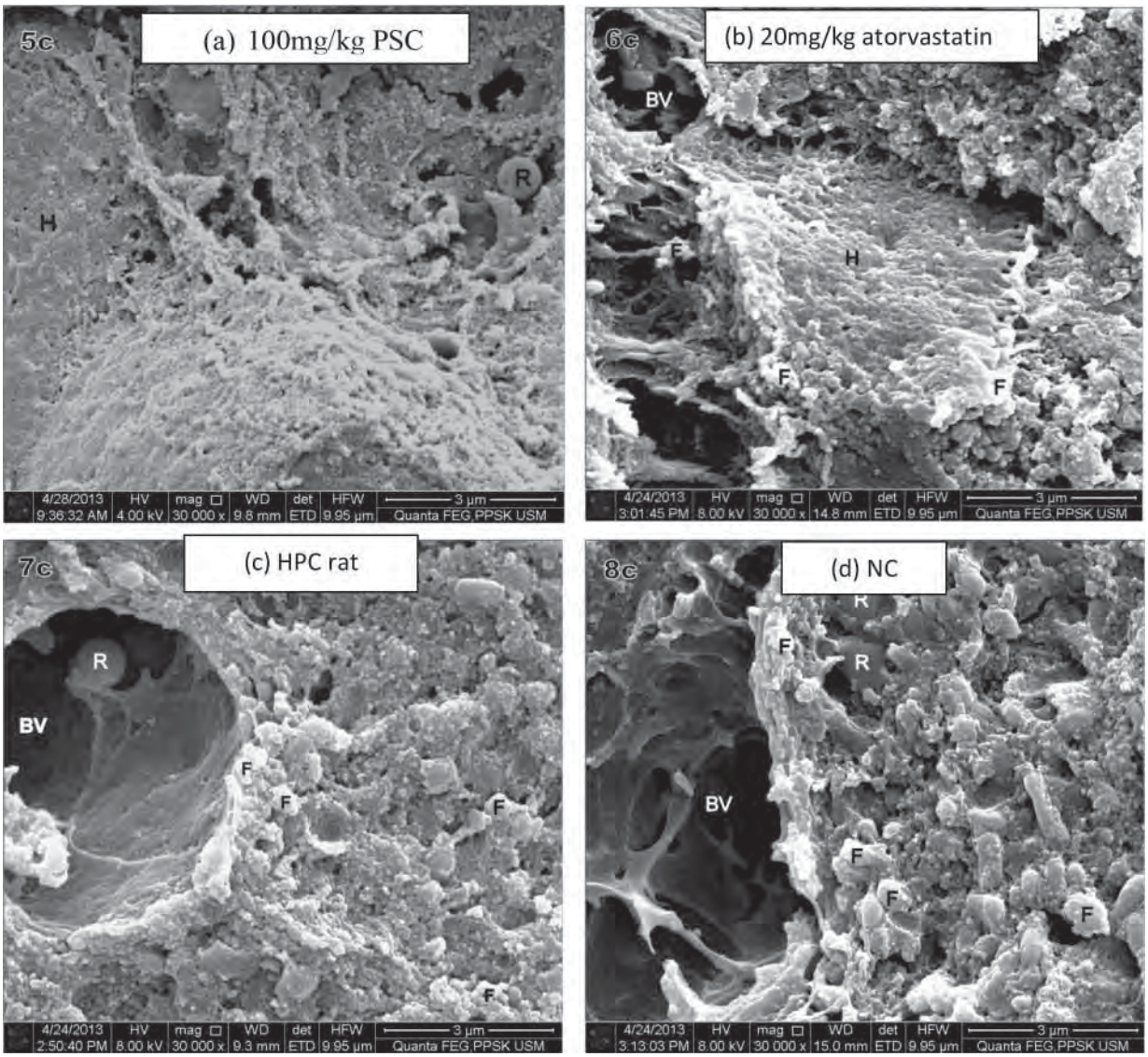

Fig 10 (a): Micrographs of rat liver after 100 mg/kg PSC treatment; **(b):** atorvastatin treatment; **(c):** HPC control; **(d):** normal control. (H: hepatocytes; arrowhead: bile canaliculi; BV: blood vessel; R: red blood cell) (30 000 x magnification)

on biochemical and histological function in hypercholesterolemic rats. *Journal of research in medical sciences: the official journal of Isfahan University of Medical Sciences* **16**(6), 776.

Alam, N., Yoon, K. N., Lee, J. S., Lee, M. W. and Lee, T. S. (2011) Evaluation of Biochemical and Histological Effectiveness of Pleurotus Citrinopileatus on Plasma, Feces and Liver in Hypercholesterolemic Rats. *Advances in Environmental Biology* **5**(6), 1095-1103.

Alarcon, J., Aguila, S., Arancibia-Avila, P., Fuentes, O., Zamorano-Ponce, E. and Hernandez, M. (2003) Production and purification of statins from Pleurotus ostreatus (Basidiomycetes) strains. *Zeitschrift Fur Naturforschung C,* **58**(1/2), 62-64.

Alberts, A., Chen, J., Kuron, G., Hunt, V., Huff, J. and Hoffman, C. (1980) Mevinolin: a highly potent competitive inhibitor of hydroxymethylglutaryl-coenzyme A reductase and a cholesterol-lowering agent. *Proceedings of the National Academy of Sciences* 77(7), 3957-3961.

Altunkaynak, B. Z. and Ozbek, E. (2009) Overweight and structural alterations of the liver in female rats fed a high-fat diet: a stereological and histological study. *Turkish Journal of Gastroenterology* **20**(2), 93-103.

Austin, M. A., Hutter, C. M., Zimmern, R. L. and Humphries, S. E. (2004) Familial hypercholesterolemia and coronary heart disease: a HuGE association review. *American Journal of Epidemiology* **160**(5), 421-429.

Beltowski, J., Wojcicka, G. and Jamroz-Wisniewska, A. (2009) Adverse effects of statins - mechanisms and consequences. *Current Drug Safety* **4**(3), 209-228.

Bobek, P., Hromadová, M. and Ozdin, L. (1995) Oyster mushroom (*Pleurotus ostreatus*) reduces the activity of 3-hydroxy-3-methylglutaryl CoA reductase in rat liver microsomes. *Experientia* **51**(6), 589-591.

Bobek, P., Ozdín, L. and Galbavý, Š. (1998). Dose-and Time-Dependent Hypocholesterolemic Effect of Oyster Mushroom (*Pleurotus ostreatus*) in Rats. *Nutrition* **14**(3), 282-286.

Bobek, P., Ozdin, L. and Kuniak, L. (1994) Mechanism of hypocholesterolemic effect of oyster mushroom (*Pleurotus ostreatus*) in rats: reduction of cholesterol absorption and increase of plasma cholesterol removal. *Zitschrift Für Ernährungswissenschaft* **33**(1), *44-50.*

Calderon, R. M., Cubeddu, L. X., Goldberg, R. B. and Schiff, E. R. (2010) Statins in the treatment of dyslipidemia in the presence of elevated liver aminotransferase levels: a therapeutic dilemma. *Mayo Clin Proc* **85**(4), *349-356.*

Chang, S. and Miles, P. (1989) The nutritional attributes and medicinal value of edible mushrooms (pp. 27-40): CRC Press, Boca Raton, FL.

Chang, S. T. (1992) Mushroom biology-A new discipline. *The Mycologist* **6**, 64-65.

Chorváthová, V., Bobek, P., Ginter, E. and Klvanová, J. (1993) Effect of the oyster fungus on glycaemia and cholesterolaemia in rats with insulin-dependent diabetes. *Physiological research/ Academia Scientiarum Bohemoslovaca* **42**(3), 175

Jayakumar, T., Ramesh, E. and Geraldine, P. (2006) Antioxidant activity of the oyster mushroom Pleurotus ostreatus induced liver injury in rats. *Food and Chemical Toxicology* **44**(12), 1989-1996.

Khan, M. A., Rahman, M. M., Tania, M., Uddin, M. N. and Ahmed, S. (2011) *Pleurotus sajor-caju* and *Pleurotus florida* Mushrooms Improve Some Extent of the Antioxidant Systems in the Liver of Hypercholesterolemic Rats. *The Open Nutraceuticals J* **4**, 20-24.

Khan, M. A. and Tania, M. (2012) Nutritional and medicinal importance of pleurotus mushrooms: an overview. *Food Reviews International* **28**(3), 313-329.

Magosso, E., Ansari, M. A., Gopalan, Y., Abu Bakar, M., Karim Khan, N. and Wong, J. (2010). Prevalence of non-alcoholic fatty liver in a hypercholesterolemic population of northwestern peninsular Malaysia. *Southeast Asian Journal of Tropical Medicine and Public Health* **41**(4), 936.

Manzi, P., Marconi, S., Aguzzi, A. and Pizzoferrato, L. (2004) Commercial mushrooms: nutritional quality and effect of cooking. *Food Chemistry* **84**, 201-206.

Mishra, S. and Singh, R. B. (2010) Effect of Mushroom on the Lipid Profile, Lipid Peroxidation and Liver Functions of Aging Swiss Albino Rats. *The Open Nutraseuticals Journal* **3**, 248-253.

Mohd Adzim Khalili, R., Norhayati, A. H., Rokiah, M. Y., Asmah, R., Siti Muskinah, M. and Abdul Manaf, A. (2009) Hypocholesterolemic effect of red pitaya (*Hylocereus sp.)* on hypercholesterolemia induced rats. *International Food Research Journal* **16**, 431-440.

Sumy, A. K., Jahan, N. and Sultana, N. (2010) Study on the Hepatoprotective effect of oyster mushroom (Pleurotus florida) against paracetamol induced liver damage in Wistar albino rats. *Journal of Bangladesh Society of Physiologist* **5**(2), 46-52.

Immunological Study on the Effect of Some Free Radicals and Antioxidants on the Placenta of Pregnant Women with Rheumatic Heart Diseases

Anwar I. S. Al-Assaf[a], Ragwa H.I. Al-Rubai[b], Imad M. Al-Ani[c*], Salim R. Al-Ubeidie[d]
[a] *Department of Biology, Ibin Al- Haithum college of Education, Baghdad University, Baghdad, Iraq.*
[b] *Department of Biology, College of Science, Al-Mustansiriyah University, Baghdad, Iraq.*
[c] *Department of Basic Medical Science, Kulliyyah of Medicine, International Islamic University Malaysia, Kuantan, Malaysia.*
[d] *Department of Pathology, College of Medicine, Baghdad University, Baghdad, Iraq.*
**Corresponding author: Tel. +60179776014. E-Mail: imad_alani@yahoo.com*

ABSTRACT

***Introduction*:** The present study was undertaken to assess the role of heart diseases on pregnancy status. Twenty-six pregnant women with rheumatic heart disease **(**RHD), five pregnant women with non rheumatic heart disease (NRHD) and ten healthy pregnant control groups were investigated.
Methods: Immunological responses were investigated, and the activity of adenosine deaminse (ADA) was measured. Radial immunodiffusion (RID) technique, was used to quantify the immunoglobulin level, such as, IgG ,IgM and IgA , in addition to the complement components C3 and C4 , in serum and placental tissue, blood films with Leishman's stain and the granulocytes were prepared.
***Results*:** The results indicated that there is a significant depression in tissue IgG and IgA levels in patients as compared with control groups, while the level of IgM is very low in tissue and less than normal value. Serological tests such as, anti streptolycinO–titer (ASO-T) , venereal disease research laboratories (VDRL) , anti - nuclear antibody (ANA) and anti - cardiolipin antibody (ANCA) gave negative results except for two cases with positive (ASO-T) titers.

Keywords: Granulocytes, **I**mmunoglobulin, Pregnant women, Rheumatic heart disease.

INTRODUCTION

The placenta is a temporary organ which separates the maternal and fetal circulations, nourishes the fetus, eliminates fetal wastes and produces hormones vital to pregnancy (Tietz, 1987). It is an effective barrier to the movement of large proteins and hydropic compounds bound to plasma proteins. Maternal IgG crosses the placenta via receptor mediated endocytosis (Tietz, 1987). Because of its long half–life, maternally produced IgG protects a newborn for the first 6 months of life and confers a high degree of natural passive acquired immunity to the newborn (Roitt *et al*. 2001). Maternal cardiac disease complicates 0.5 % to 1% of pregnancies. Rheumatic lesions are responsible for fewer than half the cases of heart disease that complicate pregnancy, the majority being due to congenital lesions. Rheumatic heart disease in women usually involves the mitral valve, and mitral stenosis account for 90% of rheumatic heart disease seen in pregnancy (Scott *et al*. 1990). It follows an attack of *Streptococcal pharangitis* and occurs mainly in children and young adults. It starts with acute febrile illness in which lesions occur in the heart, the joints and subcutaneous tissue. After this there is an interval of 5-30 years of apparent good health before the clinical features of valvular disease develop (Anderson, 1987). Rheumatic fever is a multisystemic inflammatory disease with presence of circulating antibodies directed at cardiac tissue and groups "A" streptococci antigens, in addition to deposition of immunoglobulin and complement in myocardial and valvular tissues (Stites *et al*. 1997). According to the immunological disorders in pregnancy, the principle function of the host immune system is to maintain the baby's integrity by defending and destroying invaders or antigens of extrinsic origin. The present study was undertaken to investigate some changes in the immunological parameters that might occur in pregnant women with rheumatic heart diseases.

MATERIAL AND METHODS

Thirty one pregnant women, with ages of 20-39 years; twenty–six of them were with a provisional diagnosis of rheumatic heart disease **(**RHD) and five pregnant women with non rheumatic heart disease (NRHD)attending Baghdad Teaching Hospital, Baghdad, (January 2002 to January 2003). Ten healthy pregnant women aged 19-35 years were taken as control. All women selected had no previous disease, which may interfere with the parameters included in this study.

The placenta were collected from maternity ward; the cord and membrane were removed and placenta was drained of blood before clotting occurred and then free the placenta of blood, dried with filter paper, weighed, then the maternal portion were cut into small pieces (5 grams each), dried with blotting paper and weighed for extraction of the placental protein (Rakonczay *et al*. 1981). Five milliliter of venous blood was obtained from each patient and from healthy pregnant for immunological tests in this study Serum was separated by centrifugation of blood (3000 r.p.m. for 10 minutes. Adenosin deaminase activity (ADA) was assay according to Giusti (Giusti, 1974). The concentration of IgG, IgM and IgA immunoglobulins and the components C3, C4 of the complement were measured by using the method of (Single Radial Immunodiffusion) (RID) (Mancini *et al*. 1981). Placental protein was extracted using the method of Rakonczay *et al*. (1981). The low level immunoglobulins IgG, IgM in the extract of the placenta was measured using the single radial immunodiffusion method (AL-Najjar, 2002).

To show the nature of eosinophils and to assess the frequency of eosinophilic inflammation in cases of peripartum cardiac disease (Bonezuk *et al*. 1997); thin blood smears were prepared and stained with Giemsa and Leishman stains. The anticardiolip in IgG / IgM antibodies was measured by immunoassay kit (Biomaghreb).To detect the semiquantitative of human auto- antibodies, the antinuclear auto- antibodies in the test sample were measured by immunoassay kit (Biomaghreb). To determine the antistreptolysin O titer “ASO-T”, rheum jet ASO, bio kit, S. A was used in this study.

Statistical Analysis

Statistical analysis was performed using SPSS Statistical program. Results were analysed statistically using Student’s t-test and paired samples t-test to compare the significance of the differences between the means of patients and control studied group. The results were expressed as mean±standard deviation. P values less than 0.05 were considered to be significant and less than 0.01 as highly significant.

RESULTS AND DISCUSSION

Adenosine deaminase enzyme (ADA) in serum:

Table (1) shows the mean values of serum ADA enzyme (U/mg) in RHD pregnant were (0.20 ± 0.0107), in NRHD pregnant were (0.21 ± 0.0213), while in control pregnant women were (0.13 ± 0.0092). Statistically, there is a significant difference ($P<0.05$) in serum ADA enzyme between RHD and NRHD pregnant women as compared with the control group.

Table (1): Level values of serum ADA enzyme (U/mg) in control, RHD and NRHD groups.

Groups	**No.**	**Mean (U/mg) ±Sd**
RHD	26	0.20* ± 0.0107
NRHD	5	0.21* ± 0.0213
Control	10	0.13 ± 0.0092

*Significant ($P<0.05$) to their control.

Adenosine deaminase enzyme (ADA) in lyophilized Placental tissue

Table (2) shows the mean value of lyophilized placental tissue ADA enzyme (U/mg) in rheumatic heart disease pregnant were (0.20 ± 0.021), in NRHD were (0.044 ± 0.0024), while in control pregnant were (0.074 ± 0.0094). Statistically, there is a significant difference (P<0.05) in placental ADA enzyme between RHD and NRHD pregnant also between RHD and control pregnant.

Table (2): Level values of placental ADA enzyme (U/mg) in control, RHD and NRHD groups.

Groups	No.	Mean (U/mg) ±Sd
RHD	26	$0.20^{*\#} \pm 0.021$
NRHD	5	$0.044^{*} \pm 0.0024$
Control	10	0.074 ± 0.0094

*Significant (P<0.05) to their control. #Significant (P<0.05) to NRHD group.

The activity of ADA enzyme is now considered as an indicator for cellular immune response, because of its role in proliferation and differentiation of T-cells, monocytes and epithelial cells (Moriwake *et al*. 1999). The results reported in this study showed activation and elevated levels of ADA enzyme .It can be concluded that the increase of ADA activity in sera of heart disease patients is predictable since rheumatic heart disease is an inflammatory disease in which the immune system is stimulated in response to antigenic stimuli, and ADA has probably leaked from activated lymphocytes or from the damaged activated inflammatory cells e.g. neutrophils (Ungere JP and Grobler 1988). These finding are in agreement with the findings obtained by Abd-AL Qader, (2001) who reported high levels of ADA enzyme in serum of patients with tonsillitis, especially those of chronic status. The activity of the enzyme may result from the increase of T– cell mass, and this suggestion is in concordance with Bonezuk, *et al*. (1997) that there is increase numbers of lymphocytes and granulocytes (eosinophils) in patients of heart diseases which scavenges the Ag – Ab complexes.

Serum immunoglobulins, C3 and C4

Table (3) shows the mean values of serum IgG, IgM and IgA (mg/dl) in RHD pregnant were (879.10 ± 52.99), (118.41 ± 4.61), (141.14 ± 8.85) respectively. In NRHD pregnant were (1385.24 ± 30.30),(124.98 ± 5.62), (140.38 ± 13.07) respectively, while in control pregnant were (1124.47 ± 23.74), (163.52 ± 11.96), (208.88 ± 2.96) respectively. Statistically, there is a significant difference (P<0.05) in serum IgG level between RHD with NRHD pregnant women and between RHD with the pregnant group. Also, there is a significant difference (P<0.05) in serum IgM as well as IgA levels between RHD and NRHD pregnant as compared with control group.

Table (3): Mean values of serum immunoglobulins IgG, IgM and IgA levels (mg/dl) in control, RHD and NRHD groups.

Groups	No.	IgG	IgM	IgA
		Mean (mg/dl) ± S. R.M.		
RHD	**26**	$879.10^{*\#} \pm 52.99$	$118.41^{*\#} \pm 4.61$	$141.14^{*\#} \pm 8.85$
NRHD	**5**	$1385.24^{*} \pm 30.30$	$124.98^{*} \pm 5.62$	$140.38^{*} \pm 13.07$
Control	**10**	1124.47 ± 23.74	163.52 ± 11.96	208.88 ± 2.96
Normal value		710 – 1520	40 – 310	90 – 310

*Significant (P<0.05) to their control. #Significant (P<0.05) to NRHD group.

Table (4) shows the mean values of complement components C3 and C4 (mg/dl) in serum of RHD pregnant women were (137.93 ± 6.74), (37.36 ± 2.40) respectively, in NRHD pregnant women were (202.34 ± 9.47), (40.23 ± 3.56) respectively, while in control group were (151.98 ± 3.58), (35.02 ± 1.20) respectively. Statistically, there is a significant difference (P<0.05) in serum level between RHD and NRHD pregnant, also between NRHD pregnant with control pregnant. About C4 level, there is no significant difference (P<0.05) in serum C4 level between RHD, NRHD and control groups.

Table (4): Mean values of serum immunoglobulins IgG, IgM and IgA levels (mg/dl) in control, RHD and NRHD groups.

Groups	No.	IgG	IgM	IgA
		Mean (mg/dl) ± S. R.M.		
RHD	26	879.10*# ± 52.99	118.41*# ± 4.61	141.14*# ± 8.85
NRHD	5	1385.24* ± 30.30	124.98* ± 5.62	140.38* ± 13.07
Control	10	1124.47$ ± 23.74	163.52 ± 11.96	208.88 ± 2.96
Normal value		710 – 1520	40 – 310	90 – 310

*Significant (P<0.05) to their control. #Significant (P<0.05) to NRHD. $Significant (P<0.05) to normal value.

Our results indicated that there is decreased IgG, IgM and IgA levels in the serum of RHD pregnant women when compared to that of control; however the IgG, IgM and IgA values difference was significant in control group when compared with normal range. These decreased levels may be due to the physiological changes in pregnancy and its effects on the immune activity which occur in pregnancy which may significantly modify the primary disease, for example the raised levels of steroids and other hormones during pregnancy may have a beneficial effect in rheumatic disease (Chapel *et al*. 1999). However, these results are not correlated with the results obtained by Gupta *et al*. (l985) who observed elevations in serum immunoglobulins (IgG, IgM and IgA) and C3 in majority of RHD patients.

Immunoglobulins IgG and IgA in placental protein

Table (5) shows the mean values of IgG and IgA in liquid protein of placenta (mg/dl) in RHD were (16.47 ± 0.98). (1.06 ± 0.064) respectively, in NRHD pregnant women were (14.02 ± 1.15), (1.16 ± 0.16) respectively, while in control. There is a significant difference (p<0.05) in placental immunoglobulin levels between RHD and NRHD pregnant women when compared to that of control pregnant women.

Table (5): Mean values of placental immunoglobulins IgG and IgA levels (mg/dl) in control, RHD and NRHD groups.

Groups	No.	IgG	IgM
		Mean (mg/dl) ± S. R.M.	
RHD	26	16.47* ± 0.98	1.06* ± 0.064
NRHD	5	14.02* ± 1.15	1.16* ± 0.16
Control	10	24.30 ± 1.12	1.77 ± 0.077
Normal value		25 - 354	2 – 25

*Significant (P<0.05) to their control.

This study revealed the presence of IgG and IgA in the placental extract, these results are in agreement with the study of Malek *et al*. (1995) who detected the existence of IgG antibodies in both maternal and fetal components of the placenta and lowered IgG antibodies may be due to its transference from maternal circulation to the placenta then to the fetus for protection (McGillivary, 2006).

As the IgM is the predominant antibody in primary immune response (Roitt *et al*. 2001), the low level (less than the normal level) in placental extract of pregnant women may be related to chronic RHD disease. The lowered amount of IgA antibodies in placental tissue may consider that IgA was mostly surface antibody defense mechanisms than that of deeper tissues (Scott and Dawson, 1985).

An immunohistological study of human placenta demonstrated the presence of "Fibrinoid" material in the villi of the placenta and the presence of IgG and IgM in relation to the fibrinoid deposits suggests that some immunological reaction may be involved in the formation of these deposits, thus the fibrinoid material with its content of immunoglobulins, complement and fibrin may represent the " immuno-debris " of an immunological reaction with some undetermined placental or fetal antigen (McCormik *et al*. 1971).

Eosinophils percentage in blood smears

Table (6) shows the mean values of eosinophils percentage (%) in blood smear of RHD pregnant were (9 ± 0.50), in NRHD pregnant women were (6 ± 0.89), while in control pregnant were (2 ± 0.20). Statistically, there is a significant difference was observed ($P<0.05$) in eosinophils percentage of patients when compared to that of control group and between RHD and NRHD pregnant women.

Table (6): Mean values of eosinophils percentage (%) in blood smears of control, RHD and NRHD groups.

Groups	**No.**	**Eosinophils percentage**
		Mean(%) ± S.E M.
RHD	26	$9^{*\#} \pm 0.50$
NRHD	5	$6^{*} \pm 0.89$
Control	10	2 ± 0.20

*Significant ($P<0.05$) to their control. #Significant ($P<0.05$) to NRHD group.

Our findings applies with study of (Janewy *et al*. (2001) which emphasis the increased numbers of eosinophils in the circulation of blood synonymous with endocrdium damage as in (Fig. 2). The results of this study are in agreement with Bonezuk *et al*. (1997) who suggested the possibility of raises role of eosinophils in the spontaneous coronary dissection and myocarditis in the postpartum period. The rheumatic heart disease is the most usual manifestation of humoral and cell – mediated reactivity in patients; due to cardiotoxicity of eosinophils, endomyocardil diseases with eosinophils are developed (Kolbas, 1990).

Anticardiolipin antibody (ANCA) test

The ANCA was negative in RHD pregnant group, this test is might be not suitable for RHD, but it have been found in some of non–thrombotic neurological disorders like cardiovascular insufficiency, cerebral ischemia or chorea and myocardial infarction (Hughes *et al*. 1986).

Antinuclear antibody (ANA) test

The ANA test was negative in the RHD pregnant group; this might be related to the decreased amount of antibodies performance in chronic status and because the typical reaction occur in acute

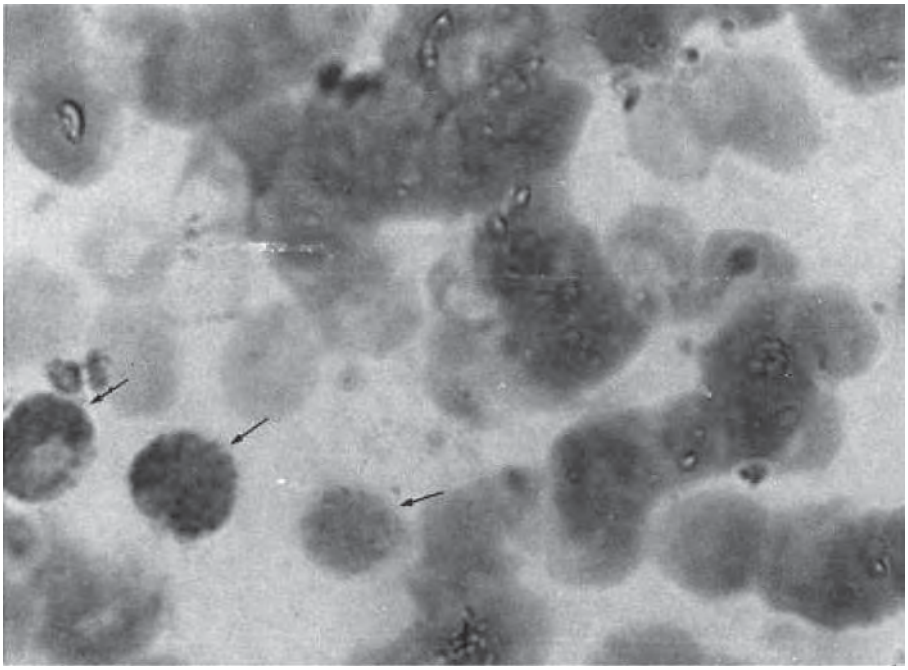

Fig. (1): Blood smear from RHD pregnant woman showing granulocytes (eosinophils) and eosinophils ghost (arrows) (Leishman stain X 1000).

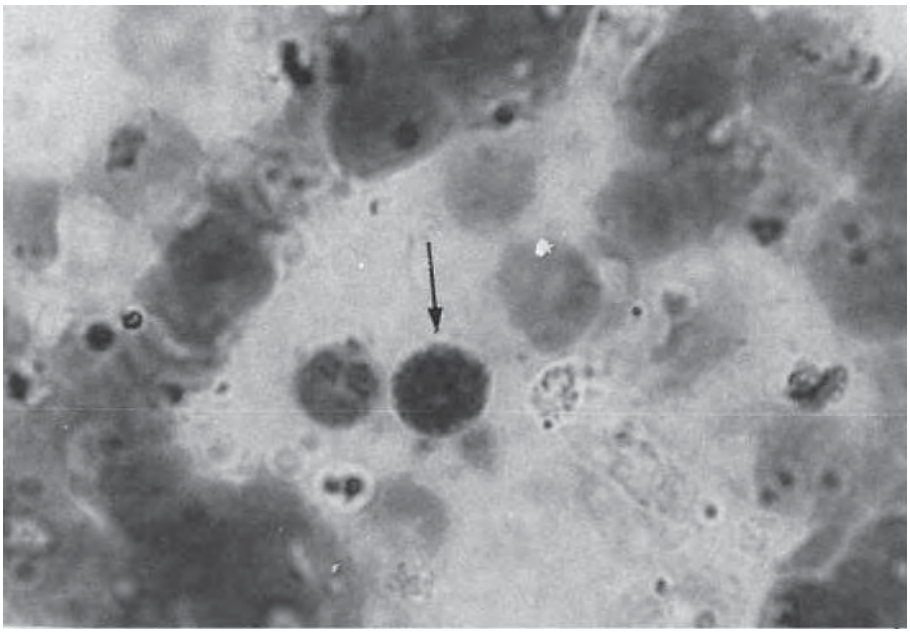

Fig. (2): Blood smear from RHD pregnant woman shows the eosinophil cell (arrow) with its heavily stained cytoplasmic granules. (Leishman stain X 1000).

phase (rheumatic fever) of the patients (Janewy *et al*. 2001).

Venereal disease research laboratories VDRL test

The VDRL test was negative in RHD pregnant group**;** these findings emphasised that the reason for RHD in these patients is due to early streptococci infection and not to syphilis infection (Cecil and Lobe, 1959).

Antistreptolycin O – titer:

Table (8): shows the percentage of ASO – T titer in Rheumatic heart disease pregnant.

RHD pregnant women No.	**ASO – T (+ ve) No.**	**%**
26	2	7.6 %

The ASO – T is considered as a specialized confident assay for group A streptococcus (GAS) which has the ability to secrete streptolycin –O enzyme (Alouf, 1997). This enzyme can stimulate the immune system to produce IgG immunoglobulins in serum of patients with GAS (Alouf, 1997). Our results indicated that there is a decreased level of ASO in patients with chronic RHD, because antibody to streptolycin O (antistreptolycin O, ASO) develops following infection (Hyde, 1989),or this depression may be due to previous taking the antibiotics (Benzathen penicillin) which will lead to increase the analysis of ASO level in blood (Chapel *et al*. 1999).

REFERENCES

Abd –AL Qader LS (2001). Bacteriological and immunological study on tonsillitis patients. M. Sc. Thesis. Ibn-AL Haithum College of Education; University of Baghdad.

AL-Najjar EW (2002). Histopathological and biochemical study for pregnant and abortion women. M. Sc. Thesis. College of Science; AL-Mustansiriyah University.

Alouf JE (1997). Streptococcal pyrogenic exotoxin Streptolycin O, exoenzymes, serotype and biotype profiles of *Streptococcus pyrogenes* isolated from patients with toxic shock syndrome and other sever infections. *Zb 1-Bakt*. 286: 421-433.

Anderson JR (1987). Muir's Textbook of Pathology. 12th Ed., Chapter 14, 15.

Bonezuk AC, Vn-Hoeven KH and Factor SM (1997). Review and hypothesis: the eosinophils and peripartum heart disease. *Cardiovascular Research*. 33: 527-32.

Cecil RL and Lobe RF (1959). Textbook of Medicine. 10th Ed., W. B. Saunders Company. London: 1212.

Chapel H, Haeney M, Misbah S and Snowden N (1999). Essential of clinical Immunology. 4th Ed., Black Well Science Ltd., U. K.: 304-320.

Giusti G (1974). Adenosin deaminase. In: Bergmeyer, HV (Ed). Methods of enzymatic analysis, Vol. 2, 2nd Ed., Academic Press, New York: 1092.

Gupta RK, Gupta S, Dubey VK, Mishra DN (1985). Serum immunoglobulins and C3 in rheumatic heart disease. *Indian Heart Journal*. 37: 377-379.

Hughes, G. R. V.; Harris, E. N. and Gharavi, A. E. (1986): *The Journal of Rheumatology*. 13: 486- 489.

Hyde MR (1989). β – Hemolytic streptococcal, I: Microbiology Oklahoma Notes. 2nd Ed., Sprigger-Verlag. New York : 135.

Janeway CA, Travers P, Walport M and Shlomchik M (2001). Immunobiology (The immune system in heart disease), 5th Ed., Garland Publishing, United State of America: 482-484.

Kolbas V (1990). Immunology of cardiovascular disease in children. *Lijec-Vjesn*. 112 : 404-407.

Malek A, Sager R, Zakher A and Schneider H (1995). Transport of immunologlobulin G and its subclasses across the in vitro-perfused human placenta. *America Journal of Obstetrics and Gynecology*. 173; 760-67.

Mancini G, Carbonar AO, Hesemans JF(1965). Immunochemical quantitation of antigen by single radial immunodiffusion. Immunochemistry. 2: 235–254.

McCormik JN, Fox H, Faulk WP and Fudenberg HH (1971). Immunohistological and elution studies of human placenta. *Journal of Experimental Medicine*. 133:1–18.

McGillivary I (2006). Surgical procedures for rheumatoid arthritis. Cambridge University Press

Moriwake Y, Yamamoto T and Higashino K(1999). Invited review enzymes involved in purin metabolism - A review of histochemical localization and functional implications. *Histology Histopathology*. 14: 1321-1340.

Rakonczay Z, Mallof J, Schenk H and Zanetta JP(1981). Heterogeneity of rat brain acetylcholinesterase: a stury by gel filtration and gradient centrifugation. *Journal of Neurochemistry*. 37: 662-669.

Roitt I, Brostoff J and Male D (2001). Immunology. 6th Ed., W.B. Saunders: 65-80.

Scott JR, Disaia Ph J, Hammond ChB and Spellacy WN(1990). Danforth's Obstetrics and Gynecology. 6th Ed., Lippincoltt Company, Philadelphia: 432-495.

Scott DW and Dawson JR (1985). Key Facts in Immunology.1st Ed., Churchil Livingstone, U.S.A.:11-29.

Stites DP, Stobo JD and Wells JV(1997). Basic & Clinical Immunology. 6th Ed., Middle East Edition, Nor Walk, Connecticut / Los Altos, California, printed in Lebanon by Typorress: 356-360.

Tietz WN (1987). Fundamental of Clinical Chemistry. 3rd Ed., W.B. Saunders Company, Philadelphia. London, Torento; 7. 54-759.

Ungere JP and Grobler A (1988). Molecular forms of adenosine deaminase in pleural effusions. *Enzyme*. 40:7-13.

The Role of Microscopy and the Potential of Propolis Mineral Trioxide Aggregate (MTA) In Mineralization of Matrix

M.M.H. Massoud[*], SA Sulaiman[1], Z Ariffin[2], Farid C. Ghazali[3]

[*] *Biomedical Sciences programme, School of Health Sciences, Universiti Sains Malaysia, Kubang Kerian, 16150, Malaysia.*

[1]*Department of Pharmacology, School of Medical Sciences, Universiti Sains Malaysia, Kubang Kerian, 16150, Malaysia.*

[2]*School of Materials And Mineral Resources, Univeristi Sains Malaysia, Nibong Tebal 14300, Malaysia*

[3]*School of Health Sciences, Universiti Sains Malaysia, Kubang Kerian, 16150, Malaysia*

Corresponding authors: Email: mostafahasaballa@gmail.com & farid@usm.my

ABSTRACT

Mineral Trioxide Aggregate (MTA) is a novel retrograde restorative material with numerous exciting clinical applications. MTA promises to be one of the most versatile materials of this century in the field of dentistry. Some of the appreciable properties of MTA include its good physical characterized properties and its ability to stimulate viable body tissue regeneration as well as good dental-pulp response. In this write-up, an electronic literature search of scientific papers from January 1993 to January 2014 was carried out on the MEDLINE and Scopus databases using specific key words. The papers that dealt with MTA and Portland Cement (PC) in a relevant way was reviewed. The potential of fabrication and introduction of MTA-based natural product and its possible availability, composition, manipulation properties will be discussed and reviewed**.**

Keywords: Osteogenesis; MTA (Mineral Trioxide Aggrgate); propolis; mineralization; PC (Portland Cement).

INTRODUCTION

The quests for newer tangible, novel nanomaterials are never ending dynamic episodes in present day research especially in transforming practice in the field of dental science. Various materials have been formulated, tested and standardized to obtain maximum benefits for good clinical performance. One such new material is Mineral Trioxide Aggregate (MTA). The introduction of Mineral Trioxide Aggregate (MTA) materials by Torabinejad in 1993, was really a landmark event in dentistry and in the field of endodontics (Roberts *et al*. 2008, Gera 2006).

In 1998, Koh *et al* studied the cytomorphology of osteoblasts and cytokine production in the presence of MTA. They reported that MTA offers a biologically active substrate for bone cells and stimulates interleukin production. MTA has also been identified to have a favorable bone reaction when implanted in the tibia and mandible of guinea pigs.

A root-end filling material, MTA, has shown antimicrobial properties with no cytotoxic effect proved, able to stimulate cytokine release from osteoprogenitor bone cells, which actively promotes hard tissue formation (Fig. 1) (Holan, G., E. Eidelman, and A.B. Fuks, 2005).

Research in MTA optimized with natural product creating or impregnation as variables are ongoing research activities. Little is known of the universal effect of propolis MTA role in osteogenesis *in-vitro.* However, there have not been any reports till date that compared the bone reaction to a propolis MTA in-culture.

Malaysia tualang honey is one of the best options available as it contains antioxidant as well as exerting anti-inflammatory effect which can act as a free radical scavenger, reducing the oxidative stress level as well as inhibiting proinflammatory cytokine. This will result in survival of osteoblasts, reduced osteoclastogenic activity, and consequently, reduce bone loss. Hence, tualang honey can be used as an alternative treatment of postmenopausal osteoporosis with minimal side effects (Mohd Effendy *et al*. 2012).

While propolis honey is a resinous substance that honey bees (*Apis mellifera* L.) collected from various plant species; a mixture of wax and other inert substances. Propolis honey as the tualang honey contains antioxidants (Ahuja, V. and A. Ahuja, 2011, Costa-Neto, 2005) that also effectively reduces osteoclastogenic activity (Regan, J.D., 2005). However surgical endodontic intervention procedures accomplished by bone removal to expose surgical site for application of material to pomote healing and bone formation is an essential intervention (Meister *et al*. 1979, Roda R.S. and B.H. Gettleman, 2006, Roda R.S., 2006). Bone remodeling and mineralization is an important observed features related to biomaterials used as sealing materials in endodontic treatment. Unfortunately**,** it seems that none of these sealing materials are able to meet the holistic requirements of an ideal seal (Roberts *et al*. 2008, Gera 2006). Little is also known if the combined usage of local honey and MTA can accommodate an ideal osteogenesis.

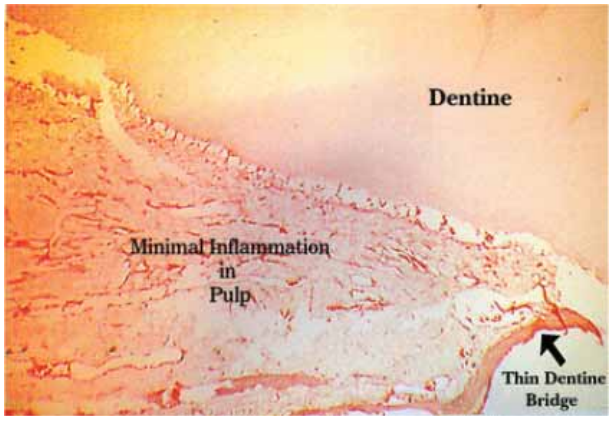

Fig. 1: Photomicrograph representation of hard tissue formation (pulp cap with MTA) observed under light microscope (adapted from Parolia *et al*. 2010).

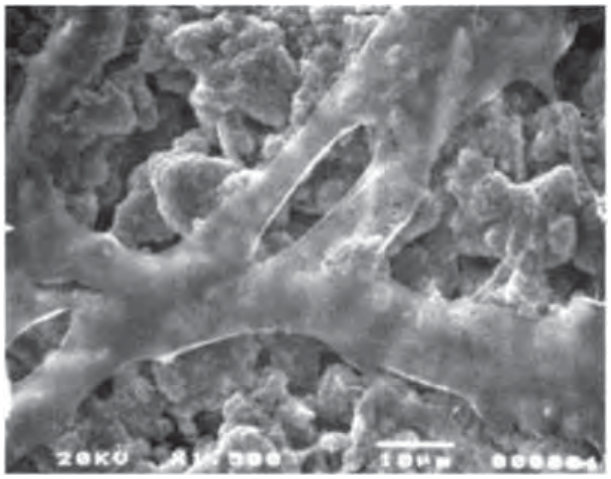

Fig. 2: Scanning electron photomicrograph of human cementum-derived cells (HCDCs) grown on white MTA (adapted from Clauder, T. and S. Shin, 2006.

Agents that reduce osteoclast numbers and activity may be useful in the treatment of traumatic injuries to the teeth. Propolis reduced the formation of actin rings in pure cultures of osteoclast-like cells (Pileggi *et al*. 2009).

Biocompatibity is the almost needed important feature of any optimised dental biomaterial. It appears that the variants of MTA are biocompatible and suitable for use in clinical trials (Mitchell *et al*.,1999), as a bioactive (Enkel *et al*. 2008), are conductive (Moretton *et al*. 2000) material in hard bone tissue formation. Biocompatibility of MTA paste containing propolis had been proven compatible to subcutaneous tissue of rats (Garcia *et al*. 2011). This compatibility feature proves further that MTA tested on dogs pulpotomy with calcium chloride as a variable was also tangible (Bortoluzzi *et al*. 2008).

In this decade, modification or fabrication by combination of the old with new materials that is more compatible and non detrimental can be used in periodontal treatment, oral surgery (dry sockets and alveolar bone defects) other than conventional materials used in endodontic and to determine the best results of using MTA in apexification, pulpotomy, pulp caping, root perforation repairs and root-end filling material (Wang, Wang, and Ni, 2009).

Statement of the problem:

MTA's long setting time; handling and difficult manipulation dilemma are the major drawbacks of the material. In order to enhance the selective properties of MTA, the addition of various liquids might adversely affect other properties of the material such as antibacterial property. *Per se*, an investigation is thus proposed by incorporating a natural product propolis honey to this clinical biomaterial to harness its properties especially also in an effort to harness the antibacterial

and antifungal properties of MTA and thus its therapeutic role and clinical capabilities. This work is proposed and performed to overcome any clinical disadvantages. Testing cytotoxicity against cell lines culture hopefully will provide evidence based insight into how inert viable tissue will respond to a new adulterated or mixed with a natural product based accelerated biomaterial.

Based on literature review and as elucidated via microscopy notes, we will discuss that the potential novel propolis MTA mixed with or without calcium chloride (which reduce setting time of MTA) to be a better biocompatible material and has the ability for osteogenesis, thus promoting the healing process.

MTA (Mineral Trioxide Aggregate)

MTA has been shown to be biocompatible, as have Portland cement and PC accelerated by

Fig. 3: Commercially available ProRoot MTA (adapted from Torabinejad *et al*. 1995).

calcium chloride ($CaCl_2$). Fifty papers from January 1993 to January 2009 conformed to the applied criteria showed that MTA and PC have the same clinical, biological, and mechanical properties (Steffen and Van Waes, 2009). Several studies have demonstrated that MTA and construction-grade PC are very similar in chemical and physical characteristics. This fact leads one to believe that adding a construction grade PC accelerator to induce faster setting of MTA would be feasible. One study showed that the initial setting time for MTA was reduced significantly by using another PC accelerator (Calcium formate [CF]) at 5% by weight. Yet another construction-grade set accelerator frequently used with PC is calcium nitrite mixed with calcium nitrate (CN/N). Although the cytotoxicity of CF and CN/N when combined with MTA has not yet been investigated,the ability of these chemicals to accelerate MTA setting time could be of interest.

Mineral trioxide aggregate materials are a mixture of a refined Portland Cement (PC) and bismuth oxide (to be radio-opaque), and are reported to contain trace amounts of SiO_2, CaO, MgO, K_2SO_4, and Na_2SO_4. The main component, Portland cement, is a mixture of di-calcium silicate, tri-calcium silicate, tri-calcium aluminate, gypsum, and tetra-calcium alumino-ferrate. The first MTA material was described as a fine hydrophilic powder with added bismuth oxide to provide radio-opacity greater than dentin (Roberts *et al*. 2008). MTA products have an initial pH of 10.2, which rises to 12.5 three hours after mixing. MTA compressive strength has been reported to increase in the presence of moisture for up to 21 days.

MTA has the potential to undergo solidification similar to other mineral cements, The effect of mixing MTA powder with different liquids and additives has shown that the choice of preparation liquid can have an effect on setting time and compressive strength. It seems to reason that the setting reaction of MTA products, like its Portland cement parent compound, is a hydration reaction; sufficient water in potential preparation liquids must be present for the reaction. However, in many cases, dentists must allow time for the material to set, which has been reported to be

anywhere between 75 minutes to 4 hours, and even up to 72 hours, before proceeding to the next step in the procedure. The slow s*et al*so results in challenging handling characteristics. Irrigation of an area containing newly placed MTA can lead to washout of the material. Although incredibly useful, MTA could be even more so if it could set faster in certain situations. When appropriate, a dentist could complete a case without another appointment to check the set and finalize the restoration. Moreover, *in vitro* studies revealed its good sealing ability because of its biological properties and the fact that it provides favorable conditions for repair. MTA has been the material of choice in the treatment of perforations and as a retrograde filling material.

There was two categories of MTA commercially available, white MTA (WMTA) or ProRoot MTA (Fig. 3) and Grey MTA (GMTA). Scanning electron microscopy (SEM) and electron probe microanalysis was used to characterize the differences between GMTA and WMTA and was found that the main difference between GMTA and WMTA is within the concentrations of Al_2O_3, MgO, and FeO. WMTA was found to have 54.9% less Al_2O_3, 56.5% less MgO, and 90.8% less FeO, which leads to the conclusion that the FeO reduction is most likely the cause for the color change. WMTA was also reported to possess an overall smaller particle size than GMTA while it was also suggested the reduction in magnesium could also contribute to the lighter color of WMTA (Roberts *et al*. 2008). At present, the commercially available MTA are ProRoot MTA (Dentsply), White ProRoot MTA (Dentsply), MTA-Angelus (Solucoes Odontontlogicas), MTA-Angelus Blanco (Solucoes Odontologicas), MTA Bio (Solucoes Odontologicas).

MTA has multiple uses in dentistry. MTA can be considered a very effective option for dental root apexification with the advantage of reduced treatment time, good sealing ability (Witherspoon, D. and K. Ham, 2001), and high biocompatibility (Fig. 2) (Pinar Erdem, A. and E. Sepet, 2008). MTA thus shows promise as a valuable material for use in one-visit apexification treatment, primarily for treating immature teeth with necrotic pulps (Giuliani *et al*. 2002). MTA is used also in pulpotomy as a pulp caping material (Torabinejad and Chivian, 1999, Abedi and Ingle, 1995), repair of root perforation (Lee *et al*. 1993) apically, laterally and furcation area (surgically and non- surgically) (Fig. 4). MTA can be used as an alternative to existing materials in the proplylactic treatment of dens evaginatus and as root-end filling materials (Koh *et al*. 2001). Some researchers have also reported that the use of MTA as‘ apical plug’ seems to be an appropriate application in the treatment of horizontal root fractures (Kusgoz *et al*. 2009, Moule and Moule, 2007).

Delayed setting times may limit the use of mineral trioxide aggregate (MTA) in endodontic procedures (Kogan *et al*. 2006). The addition of $CaCl_2$ provided a significant reduction (50%) in the initial setting time of cements. The addition of $CaCl_2$ increased the pH of WMTA in the immediate period and at 24 and 72hr. NaOCl gel, K-Y Jelly and 5% $CaCl_2$ decreased the setting time to 20 to 25 min; compressive strengths of these set materials were significantly lower than MTA mixed with water ($p<0.05$) (Kogan *et al*. 2006).

DISCUSSION

The growth of biotechnological intervention, revolving around user-friendly product based on evolution and continuous introduction of new endodontic material for different therapeutical applications make the evaluations of the biological properties of these new nano-based particles or biomaterials products essentially a mandatory condition. As such, these materials must and do not have any deleterious effect when in contact with vital tissues before they can be commercially marketed and actually utilized routinely in the clinical scenario.

Torabinejad *et al.* (1995) showed a more significant and less organized tissue response in pulps capped with calcium hydroxide compared with pulps capped with MTA. Therefore, the data from the morphology and localisation of the hard tissue barriers formed in the proposed study suggest that there should be an establishment of information and documentation preferable photomicrograph images of a physical “well-defined” pH and the bone cells in-culture response pattern. Hence the initial information is needed. pH of MTA and propolis MTA must be noted.

The earliest expected morphological feature of this study or expected process involved may likely be: cell shrinkage and this is followed by the loss of intercellular connections, cell detachment to substrate, and finally the cell fragments. The previous scoring method was based on the extent of cell cover over the surface of the material. However, the extent of cell coverage may not be an ideal marker of cell-material interaction because the quantity of cell growth and its

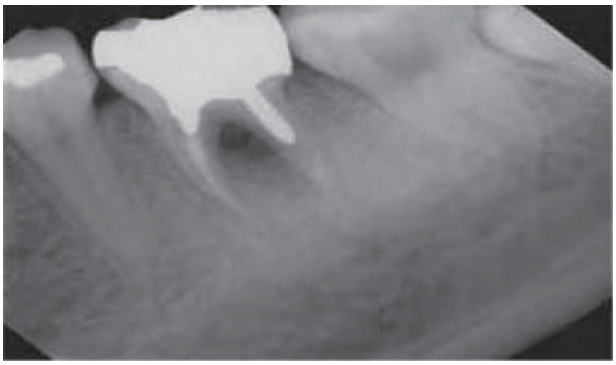

Fig.4 (a): Radiological micrograph revealing furcation defect (FD) post lateral perforation.

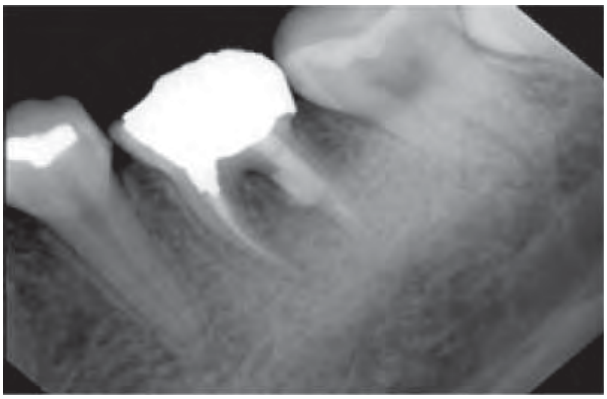

Fig.4 (b): Radiological micrograph revealing excellent healing after 6 months post MTA application.

spread is ultimately dependent on time.

Among the scientific elucidated properties of Mineral Trioxide Aggregate are as such:

1.1.Compressive Strength

It takes an average of three to four hours for the MTA to completely solidify. It has been shown that once it is set, it has a compressive strength equal to IRM and Super EBA but less than amalgam. Compressive strength of MTA within 24 hours of mixing was about 40.0 MPa and increases to 67.3 MPa after 21 days (Torabinejad *et al*. 1995). In comparison, grey MTA exhibited greater compressive strength than white MTA. Several factors might influence MTA's compressive strength, including the type of MTA, the liquid that is mixed with the material (Holt *et al*. 2007), the pH value of the mixing liquid, and the condition of MTA storage.

1.2. Radio-opacity

MTA is less radio opaque than IRM. Super EBA, Amalgam or gutta-percha and has similar radiodensity as Zinc Oxide Eugenol (Ding *et al*. 2008). The mean radio opacity of MTA is 17.7 mm of equivalent thickness of aluminium, which is sufficient to make it easy to visualize radiographically (Torabinejad *et al*. 1995).

1.3. Solubility

Although the set MTA shows no signs of solubility, the solubility might increase if more water is used during mixing. The set MTA when exposed to water releases calcium hydroxide which might be reponsible for its cementogenesis inducing property (Budig, C.G. and P.D. Eleazer, 2008). An acidic environment does not interfere with the setting of the MTA (Roy *et al*. 2001).

1.4. Antibacterial and Antifungal Properties of MTA

The antibacterial and antifungal properties of MTA have been extensively evaluated, with conflicting reports (Holt *et al*. 2007, Stowe *et al*. 2004, Estrela *et al*. 2000 Torabinejad *et al*. 1995, Al-Nazhan and Al-Judai, 2003, Miyagak *et al*. 2006, Al-Hezaimi *et al*. 2005, Al-Hezaimi *et al*.

2006, Mohammadi *et al*. 2006, Eldeniz *et al*. 2006, Yasuda *et al*. 2008, Tanomaru-Filho *et al*. 2007, Asgary and Kamrani 2008, Zhang *et al*. 2009). Several investigations reported that MTA has limited antimicrobial effect against some microorganisms (Estrela *et al*. 2000, Torabinejad *et al*. 1995, Miyagak *et al*. 2006, Yasuda *et al*. 2008). An investigation (Torabinejad *et al*. 1995) on facultative and strict anaerobic bacteria showed that MTA has an antibacterial effect on some facultative bacteria and no effect on any species of strict anaerobes.

1.5. Biocompatibility

Any material that is identified to be used in humans or animals should be biocompatible without having toxic or injurious effects on biologic tissues and their functions. Kettering and Torabinejad studied MTA in detail and found that it is not mutageneic and is much less cytotoxic compared to Super EBA and IRM (Kettering and Torabinejad, 1995). This supports the superiority of MTA over formocresol as a pulpotomy medicament. Genotoxicity tests of cells after treatment of peripheral lymphocytes with MTA showed no DNA damage (Braz *et al*. 2006). On direct contact they produce minimal or no inflammatory reaction in soft tissue regeneration (Sumer *et al*. 2006). In animal studies, MTA produced cementum growth which was very unique compared to other root-end filling materials (Torabinejad *et al*. 1995). Arens and Torabinijad reported osseous repair of furcation perforations treated with MTA. MTA showed good interaction with bone-forming cells: cells remained viable and released collagen even after 72 hours with good adherence (Pelliccioni *et al*. 2004). Investigations by Kot *et al. 1998* revealed that MTA offers a biologically active substrate for bone cells and stimulates interleukin production. MTA is also said to stimulate cytokine production in human osteoblasts.

1.6. Tissue regeneration

MTA is capable of activation of cementoblasts and production of cementum (Torabinejad *et al*. 1995). It consistently allows for overgrowth of cementum and also facilitates regeneration of the periodontal ligament. MTA allows bone healing and eliminates clinical symptoms in many cases (Schwartz *et al*. 1999).

1.7. Mineralization

MTA, just like calcium hydroxide,induces dentin bridge formation. Many investigators believe that the hard tissue bridge deposited next to MTA is because of sealing property, biocompatibility, alkalinity and other properties associated with this material. Holan *et al (2005).* found calcite crystals nearest to the opening of the dentinal tubules close to MTA. They theorized that the tricalcium oxide in MTA reacts with tissue fluids to form calcium hydroxide, resulting in hard-tissue formation in a manner similar to that of calcium hydroxide.

The role of microscopy in characterization and research pertaining to MTA.

Scanning electron microscopy (SEM) have been used to assess the topographical morphology, localization and extension of the reparative hard tissue barriers (fig. 6). *Per se* literature seems to suggest that Scanning Electron Microscopy (SEM) studies of MTA-dental pulp interface are still considered a very rare episode (Stefanescu *et al*.,). The attachment, spreading of the cells on a material surface and morphology of human periodontal ligament fibroblasts to mineral trioxide aggregate (MTA) have been evaluated using a scanning electron microscope (Balto, 2004). However nowadays, Transmission Electron Microscope (TEM), which has long been used as an “eye” capable of ultimate zooming onto a nano object of interest down to the atomic resolution, has become a powerful “arm” capable of manipulating and engineering an object, composite or aggregate while using all the pre-existing spatial and energy resolution tools, such as high-resolution imaging, electron diffraction energy disperative x-ray and electron energy loss spectroscopy analyses. Many intriguing properties of nanomaterials have been uncovered

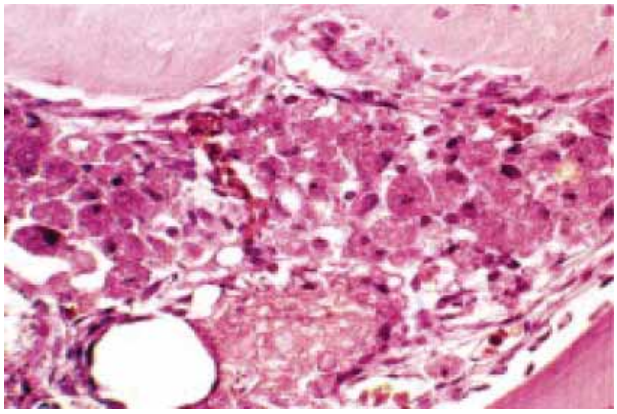

Fig. 5: Photomicrograph of ProRoot implant at the 12-week observation period. A significant accumulation of macrophages is seen in tissue between the healing bone and the implant material. The macrophages are filled with particles (hematoxylin-eosin, original magnification ×250) (Saidon *et al*. 2003).

using these novel *in situ* techniques. The directions of all works conducted worldwide may be generally categorized into four main streams (i) analysis of mechanical, electrical, thermal and electromechanical properties of various nanoparticles or aggregates; (ii) property explorations of booming structures; (iii) inert property investigations and (iv) reconstruction.

The potential role of natural prducts incorporated MTA in matters pertaining to tissue mineralization (osteogenesis, osteointergration, cementogenesis etc).

The tangible morphological restoration of bony osseous and oro-dental defects requires a biocompatible nano-biomaterial capable of inerty integrating with regional tissues and it's supporting biological entities. The biomaterials that are identified mainly microscopically orchestered and in close association with bone mineralization or osteointegration must act as 'osteoconductive' biomaterials capable of promoting sustainable bone turnover and is also insoluble in tissue fluids. As such, over the years a new class of dental restorative biomaterial called mineral trioxide aggregate (MTA) was introduced into the field of dental science and ortho biomaterials research.

In tandem with this, natural product incorporation into medicinal biotechnological polymeric micro-particle systems, micro carriers, smart drugs, etc is purposed to increases the bioavailability of these compounds, cosequently improving their therapeutic properties. While bone metabolism involves a complex balance between the deposition of the matrix and mineralization and resorption. There is now good evidence that dietry components and herbal products can influence these processes, particularly by inhibiting bone resorption, thus having beneficial effects on the skeleton. For example, it has been reported that a number of common vegetables, including onion, garlic and parsley, can inhbit boneresorption in ovariectomized rats. Essential oils derived from sage, rosemary, thyme and other herbs inhibit osteoclasts activity *in vitro* and *in vitro* and leading to an increase in bone mineral density. Soya, a rich source of isoflavones, has shown promising results and epidemiological evidence to support its use in maintaing bone health, and various traditional herbal formulae in Chinese and Ayurevedic medicine have been shown to have effects in pharmacological models of osteoporosis. There seems to be a lacuna in studies pertaining to the effects of pairing natural or synthetic drugs with MTA. These potential combinations may present numerous advantages, such as optimization or prolonging sustainable residence in the tissue, decreasing metabolic degradation by hydrolytic enzymes, and reducing or eliminating the immunogenecity of proteins. It is likely that the development of drugs that incorporate natural materials will be able to reduce side effects, decrease costs, and maximize the benefits of natural product formulations to avoid the afore-mentioned problems.

Osteogenesis induced by biomaterial can detect the mineralization of matrix involving non-collagenous proteins, such as osteonectin and nodule formation that stimulate cytokine release from bone cells and reduce the formation of actin rings in pure cultures of osteoclast-like cells

(Ahmad *et al*.,1999). Alkaline phosphatase enzyme assay, Alizarin Red-S stain and Polymerase chain reaction can be helpful in determination of osteogenesis of the novel material (Min *et al*. 2009). It is purposed and hypothesized that if this process can be observed in MTA and propolis option, an optimized novel MTA with propolis can be of a commercial viable entity.

The biocompatibility of MTA has been investigated in a number of ways, using cell expression and growrh subcutaneous and intra-osseous implantation and direct contact with dental tissues *in vivo*. In cytological investigation with pertinent to MTA biocompatibility, it was documented that, Osteocalcin levels were increased in the presence of MTA (Botushanov *et al*. 2001), induced alkaline phosphatase expression. In subcutaneous and intra-osseous implantation studies, there is histological osseous implantation of the materials in test animals. Subcutaneous implantation in rats showed that MTA (ProROOT) initially elicited severe reactions with coagulation necrosis and dystrophic calcification (Moretton *et al*. 2000, Yaltirik *et al*. 2004). These initial reactions, however were observed to subside with time.

Literaure have also been documented and revealed that MTA offers a biologically active substrate for bone cells and also permits cementoblasts attachment, growth, and the production of mineralized matrix gene and osteocalcin expressions (Koh *et al*. 1998, Thomson *et al*. 2003).

Propolis:

Propolis is a resinous mixture. It is dark brown in color, but it can be found in green, red, black and white hues, depending on the sources of resin found in the particular hive area. Propolis is also identified as an antimicrobial apex (Andrade Ferreira *et al*. 2007), an emollient (Hounuter *et al*. 2004), an immunomodulator (Ocakci *et al*. 2006), a dental antiplaque agent (Botushanov *et al*. 2001, Koo *et al*. 2002, Duarte *et al*. 2006), an antitumor growth agent (Sugimoto *et al*. 2003) and a radioprotector. Propolis is effective in reducing and delaying radiation-induced mucositis in an animal model (Mirzoeva and Calder,1996). Propolis is an antioxidant and using diet rich in propolis extract could be a beneficial way to overcome the reproductive toxicity of chlorpyrifos (Tan-No *et al*. 2006). Propolis bee preparations revealed good antibacterial (particularly against Gram-positive bacteria), antifungal (against those responsible for superficial and dermatomycoses) and antiinflammatory (against acute and chronic models of inflammation) effects but no antiamoebic or antipyretic potentials (Dobrowolski *et al*. 1991). In dentistry, propolis used as pulp caping material as the response of pulps to propolis as a pulp caping agent was comparable to MTA and dycal (Parolia *et al*. 2010) (Fig. 6).

Propolis honey contains a balsam-like substances and there were a few well-documented cases of systemic contact dermatitis with propolis (Veien, 2011). The ethanol extract of propolis suppressed prostaglandin and leukotreine generation by murine peritoneal macrophage *in-vitro*

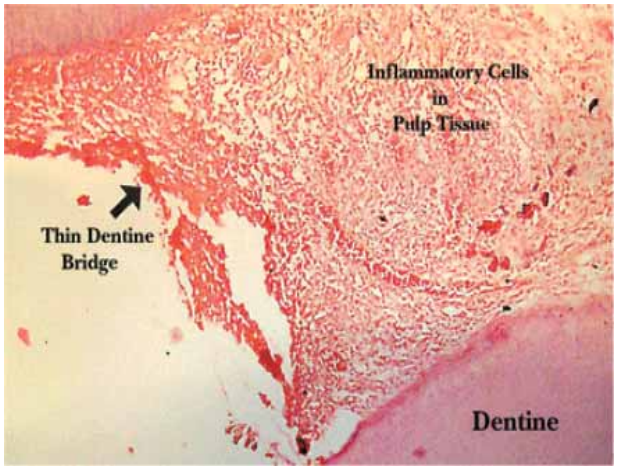

Fig. 6: Light photomicrograph of pulp cap built-up with propolis honey (Adapted from Parolia, A. (Parolia *et al*. 2010).

and during zymosan-induced acute peritoneal macrophages *in- vivo*. Dietary propolis significantly suppressed the lipoxagyenase pathway of arachidonic acid metabolism during inflammation *in-vivo*. Caffeic acid phenethyl ester was the most potent modulator of the arachidonic acid cascade among the propolis components (Mirzoeva and Calder, 1996) and the anti-inflammatory effect of propolis through inhibition of nitric oxide production have also been reported (Tan-No *et al*. 2006).

As such the systemic use of propolis may hasten new bone formation at the expanded suture in rats (Yoshimine *et al*. 1996). In tandem to this artificially induced bone tissue losses after the application of ethanol extract of propolis (EEP) have also been reported to show an accelerated rate of ossification (Knabe *et al*. 2000).

CONCLUSION

In conclusion, the existing literature gives a solid base for clinical studies with propolis MTA to replace conventional MTA as an endodontic material. The potential of an innovative, optimised usage of propolis MTA in chemical root canal sclerosis is a scientific approach of tangible characteristic elucidation.

REFERENCES

Abedi, H. and J. Ingle, Mineral trioxide aggregate: a review of a new cement. Journal of the California Dental Association, 1995. 23(12): p. 36.

Ahmad, M., M. McCarthy, and G. Gronowicz, An in vitro model for mineralization of human osteoblast-like cells on implant materials. Biomaterials, 1999. 20(3): p. 211-220.

Ahuja, V. and A. Ahuja, Apitherapy-A sweet approach to dental diseases. Part II: Propolis. Journal of Academy of Advanced Dental Research, 2011. 2(2).

Al-Hezaimi, K. *et al*. Effect of White-Colored Mineral Trioxide Aggregate in Different Concentrations on Candida albicans. In Vitro. Journal of Endodontics, 2005. 31(9): p. 684-686.

Al-Hezaimi, K. *et al*. Antibacterial Effect of Two Mineral Trioxide Aggregate (MTA) Preparations Against Enterococcus faecalis and Streptococcus sanguis. In Vitro. Journal of Endodontics, 2006. 32(11): p. 1053-1056.

Al-Hezaimi, K. *et al*. Comparison of Antifungal Activity of White-Colored and Gray-Colored Mineral Trioxide Aggregate (MTA) at Similar Concentrations Against Candida albicans. Journal of Endodontics, 2006. 32(4): p. 365-367.

Al-Nazhan, S. and A. Al-Judai, Evaluation of antifungal activity of mineral trioxide aggregate. Journal of Endodontics, 2003. 29(12): p. 826-827.

Andrade Ferreira, F.B. *et al*. Antimicrobial effect of propolis and other substances against selected endodontic pathogens. Oral Surgery, Oral Medicine, Oral Pathology, Oral Radiology and Endodontology, 2007. 104(5): p. 709-716.

Asgary, S. and F.A. Kamrani, Antibacterial effects of five different root canal sealing materials. Journal of oral science, 2008. 50(4).

Baek, S.-H., H. Plenk Jr, and S. Kim, Periapical tissue responses and cementum regeneration with amalgam, SuperEBA, and MTA as root-end filling materials. Journal of Endodontics, 2005. 31(6): p. 444-449.

Balto, H.A., Attachment and morphological behavior of human periodontal ligament fibroblasts to mineral trioxide aggregate: a scanning electron microscope study. Journal of Endodontics, 2004. 30(1): p. 25-29.

Bortoluzzi, E.A. *et al*. Mineral trioxide aggregate with or without calcium chloride in pulpotomy. Journal of Endodontics, 2008. 34(2): p. 172-175.

Botushanov, P., G. Grigorov, and G. Aleksandrov, A clinical study of a silicate toothpaste with extract from propolis. Folia medica, 2001. 43(1-2): p. 28.

Braz, M. *et al*. Evaluation of genetic damage in human peripheral lymphocytes exposed to mineral trioxide aggregate and Portland cements. Journal of Oral Rehabilitation, 2006. 33(3): p. 234-239.

Budig, C.G. and P.D. Eleazer, In Vitro Comparison of the Setting of Dry ProRoot MTA by Moisture Absorbed through the Root. Journal of Endodontics, 2008. 34(6): p. 712-714.

Clauder, T. and S. Shin, Repair of perforations with MTA: clinical applications and mechanisms of action. Endodontic Topics, 2006. 15(1): p. 32-55.

Costa-Neto, E.M., Entomotherapy, or the medicinal use of insects. Journal of Ethnobiology, 2005. 25(1): p. 93-114.

de Andrade Ferreira, F.B. *et al*. Antimicrobial effect of propolis and other substances against selected endodontic pathogens. Oral Surgery, Oral Medicine, Oral Pathology, Oral Radiology, and Endodontology, 2007. 104(5): p. 709-716.

Ding, S.J. *et al*. The Physical and Cytological Properties of White MTA Mixed with Na sub 2 sub HPO sub 4sub as an Accelerant. Journal of Endodontics, 2008. 34(6): p. 748-751.

Dobrowolski, J.W. *et al*. Antibacterial, antifungal, antiamoebic, antiinflammatory and antipyretic studies on propolis bee products. Journal of ethnopharmacology, 1991. 35(1): p. 77-82.

Duarte, S. *et al*. The influence of a novel propolis on mutans streptococci biofilms and caries development in rats. Archives of oral biology, 2006. 51(1): p. 15-22.

Eldeniz, A.U. *et al*. Antibacterial effect of selected root-end filling materials. Journal of Endodontics, 2006. 32(4): p. 345-349.

Enkel, B.n.d. *et al*. Bioactive materials in endodontics. 2008.

Estrela, C. *et al*. Antimicrobial and chemical study of MTA, Portland cement, calcium hydroxide paste, Sealapex and Dycal. Brazilian Dental Journal, 2000. 11(1): p. 3-9.

Garcia, L. *et al*. Biocompatibility assessment of pastes containing Copaiba oilresin, propolis, and calcium hydroxide in the subcutaneous tissue of rats. Journal of Conservative Dentistry, 2011. 14(2): p. 108.

Gera, D., A Comparative Analysis Of Microleakage Of Three Root End Filling Materials“An In vitro Stereomicroscopic Study. 2006.

Giuliani, V. *et al*. The use of MTA in teeth with necrotic pulps and open apices1. Dental Traumatology, 2002. 18(4): p. 217-221.

Gomes-Filho, J.o.E. *et al*. A mineral trioxide aggregate sealer stimulated mineralization. Journal of Endodontics, 2009. 35(2): p. 256-260.

Holan, G., E. Eidelman, and A.B. Fuks, Long-term evaluation of pulpotomy in primary molars using mineral trioxide aggregate or formocresol. Pediatric Dentistry, 2005. 27(2): p. 129-36.

Holt, D.M. *et al*. The Anti-microbial Effect Against Enterococcus faecalis and the Compressive Strength of Two Types of Mineral Trioxide Aggregate Mixed With Sterile Water or 2% Chlorhexidine Liquid. Journal of Endodontics, 2007. 33(7): p. 844-847.

Hounuter, M.b. *et al*. The effect of CAPE on lipid peroxidation and nitric oxide levels in the plasma of rats following thermal injury. Burns, 2004. 30(2): p. 121-125.

Kettering, J.D. and M. Torabinejad, Investigation of mutagenicity of mineral trioxide aggregate and other commonly used root-end filling materials. Journal of Endodontics, 1995. 21(11): p. 537-539.

Knabe, C. *et al*. Evaluation of calcium phosphates and experimental calcium phosphate bone cements using osteogenic cultures. Journal of Biomedical Materials Research, 2000. 52(3): p. 498-508.

Kogan, P. *et al*. The effects of various additives on setting properties of MTA. Journal of Endodontics, 2006. 32(6): p. 569-72.

Koh, E. *et al*. Prophylactic treatment of dens evaginatus using mineral trioxide aggregate. Journal of Endodontics, 2001. 27(8): p. 540-542.

Koh, E.T. *et al*. Cellular response to mineral trioxide aggregate. Journal of Endodontics, 1998.

24(8): p. 543-547.
Koo, H. *et al*. Effect of a mouth rinse containing selected propolis on 3-day dental plaque accumulation and polysaccharide formation. Caries Research, 2002. 36(6): p. 445-448.
Kusgoz, A. *et al*. Treatment of horizontal root fractures using MTA as apical plug: report of 3 cases. Oral Surg Oral Med Oral Pathol Oral Radiol Endod, 2009. 107(5): p. 68-72.
Lee, S.-J., M. Monsef, and M. Torabinejad, Sealing ability of a mineral trioxide aggregate for repair of lateral root perforations. Journal of Endodontics, 1993. 19(11): p. 541-544.
Meister, F. *et al*. Endodontic perforations which resulted in alveolar bone loss: Report of five cases. Oral Surgery, Oral Medicine, Oral Pathology, 1979. 47(5): p. 463-470.
Min, K.-S. *et al*. Effect of radiopaque Portland cement on mineralization in human dental pulp cells. Oral Surgery, Oral Medicine, Oral Pathology, Oral Radiology, and Endodontology, 2009. 108(4): p. 82-86.
Mirzoeva, O. and P. Calder, The effect of propolis and its components on eicosanoid production during the inflammatory response. Prostaglandins, Leukotrienes and Essential Fatty Acids, 1996. 55(6): p. 441-449.
Mitchell, P. *et al*. Osteoblast biocompatibility of mineral trioxide aggregate. Biomaterials, 1999. 20(2): p. 167-173.
Miyagak, D.C. *et al*. In vitro evaluation of the antimicrobial activity of endodontic sealers. Brazilian Oral Research, 2006. 20(4): p. 303-306.
Mohammadi, Z., J. Modaresi, and M. Yazdizadeh, Evaluation of the antifungal effects of mineral trioxide aggregate materials. Australian Endodontic Journal, 2006. 32(3): p. 120-122.
Mohd Effendy, N. *et al*. The Effects of Tualang Honey on Bone Metabolism of Postmenopausal Women. Evidence-Based Complementary and Alternative Medicine, 2012. 2012.
Moretton, T.R. *et al*. Tissue reactions after subcutaneous and intraosseous implantation of mineral trioxide aggregate and ethoxybenzoic acid cement. Journal of Biomedical Materials Research, 2000. 52(3): p. 528-533.
Moule, A. and C. Moule, The endodontic management of traumatized permanent anterior teeth: a review. Australian Dental Journal, 2007. 52(s1): p. S122-S137.
Ocakci, A. *et al*. Role of caffeic acid phenethyl ester, an active component of propolis, against NAOH-induced esophageal burns in rats. International Journal of Pediatric Otorhinolaryngology, 2006. 70(10): p. 1731-1739.
Parolia, A. *et al*. A comparative histological analysis of human pulp following direct pulp capping with Propolis, mineral trioxide aggregate and Dycal. Australian Dental Journal, 2010. 55(1): p. 59-64.
Pelliccioni, G. *et al*. Evaluation of osteoblast-like cell response to Proroot MTA (mineral trioxide aggregate) cement. Journal of Materials Science: Materials in Medicine, 2004. 15(2): p. 167-173.
Pileggi, R. *et al*. Propolis inhibits osteoclast maturation. Dental Traumatology, 2009. 25(6): p. 584-588.
Pinar Erdem, A. and E. Sepet, Mineral trioxide aggregate for obturation of maxillary central incisors with necrotic pulp and open apices. Dental Traumatology, 2008. 24(5): p. e38-e41.
REGAN, J.D., D.E. WITHERSPOON, and D. FOYLE, Surgical repair of root and tooth perforations. Endodontic Topics, 2005. 11(1): p. 152-178.
Roberts, H.W. *et al*. Mineral trioxide aggregate material use in endodontic treatment: a review of the literature. Dental Materials, 2008. 24(2): p. 149-164.
Roda, R.S. and B.H. Gettleman, Etiology Of Persistent Apical Periodontitis, 2006.
Roda, R.S., Clinical Showcase. 2006. 3: p. 786-821.
Roy, C.O., B.G. Jeansonne, and T.F. Gerrets, Effect of an acid environment on leakage of root-end filling materials. Journal of Endodontics, 2001. 27(1): p. 7-8.
Saidon, J. *et al*. Cell and tissue reactions to mineral trioxide aggregate and Portland cement. Oral Surgery, Oral Medicine, Oral Pathology, Oral Radiology, and Endodontology, 2003. 95(4): p.

483-489.
Schwartz, R.S. *et al*. Mineral trioxide aggregate: a new material for endodontics. Journal-American Dental Association, 1999. 130: p. 967-976.
Stefanescu, T., C. Craciun, and L. Barbu-Tudoran, SCANNING ELECTRON-MICROSCOPE STUDY UPON THE MTA-PULP INTERFACE. Analele Societatii Nationale de Biologie Celulara. 17(2).
Steffen, R. and H. Van Waes, Understanding mineral trioxide aggregate/Portlandcement: A review of literature and background factors. European Archives of Paediatric Dentistry, 2009. 10(2): p. 93-97.
Stowe, T.J. *et al*. The effects of chlorhexidine gluconate (0.12%) on the antimicrobial properties of tooth-colored ProRoot mineral trioxide aggregate. Journal of Endodontics, 2004. 30(6): p. 429-431.
Sugimoto, Y. *et al*. Inhibitory effects of propolis granular AP C on 4-(methylnitrosamino)-1-(3-pyridyl)-1-butanone-induced lung tumorigenesis in A/J mice. Cancer Letters, 2003. 193(2): p. 155-159.
Sumer, M. *et al*. Reactions of connective tissue to amalgam, intermediate restorative material, mineral trioxide aggregate, and mineral trioxide aggregate mixed with chlorhexidine. Journal of Endodontics, 2006. 32(11): p. 1094-1096.
Tan-No, K. *et al*. Anti-inflammatory effect of propolis through inhibition of nitric oxide production on carrageenin-induced mouse paw edema. Biological and Pharmaceutical Bulletin, 2006. 29(1): p. 96-99.
Tanomaru-Filho, M.r. *et al*. In vitro antimicrobial activity of endodontic sealers, MTA-based cements and Portland cement. J Oral Sci, 2007. 49(1): p. 41-5.
Thomson, T.S. *et al*. Cementoblasts maintain expression of osteocalcin in the presence of mineral trioxide aggregate. Journal of Endodontics, 2003. 29(6): p. 407-412.
Torabinejad, M. and N. Chivian, Clinical applications of mineral trioxide aggregate. Journal of Endodontics, 1999. 25(3): p. 197-205.
Torabinejad, M. *et al*. Antibacterial effects of some root end filling materials. Journal of Endodontics, 1995. 21(8): p. 403-406.
Torabinejad, M. *et al*. Investigation of mineral trioxide aggregate for root-end filling in dogs. Journal of Endodontics, 1995. 21(12): p. 603-608.
Torabinejad, M. *et al*. Physical and chemical properties of a new root-end filling material. Journal of Endodontics, 1995. 21(7): p. 349-353.
Veien, N.K., Systemic contact dermatitis. International Journal of Dermatology, 2011. 50(12): p. 1445-1456.
Wang, P., S. Wang, and L. Ni, The combination of a mineral trioxide aggregate and an adhesive restorative approach to treat a crown-root fracture coupled with lateral root perforation in a mandibular second molar: a case report. Operative Dentistry, 2009. 34(4): p. 497-502.
Witherspoon, D. and K. Ham, One-visit apexification: technique for inducing root-end barrier formation in apical closures. Practical Procedures & Aesthetic Dentistry, 2001. 13(6): p. 455.
Yaltirik, M. *et al*. Reactions of connective tissue to mineral trioxide aggregate and amalgam. Journal of Endodontics, 2004. 30(2): p. 95-99.
Yasuda, Y., A. Kamaguchi, and T. Saito, In vitro evaluation of the antimicrobial activity of a new resinbased endodontic sealer against endodontic pathogens. Journal of Oral Science, 2008. 50(3).
Yoshimine, Y. *et al*. In vitro interaction between tetracalcium phosphate-based cement and calvarial osteogenic cells. Biomaterials, 1996. 17(23): p. 2241-2245.
Zhang, H., F.G. Pappen, and M. Haapasalo, Dentin enhances the antibacterial effect of mineral trioxide aggregate and bioaggregate. Journal of Endodontics, 2009. 35(2): p. 221-224.

Limitation of Two Dimensional Imaging in the Diagnosis and Treatment of Morphoanatomical Variations of Wisdom Tooth Roots Orientation - A Case Report and Literature Review

M.M.H. Massoud[*], Farid C. Ghazali[1]
*[*1]School of Health Sciences, Universiti Sains Malaysia, Kubang Kerian, 16150, Malaysia*
Corresponding authors: Email: mostafahasaballa@gmail.com & farid@usm.my

ABSTRACT

A case of an unusual anatomical location of a left lower wisdom tooth of a 27 years old Malay gentleman is reported. The tooth was initially planned for extraction due to irreversible pulpitis and the tooth was unrestorable. On clinical inspection, the tooth crown seems to show normal anatomical features. However difficulty was encountered during extraction of which the orthopantogram then revealed presence of two mesial and distal roots. Surgical intervention was then carried out from bucco-distal approach with surgical round bur and the tooth was sectioned bucco-lingually to separate the mesial and distal root however this separation attempt was not successful. Finally the tooth was removed by luxation from the mesial aspect and notably the roots was found to be in a bucco-lingual orientation instead of that previously diagnosed as in a mesio-distal orientation.

Keywords: cone-beam computed tomography (CBCT), computed tomography (CT), malposed, luxation, hooked-shaped apices.

INTRODUCTION

The apical roots anatomical variations or orientation of the wisdom teeth can be perceived to be difficult when diagnosed using past two-dimensional radiography. Three-Dimensional (3D) imaging data that are provided by CT seem to be more useful imaging tool; however, this procedure may subject the patient to unnecessery radiation. Recently, cone-beam computed tomography (CBCT) has been made commercially available, and of potential to become a practical imaging tool in dentistry. There are however very few studies available that indicate whether CBCT provide definitive images or predict clinical accuracy for apical root discrepancy (Pinsky *et al*. 2006).

The anatomical variations of apical roots orientation of wisdom teeth are often encountered in oral surgery practice and during surgical intervention (Vertucci *et al*. 1984). Thus, in the treatment planning, it is of imperative important to accurately diagnose and locate these roots and determine their actual anatomical relationships to its adjacent teeth and other relevant viable anatomical structures within that area.

The required information was usually obtained from periapical, occlusal, or panoramic radiographs. X-Ray radiographs are important in assessing the location and possible nature of these anomalies. However, the major shortcoming of conventional radiography for the assessment of malposed or malformed teeth is the possible overlapping imaging of structures displayed on the film. This problem makes it difficult to actually distinguish very particular fine details, especially when structures differ only slightly in contrast density. CT, however, seems to be a much superior approach of imaging to other radiographic methods, especially in visualizing mineralised bone tissue (Peene *et al*. 1990).

Literature review seems to indicate that CT overcomes the limitations of conventional radiographical methods and thus, has become a useful tool for diagnosing the actual positions and help to lessen complications related to a critical antatomical root variation difficulties, malposed, malformed portions or indicated by ectopically erupting teeth position, this diagnosis method has increased frequently since 1988 (Peene *et al*. 1990, Ericson *et al*. 1988, Schmuth *et al*. 1992).

However, radiographs are basically two-dimensional representations of three-dimensional

structures and thus in certain clinical, morphological and biological features may not be definitively reflected in radiographic changes. Depending on morphological variations, surrounding bone density, x-ray angulations and radiographic contrast, these radiographic images may thus be misinterpreted. With the great technological advances of recent years, new imaging modalities have been added to dental radiology as viable diagnostic tools, among which cone beam computed tomography (CBCT) provides detailed high-resolution images of oral structures. CBCT has been used for several clinical and investigational purposes in oral surgery. The accuracy of CBCT images to identify anatomic and pathologic alterations compared to panoramic and periapical radiographs has been shown to reduce the incidence of false-negative results (Estrela *et al*. 2008).

Case Report

A healthy 27-years-old man attended a dental clinic complaining of recurrent pericoronitis and severe throbbing pain for the past three days. Panoramic radiograph (Fig. 2) revealed a deep cavity of occluso-distal position of a slightly mesio-angulated non-impacted left third mandibular tooth (Tooth number 38), slightly thickened inter-dental bone was observed between the second and third mandibular molar (38 & 37), preview no periapical radiolucency, apices of two roots away from mandibular canal, distal surface of third molar was completely out of the ascending ramus of the mandible, low level of bi-furcation and the roots seem to be presented with no modification of a fused mesial and distal root morphology.

Past medical History: Patient mentioned that he has no significant medical related problems.

Past Dental History: His regular dental check-ups, (at present recurrent pericoronitis), no history of filling or extraction.

Clinical examination revealed that occluso-distal cavity were covered by non-inflammed soft tissue features, severe pain on probing, no pain on percussion, slight pain on palpation, no swelling noted on buccal sulcus. Patient reiterated that he wants to remove the tooth. Preparation of patient for extraction had been accomplished.

Dryness of the area to be injected was swapped with gauze and local application of topical anaesthetic gel by orange stick 20%Benzocaine for 2 minutes (Strawberry 1FL OZ29.6ML CROSSTEX) (GUM NUMB NDC247942021), injection by scandonest (2% Mepivacaineine with Epinephrine 1:100,000) 2.2ml contains Mepivacaine Hydrochloride 44mg and 22ug adrenaline, slow injection done and upon checking after past 5 minutes, anaethesia was found to be profound .

Difficult luxation of the molar distally was encountered during movement by straight apexo-elevator number 2 and number 3, difficult to be luxated, trial by molar forceps resulted in jerky movement, hence difficult to be achieved .

As such, minor oral surgery (MOS) was decided , treatment plan was discussed with the patient and consent been signed. Infiltrative injection was given to achieve deep anaesthesia, incision using Bard Parker blade number 15 was initiated to create triangular flap, the triangular flap kept well away from the gingival attachment of adjacent teeth and swept down and forward from the distal aspect of the second molar to the mucobuccal fold, providing good access without the potential problems. triangular flap been reflected buccally with a Howarth's periosteal elevator, the clean white bony surface could be easily seen as the socker mops up the bleeding from a soft tissue tag. Removal of bone buccally and distally was done by surgical round bur attached to low speed hand piece and copious irrigaton with saline. Sectioning of tooth by surgical fissure bur bucco-lingually, the separation was difficult to be achieved. Separation of distal part of crown by straight elevator, luxation of the mesial part done in between second and third molar, buccal and lingual roots noted when the luxation completely achieved with hooked-shaped apices, two sockets were checked by periodontal probe, filing of irrigular inter-dental bone done, wound toilet to clear loose debris present and to avoid incidence of buccal space infection, copious irrigation

with normal saline was given, adequate haemostasis by surgicel was achieved before wound closure to minimize the risk of persistent post-operative oozing and haematoma formation to occur. Closure of the wound was done to ensure accurate apposition of wound edges by absorbable suturing material. Post-operative instructions were then given and appointment for post-operative orthopantogram was dated.

DISCUSSION

The mandibular third molar or the wisdom tooth is an unusual tooth that is characterized by considerable variability in its formation, eruption timing, morpho-variation in crown anatomy and its root morphology, orientation and, not infrequently, by agenesis (Garn *et al*. 1962, Goaz *et al*. 1994). As such, the history of wisdom teeth and orientation of its apical roots dilemma and associated problems is probably as old as the history of mankind. Discrepancies have been reported with regard to the findings of the X-ray and what could be observed clinically regarding the number and morphology of roots (Archer WH., 1975). Thus, it is crucial to evaluate to what extent the observed radiographic anatomy truly corresponds to the vaiable anatomy of the said tooth. In a comparison study between orthopantogram (OPG) and tooth *in situ* finding to evaluate the sensitivity of OPG towards the number and morphology of wisdom roots, false negative findings were frequently noted (Westesson *et al*. 1980). It was then suggested that apical root dilacerations may have not been accurately radiographed due to the path of the X-ray beam. In tandem to this, Wenzel *et al*. (1998) stated that the root bent inward rather than outward, and resulted in a difference in the radiographic and tooth *in vitro* appearannce for root dilacerations.

Whenever apical root discrepancies or lesion is observed on a radiograph, this must first be carefully described in general terms before a pathognomic differential diagnosis ia attempted. As such question pertaining to whether the root or lesion is observed is radiolucent, radioopaque, or mixed (comination of radiolucency and radiopacity)?. Where is the extent of the root or lesion well defined and located? To what extent is the apices of which neighbouring teeth are involved? What is the size of the lesion? Is the margin of the lesion ill-defined, well defined with a radiopaque border?Is the appearance of the bone surrunding the lesion: normal, porous, or sclerotic?

The various radiographic appearance of the margins of lesions and the changes in the surrounding bone have been given clinical interpretation by some diagnosticians based largely on intuitive analysis rather than on research data. Although the significance of these signs is sometimes questionable, they are useful in radiographic interpretation. An ill-defined (diffuse, irregular) periphery is suggestive of a lesion enlarging by invading the surrounding bone. A well-defined (circumscibed) periphery is suggestive of a self-contained lesion enlarging by expansion. A well-defined periphery with a hyperostatic (sclerotic) radiopaque periphery is suggestive of an extremely slow-growing self-contained lesion enlarging by expansion.

Cone beam computed tomography (CBCT), are modern low-dose three-dimensional radiographic imaging technique. CBCT results in images with a higher isotropic sub-millimeter spatial resolution than in commercially available CT scanners at a lower radiation dose (Ludlow *et al*. 2006). The first principle to adhere to when considering any radiologic investigation is that the benefit of investigation should outweigh the risk associated with investigation is made, the next rule to adhere to is the ALARA principle. ALARA stands for as low as reasonably achievable meaning that one should use the radiographic technique available that with the lowest radiation dose adequently supplies the information needed. The comparison between cone-beem CT and medical CT is another important concern. Hashimoto *et al.* reported that cone-beam CT was significantly superior to multi-detector CT in visualizing teeth and their surrounding structures (Hashimoto *et al*. 2003). Holberg *et al*. reported the opposite rersults in their clinical study (Holberg *et al*. 2005). Although direct comparison of these two modalities could determine which is superior in predicting neurovascular bundle exposure at extraction, such a clinical study should not be performed because patients would receive a signifiant radiation exposure. Interventive diagnostic

applications such as in dental implantology,endodontics, and minor oral surgical procedures have been reported (Terakado *et al*. 2000, Loftag-Hansen *et al*. 2007). However, *per se*, the modality is still relatively new and still requires further systematic and special clinical assessment to harness and confirm its tangible clinical usefulness and safe purpose.

The definition of apical root dilaceration of wisdom tooth varies in the literature (Jafarzadeh *et al*. 2007). Nevertheless, many authors define root dilaceration as a deviation or bending of 90-degree angle or greater along the axis of the tooth or root (Hamasha *et al*. 2002, Malcic *et al*. 2006, Udoye *et al*. 2009, Miloglu *et al*.). Few studies have examined this anatomical variation in the third molar teeth among different population groups, as shown in Table 1, and the prevalence has been found to be relatively higher in mandibular third molars, ranging from 3.3 to 30.92%, compared to maxillary molars that ranges from 1.33 to 8.46% (Table 1). Mechanical trauma is the most commonly accepted cause for root dilacerations. However, the increased prevalence of root dilacerations in molar teeth, which are less prone to mechanical trauma, brought other related aetiological factors into consideration. These factors include idiopathic, developmental, disturbances, hereditary factors and the effect of related anatomical structures, such as the cortical bone of maxillary sinus and the mandibular canal (Jafarzadeh *et al*. 2007).

Root dilacerations in third molars can occur anywhere along the length of the root from the coronal third to the root apex, and may include a single or all roots (Jafarzadeh *et al*. 2007, Malcic

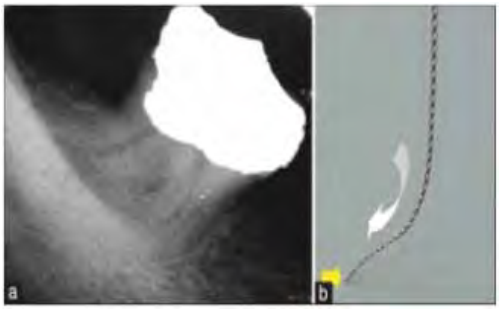

Fig. 1. (a) Mandibular third molar with dilacerated mesial and distal roots. (b) A K-file size 10 shows an apparent disto-lingual curvature of the mesio-lingual root canal. This may indicate a disto-lingual dilaceration of the mesial root.

et al. 2006, Kannan *et al*. 2002). They are usually located in a distal direction. However, buccal dilacerations have also been reported in maxillary and mandibular third molars (Malcic *et al*. 2006, Kannan *et al*. 2002). Root dilacerations may also occur in more than just one plane such as in a disto-lingual direction (Gupta 2008). Recognizing the direction of the file while determining the working length of the encased root canal, might be helpful in identifying such complex radicular morphology (Fig. 1).

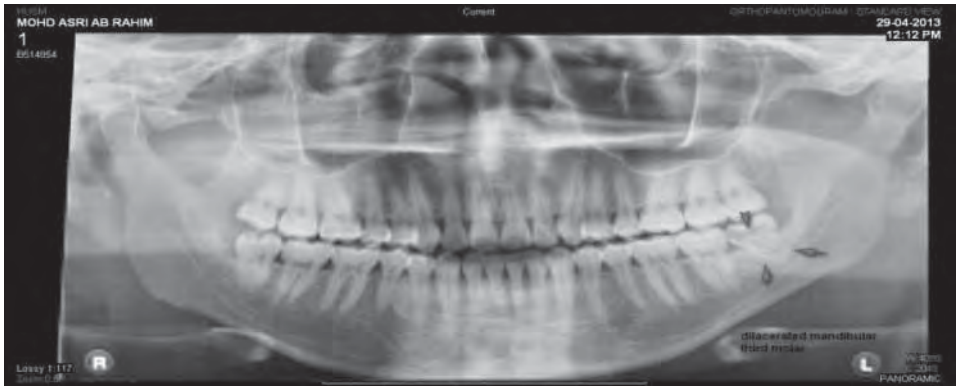

Fig. 2. Pre-operative orthopantogramic x-ray shows occlusal caries of 38, slightly mesio-angulated, low furcation and two roots seems to be mesial and distal.

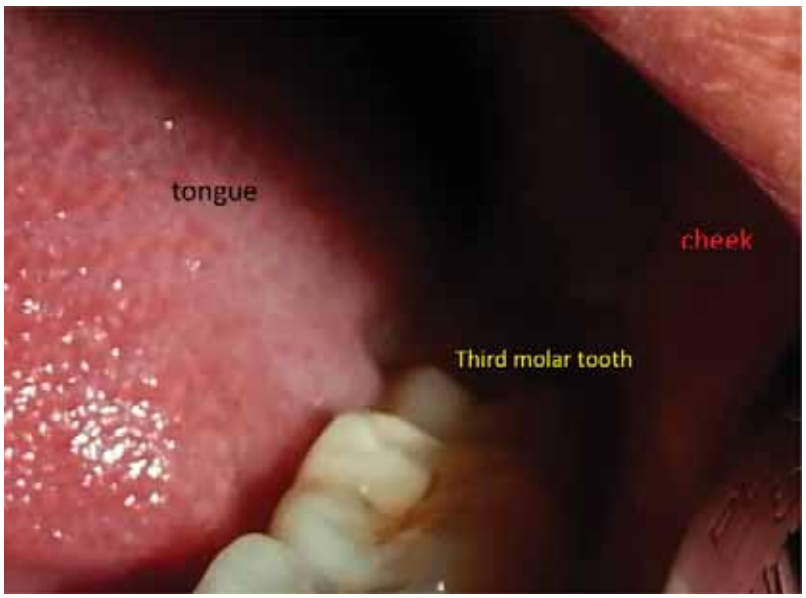

Fig. 3 (Digital photography): Intra-oral pre-operative photograph of the wisdom tooth.

Fig. 4. Shows sectioned crown and hooked-shaped apices of buccal and lingual roots.

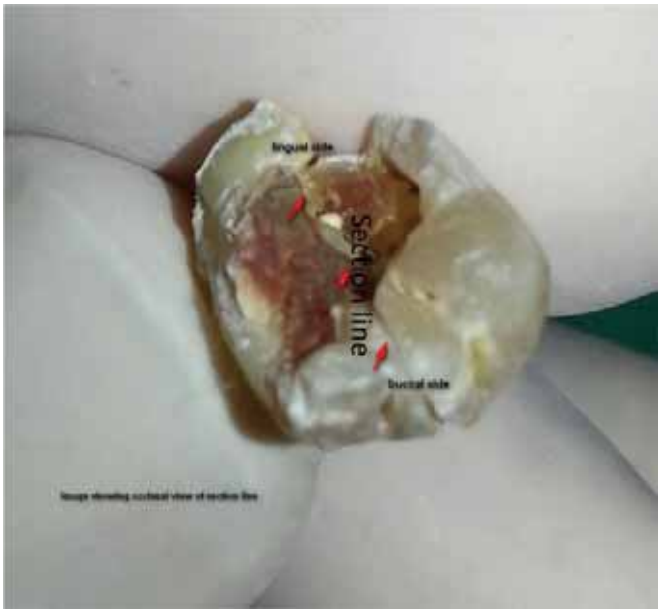

Fig. 5. Digital photography shows the assembled crown and occlual view of the section line (bucco-lingually).

Fig. 6. Buccal view shows section line and root apex.

Fig. 7. Mesial view shows buccal and lingual root, apices, wide and long bi-furcation area.

Fig. 8. 15 days post operative wound healing of socket and soft tissues.

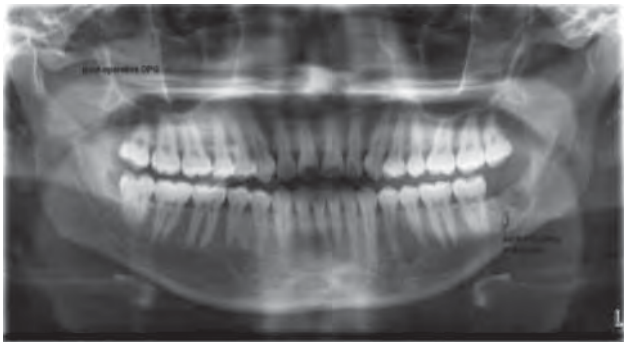

Fig. 9. Post-operative OPG shows healed socket and bone regeneration (in progress).

Regional odontodysplasia: It is a developmental abnormality of adult human dentition, usually localized to a certain anatomical quadrant and is non-hereditary. The enamel, dentin and pulp of teeth are affected and on radiographs, the teeth are described as “ghost teeth” (Tervonen *et al*. 2004).

To date, the etiology remains uncertain; although numerous factors have been suggested and considered such as local trauma, irradiation, hypophosphatasia, hypocalcemia and hyperpyrexia (Crawford and Aldred 1989). It is most commonly presented in the maxillary anterior teeth, both the permanent and primary dentition (Panat *et al*.).

In tandem with good practice, most dentists will advocate extracting the affected teeth as soon as possible and inserting a prosthetic replacement.

CONCLUSION

The introduction of Cone Beam Computed Tomography (CBCT) specifically designed for imaging the maxillofacial region is a true shift from a 2D to 3D imaging. As the CBCT requires only a single scan to capture the entire object with a cone of X-rays, effective radiation dose is significantly reduced and localized when compared when using conventional computed Tomography (CT). Periapical disease can be detected earlier with CBCT as compared with conventional radiography. Besides this, CBCT can eliminate anatomical noise, detect the true nature of resorptive lesions, assess root canal anatomy and root fractures (Dayal and Sajjan, 2012).

Anatomical variations, malposed, malformed, supernumerary and ectopically impacted

Author/s	Year	Type of report	Reported anatomy
Hemmig[29]	1979	Case report	Extraction of mandibular 3rd M fused with distomolar
Goldberg *et al.*[28]	1985	Case report	Endodontic management of mandibular 3rd M fused with 2nd M
Hou and Tsai[33]	1989	Case report	Extraction of maxillary 3rd M fused with a distomolar
Rotstein *et al.*[34]	1997	Case report	Endodontic management of mandibular 3rd M fused with 2nd M
Turell and Zmener[35]	1999	Case report	Endodontic management of mandibular 3rd M (left) fused with a distomolar
Turell and Zmener[36]	1999	Case report	Endodontic management of mandibular 3rd M (right) fused with a distomolar
Sidow *et al.*[4]	2000	*In vitro* (Clearing method)	Maxillary 3rd M: C-shaped canals in 2R= 7/150 Mandibular 3rd M: C-shaped canals in 1R= 3/150 C-shaped canals in 2R= 3/150
Gulabivala *et al.*[13]	2002	*In vitro* (Clearing method)	C-shaped canals in 1-rooted mandibular 3rd M: 1C= 5/173 2C= 9/173 3C= 4/173 4C= 1/173
Hamasha *et al.*[27]	2002	*In vivo* (Periapical radiograph) (Jordanian)	Maxillary 3rd M: Dilaceration: 4/301 (1.33%) Mandibular 3rd M: Dilaceration 63/328 (19.21%)
Kannan *et al.*[31]	2002	Case report	Dilacerated roots in four-rooted maxillary 3rd M
Malčić *et al.*[28]	2006	*In vivo* (Periapical/panoramic) (Croatian)	Maxillary 3rd M: Dilaceration: Periapical= 7/86 (8.1%) Panoramic= 45/532 (8.46%) Mandibular 3rd M: Dilaceration: Periapical= 19/79 (24.1%) Panoramic= 179/579 (30.92%)
Udoye and Jafarzadeh[25]	2009	*In vivo* (Periapical radiograph) (Nigerian)	Maxillary 3rd M: Dilaceration: 3/82 (3.7%) Mandibular 3rd M: Dilaceration: 2/60 (3.3%)
Zeylabi *et al.*[37]	2010	Case report	Endodontic management of a mandibular 3rd M fused with a distomolar
Miloglu *et al.*[39]	2010	*In vivo* (Periapical radiograph) (Turkish)	Maxillary 3rd M: Dilaceration: 30/404 (7.4%) Mandibular 3rd M: Dilaceration: 39/305 (12.8%)

M – Molar; R – Rooted

teeth are not rare anomalies in oral surgery. If the malposed and malformed teeth and their relationships to adjacent roots or other anatomical structures (eg, the mandibular canal) can be precisely determined with 3D CT or CBCT, their surgical exposure and subsequent actions to be taken can then be planned. However, the higher accuracy of CBCT images to identify anatomic and pathologic alterations compared to panoramic and periapical radiographs has been shown to reduce the incidence of false-negative results (Estrela *et al*. 2008).

CBCT has the potential to be an accurate, non-invasive, practical method to reliably determine osseous lesion size and volume. Further clinical validation will lead to a vast array of applications in oral and maxillofacial diagnosis (Pinsky *et al*. 2006).

3D CT images obtained with 3D surface reconstruction of spiral CT images is accurate and effective for examining impacted teeth and before orthodontic treatment (Chen *et al*. 2006).

Plain radiographs and 3D Dental-CT images are retrospectively reviewed by an oral radiologist for evidence of root dilaceration before operations to extract the impacted teeth are performed (Sawamura *et al*. 2003).

Cone-beam CT images are signicantly superior to panoramic images, this is of pertinent importance especially when predicting the possibility of neurovascular bundle exposed during surgical removal of impacted mandibular third molar teeth with apical root discrepancies.

REFERENCES

Archer, W.H. and W.H. Archer, Oral and Maxillo facial Surgery. 1975.

Chen, Y. *et al*. Three-dimensional spiral computed tomographic imaging: a new approach to the diagnosis and treatment planning of impacted teeth. American Journal of Orthodontics and Dentofacial Orthopedics, 2006. 130(1): p. 112-116.

Crawford, P.J. and M.J. Aldred, Regional odontodysplasia: a bibliography. Journal of Oral Pathology & Medicine, 1989. 18(5): p. 251-263.

Dayal, C. and G.S. Sajjan, Imaging solutions in endodontics: Cone beam computed tomography-A review, Endodontology, 2012. 24(1): p. 167-170.

Ericson, S. and J.r. Kurol, CT diagnosis of ectopically erupting maxillary canines"a case report. The European Journal of Orthodontics, 1988. 10(1): p. 115-120.

Estrela, C. *et al*. Method for determination of root curvature radius using cone-beam computed tomography images. Braz Dent J, 2008. 19(2): p. 114-118.

Garn, S.M., A.B. Lewis, and B. Bonné, Third molar formation and its development course. The Angle Orthodontist, 1962. 32(4): p. 270-279.

Goaz, P., S. White, and M. Pharoah, Oral radiology CV Mosby, St. 1994, Louis.

Gupta, P.V., Dental Diseases: Differential Diagnosis. 2008: Jaypee Brothers Publishers.

Hamasha, A., T. Al-Khateeb, and A. Darwazeh, Prevalence of dilaceration in Jordanian adults. International Endodontic Journal, 2002. 35(11): p. 910-912.

Hashimoto, K. *et al*. A comparison of a new limited cone beam computed tomography machine for dental use with a multidetector row helical CT machine. Oral Surgery, Oral Medicine, Oral Pathology, Oral Radiology, and Endodontology, 2003. 95(3): p. 371-377.

Holberg, C. *et al*. Cone-beam computed tomography in orthodontics: benefits and limitations. Journal of Orofacial Orthopedics/Fortschritte der Kieferorthopdie, 2005. 66(6): p. 434-444.

Jafarzadeh, H. and P.V. Abbott, Dilaceration: review of an endodontic challenge. Journal of Endodontics, 2007. 33(9): p. 1025-1030.

Kannan, S. and H. Santharam, Supernumerary roots. Indian Journal of Dental Research, 2002. 13(2): p. 116.

Lofthag-Hansen, S. *et al*. Limited cone-beam CT and intraoral radiography for the diagnosis of periapical pathology. Oral Surgery, Oral Medicine, Oral Pathology, Oral Radiology, and Endodontology, 2007. 103(1): p. 114-119.

Ludlow, J.B. *et al*. Dosimetry of 3 CBCT devices for oral and maxillofacial radiology: CB Mercuray, NewTom 3G and i-CAT. Dentomaxillofac. Radiol, 2006. 35(4): p. 219-26.

Malcic, A. *et al*. Prevalence of root dilaceration in adult dental patients in Croatia. Oral Surgery, Oral Medicine, Oral Pathology, Oral Radiology, and Endodontology, 2006. 102(1): p. 104-109.

Miloglu, O. *et al*. The prevalence of root dilacerations in a Turkish population. Med Oral Patol Oral Cir Bucal. 15: p. e441-4.

Panat, S.R. *et al*. Regional Odontodysplasia: A Case Report. Journal of Dental Sciences. 24.

Peene, P. *et al*. Resorption of the lateral maxillary incisor: assessment by CT. Journal of computer Assisted Tomography, 1990. 14(3): p. 427-429.

Pinsky, H. *et al*. Accuracy of three-dimensional measurements using cone-beam CT. Dentomaxillofacial Radiology, 2006. 35(6): p. 410-416.

Sawamura, T., K. Minowa, and M. Nakamura, Impacted teeth in the maxilla: usefulness of 3D Dental-CT for preoperative evaluation. European Journal of Radiology, 2003. 47(3): p. 221-226.

Schmuth, G. *et al*. The application of computerized tomography (CT) in cases of impacted maxillary canines. The European Journal of Orthodontics, 1992. 14(4): p. 296-301.

Terakado, M. *et al*. Diagnostic imaging with newly developed ortho cubic super-high resolution

computed tomography (Ortho-CT). Oral Surgery, Oral Medicine, Oral Pathology, Oral Radiology, and Endodontology, 2000. 89(4): p. 509-518.

Tervonen, S. *et al*. Regional odontodysplasia: a review of the literature and report of four cases. Clinical Oral Investigations, 2004. 8(2): p. 45-51.

Udoye, C.I. and H. Jafarzadeh, Dilaceration among Nigerians: prevalence, distribution, and its relationship with trauma. Dental Traumatology, 2009. 25(4): p. 439-441.

Vertucci, F.J., Root canal anatomy of the human permanent teeth. Oral Surgery, Oral Medicine, Oral Pathology, 1984. 58(5): p. 589-599.

Wenzel, A., E. Aagaard, and S. Sindet-Pedersen, Evaluation of a new radiographic technique: diagnostic accuracy for mandibular third molars. Dentomaxillofacial Radiology, 1998. 27(5): p. 255-263.

Westesson, P.-L. and L.-E. Carlsson, Anatomy of mandibular third molars: a comparison between radiographic appearance and clinical observations. Oral Surgery, Oral Medicine, Oral Pathology, 1980. 49(1): p. 90-94.

The Influence of Ante-Natal Phenytoin Therapy on Palatal Fusion in Rat Embryo

Ruwaidah F. Khaleel[1], Mohammad O. Selman[1], Imad M.Al-Ani[1*], Anam R. Al-Salihi[3]
[1]Department of Applied Embryology/ High Institute of Infertility Diagnosis and ART/ Al-Nahrain University, Baghdad, Iraq.
2Department of Basic medical Science, Kulliyyah of Medicine, International Islamic University Malaysia, Kuantan,Malaysia.
Department of Human Anatomy/ college of medicine Al-Nahrain University, Baghdad, Iraq.
***Corresponding address:** Tel. +60179776014. E-mail imad_alani@yahoo.com*

ABSTRACT

Background: Antiepileptic drug (phenytoin) is extensively used by pregnant women who have seizure disorders. It is reported to produce a variety of facial defects, and considered as an important cause of non-genetic cleft palate in their offspring.
Objective: To investigate the influence of administrating phenytoin to pregnant rats on the process of palatal fusion in rat embryos.
Material & Method: Female pregnant rats (*Rattus norvegicus*) were divided into two groups: The control group (G1) and experimental group (G2). Each group consist of (30) pregnant rats. Group 2 are subdivided into two subgroups (G2A), (G2B), each group contain 15 pregnant female rats. Each rat was given a dose of 15 mg daily phenytoin was suspended in distilled water to obtain a concentration of 15mg/kg/day , and 0.1 mg/kg that contain 3mg/rat/day was given I/P. From (E19-E16) of gestation when mothers of G2A reach (E20) of gestation cesarean section done and weighted embryos and cut the head of embryos, however when mothers of G2B reach (E21) of gestation normal delivery occur and weighted embryos and cut the head of embryos of gestation and 50 embryo from each group was used for histological preparation.
Result: At embryonic day 20 (E20) and day 21 (E21), there was delay union of palatal shelves, cartilaginous structure persist and was longer Phenytoin treated group than normals.
Conclusion: The present study did not demonstrate clefting of the palate in the phenytoin treated group. However, the histological study of the embryonic development of the palate and its morphogenesis has demonstrated that progression of fusion is taking place but with a delay in the midline seam disappearance.

INTRODUCTION

The development of the head involves the interaction of several cell populations and coordination of cell signaling pathways, which when disrupted can cause defects such as facial clefts (Yu *et al*. 2009). Cleft lip and/or palate is the most common congenital disorders worldwide; they affect an average of 1 in 700 live-born babies with ethnic and geographic variation, thus they comprise almost one-half of all craniofacial anomalies (Warrington *et al*. 2006). Cleft lip and palate are variations of a type of congenital deforming caused by abnormal facial development during gestation (Yu *et al*. 2009). It comprises a large fraction of all human birth defects, and is notable for its significant lifelong morbidity and complex etiology (Letra *et al*. 2010); there are around 7,000 infants born with facial clefts in the U.S. each year (Parker *et al*,, 2010).

Congenital structural anomalies may be caused by adverse effect of environmental factors and certain drugs that transfer across the placenta from mother into the baby's bloodstream and interfere with prenatal organ development (Brent, 2001; Gilbert-Barness, 2010). Cleft palate results from a mixture of genetic and environmental factors (Mima *et al*. 2013).

Antiepileptic drugs (AEDs) are those which decrease the frequency and/or severity of seizures in people with epilepsy (Bromfield *et al*. 2006). A large number of studies have demonstrated neonatal complications after epilepsy treatment during pregnancy (Brosh *et al*. 2011). Teratogenicity is the most important side effect of the AEDs, the most common congenital malformations identified in

newborn infants are facial dimorphism, cleft lip and palate, cardiac defects, digital hypoplasia and nail dysplasia have been found to be associated with retrospectively and prospectively identified prenatal exposure to these drugs (Brodie and Dichter, 1996). The embryotoxic and teratogenic effects of AEDs have also been experimentally demonstrated in rodents (Danielsson *et al*. 1992; Hansen *et al*. 1996). The risk for congenital malformations is approximately two to three folds higher in women exposed to AEDs compared to unexposed women; it is estimated that around 30,000 children born to epileptic mothers unexposed to antiepileptic drugs (AEDs) each year in the USA alone (Meador *et al*. 2008).

Phenytoin (PHT) is hydantoin derivative component, has minimal sedative effects and classical as antiepileptic drug, useful to treat partial seizures and generalized tonic-clonic seizures, has low affinity for resting sodium channels at hyperpolarized membrane potentials (Yaari *et al*. 1986). The teratogenicity of PHT has been established amongst clinicians and basic scientists (Hill *et al*. 2010**).** Prenatal exposure to phenytoin may result in a spectrum of congenital malformations and behavioural changes known as fetal hydantoin syndrome "FHS" (Nanda *et al*. 1989). FHS include irregular ossification of the distal phalanges, epicanthal folds, hypertelorism, broad flat nasal bridges, an upturned nasal tip, wide prominent lips and, in addition, distal digital hypoplasia, intrauterine growth retardation and mental retardation. The teratogenicity of PHT has been studied in a number of different species, including the mouse (Harbison and Becker, 1969), rat (Harbison and Becker, 1972), rabbit (McClain and Langhoff, 1980), and cat (Khera, 1979).

Normal lip development occurs between weeks 4 and 8 of gestation, the cleft lip deformity becomes established within this period of pregnancy, and is usually considered to be caused by failure of fusion of the maxillary and median nasal processes (Sadler, 2012). It may also be caused by incomplete mesodermal in-growth into these processes, with subsequent breakdown of epithelium (Yau, 2012). Facial deformity arising in association with cleft lip and palate causes special problems (Poswillo, 1988). Cleft palate occurs when the bilateral palatal shelves fail to fuse (Mima *et al*. 2013). It has been revealed that cleft of the secondary palate originates from a failure of signaling molecules and their receptors to control palatal shelf growth, elevation, and fusion involving palatal mesenchyme and epithelium (Chai and Maxson, 2006). In the fusion process, most studies have focused on the mechanisms responsible for the disappearance of the midline epithelial seam (MES); there still remains a considerable disagreement regarding the fate of the MES, such as apoptosis in the MES (Cuervo and Covarrubias, 2004) migration of the medial edge epithelium (MEE) resulting in the loss of MES (Carette and Ferguson 1992) and epithelial-mesenchymal transformation of MES (Shuler *et al*. 1992). Therefore, the present study has been conducted to evaluate effects of an antiepileptic(phenytoin) drug on palatal closure on rat embryo.

MATERIALS & METHODS

Animals

Sixty healthy mature female albino rats (*Rattus norvegicus*) (1.5-2 months old) and(150-200g body weight) obtained from the animal house of the High Institute of Infertility Diagnosis and Assistant Reproductive Technology/ University of Al-Nahrain, and kept under suitable environmental conditions (e.g. room temperature was maintained at 24 + 2 °C and exposure to 12 hours daylight). Vaginal smears were prepared to examine the regularity of at least three consecutive estrus cycles. During the estrus stage, the females were mated with males. After examination of vaginal plug to observe spermatozoa, the gestation period was started and considered the first day of pregnancy.

Experimental Design

Thirty control female pregnant rats (G1) were randomly divided into two sub groups (G1A and G1B) of 15 rats each. Each rat was injected intraperitoneally (0.1ml) distilled water. In G1A and G1B the female pregnant rats were injected at the time of palatal closure at embryonic day

(E9-E16) of gestation period to compare with Phenytoin group at embryonic day (E20, E21) respectively. When pregnant rats of G1A group reach day E20 of gestation, an incision was made in the uterus and the umbilical cord connected to the fetus was cut, while the pregnant rats of G1B group where allowed for normal delivery at day E21 of gestation. Fifty embryos from each group were used for histological preparation.

Thirty experimental pregnant female's rats (G2) were randomly divided into two sub groups (G2A, G2B) of 15 rats each. Each rat was administered daily 1.5mg/kg/day phenytoin suspended in distilled intraperitoneally from day (E9-E16) of gestation. When pregnant rats of G2A group reach day E20 of gestation, an incision was made in the uterus and the umbilical cord connected to the fetus was cut, however pregnant rats of G2B group were allowed for normal delivery at day E21 of gestation, 50 embryo from each group were used for histological preparation.

At E20 after gestation, the pregnant rats were anesthetized by intramuscular (IM) injection of a mixture of ketamine (90 mg/kg body weight) and Xylazine (10mg/kg body weight). The abdomen was incised transversely opened and the two cornua of the uterus were delivered outside the abdomen and the fetuses were delivered from the uterus. Full term pregnant female rats were allowed for normal delivery at day E21, the head of litters were transferred to 10% neutral buffered formalin (BDH) for 72 hours, then transferred to 70% ethanol, and processed for light microscopy.

The experimental animal protocol was conducted in compliance with humane animal care standards outlined in the National Institutes of Health Guide for the Care and Use of Laboratory Animals. The experimental study was with ethics approved from Al-Nahrain University.

RESULTS

Complete fusion of the secondary palatal shelves has been observed in the control group at day E20 forming complete separation between the oral cavity with the tongue well below and the nasal cavity above (Fig. 1.A). At embryonic stage E20 continuous oral cavity epithelial lining of stratified squamous epithelium is formed on the inferior surface of the fused palate. On the superior aspect, respiratory epithelium of ciliated pseudostratified columnar epithelium forms the lining of the naso-pharynx (Fig. 1.B).

Mesenchymal tissue underlying the epithelial lining is continuous from side to side. The medial epithelial edge (MEE) had fused together and their epithelial cells are opposing each other and intermingled along the mid line core of the palate (Fig. 1.B).

During the last stages of intrauterine life (E21), the medial epithelial seam (MES) which had been formed by fusion of MEE, starts to disintegrate, becoming thinner in the middle compared to its oral and nasal parts (Fig. 1. C, D). Organization and endochondral processes of ossification start in the palatal tissue (Fig. 1.D).

In the phenytoin-treated groups, the sequence of morphogenetic events was different from that of the control. Although fusion of the two sides of the palatal shelves had occurred at E20 (Fig. 2. A), the epithelial coverings of the fused palate was not well developed with scanty mesenchymal tissues underlying it. The interaction between the MEE is disorganized with distorted arrangement of the epithelial components of MEE (Fig. 2. A). Nevertheless, the palate was complete and well separated between the nasal septum and the tongue (Fig. 2. B).

At E21, the palate of the phenytoin-treated group still containing a well-formed, tightly compact MES (Fig. 2. C), which represents a delayed event compared with the control group in which the MES starts to disintegrate. Just before birth, the palate still has a MES with minimal organization of palatal tissue into its definitive components (Fig. 2. D).

DISCUSSION

The present study has demonstrated no clefting of the palate in the phenytoin-treated rats. However, the embryonic development of the palate and its morphogenesis has demonstrated a

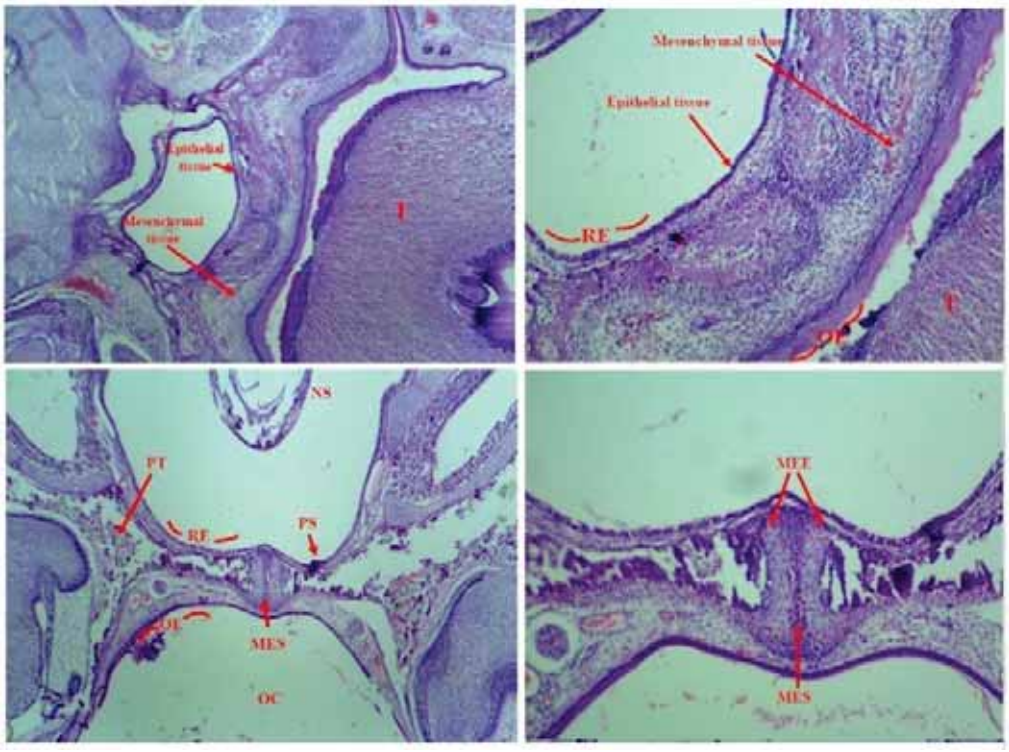

Fig. 1: Coronal sections through the palate E20 in rat fetus of control group (G1A); A/ showing complete fusion of the bilateral palatal shelves; B/ showing continuity of epithelial and mesenchymal tissues in the fused secondary palate; C/ E21 control group (G1B) in rat litter showing secondary palate with medial epithelium seam MES, D/E21 control group (G1B) showing disintegration of the medial epithelium seam. Notes: T: Tongue, RE: respiratory epithelium, OE: oral epithelium, NP: nasopharynx, NS: Nasal septum, PS: Palatal shelf, OC: oral cavity, PT: palatal triangle, MEE: Medial epithelial edge, MES: medial epithelium seam. (H&E), (original magnifications A&C 4x. B&D 10x)

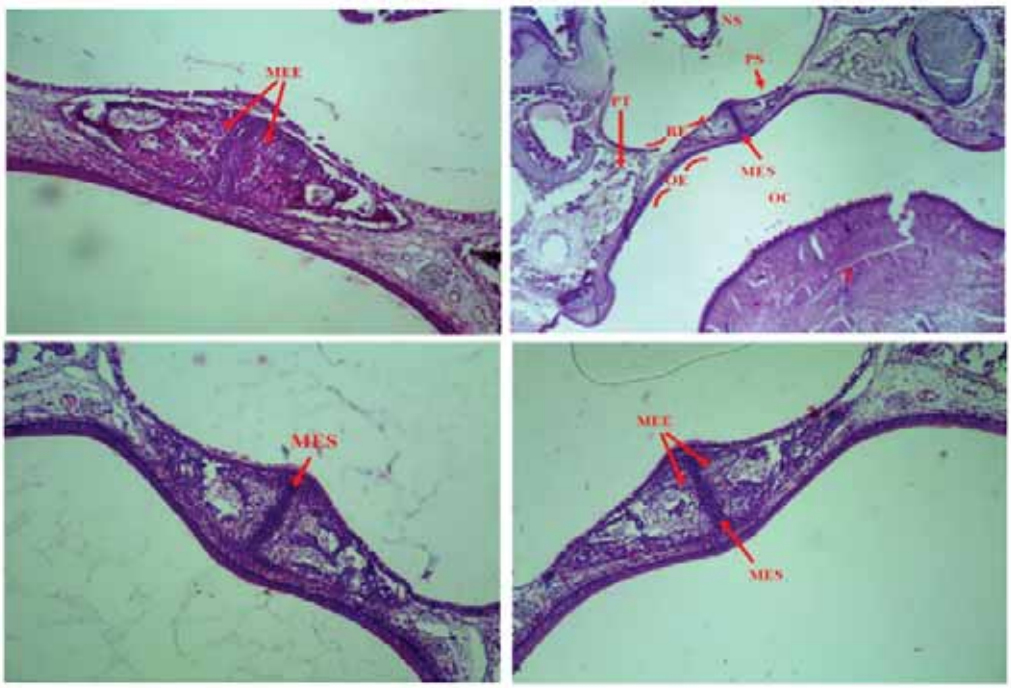

Fig. 2: Coronal sections through the palate E20 in rat fetus of Phenytoin treated group (G2A); A/ showing the site of fusion of the bilateral secondary palatal shelves; B/(G2B) coronal section through the palate E21 showing complete secondary palate; C/(G2B) Coronal section through the palate E21 litter showing tightly compact medial epithelium seam MES; D/ /(G2B) coronal section through the palate E21 showing secondary palate structure prior to birth. Notes: MEE: Medial epithelial edge, NP: nasopharynx, NS: Nasal septum, PS: Palatal shelf, OC: oral cavity, PT: palatal triangle, RE: respiratory epithelium, OE: oral epithelium, MES: medial epithelium seam, T: Tongue. (H&E), (original magnifications B 4x. A, C&D 10x)

progression of fusion with a delay in the midline seam disappearance; this delay may be attributed to the effect of phenytoin, this is in concordance with Gu *et al*. (2008) who observed a delayed closure of the secondary palate at the anterior end in *Shox2*-deficient mice embryos, leading to a failed fusion of the primary and secondary palates. The ability of the palatal shelves to fuse with other embryonic structures *in vitro* depended critically on age of palatal shelves (Ferguson, 1988).

It is still unclear whether cleft palate formation is attributable to intrinsic bio-molecular defects in the embryonic elevating palatal shelves or to an inability of the shelves to overcome a mechanical obstruction such as the tongue in Pieer Robin sequence (Sharp, 1998). This study supports the view that an intrinsic biomolecular disturbance may cause the cleft palate. The study showed that the possible mechanical obstacles, the tongue and nasal septum are far away from intervening palatal shelves to cause failure of fusion and cleft palate.

Phenytoin is well known to cause a variety of facial clefting syndrome (Paulson *et al*. 1979) and to have an influence on the glucosaminoglycan turnover (Manent *et al*. 2008).This suggests that phenytoin causes altrayion in proteoglycan structure which may be cell adhesion molecules which facilitate palatal fusion. This hypothesis which we put forward is supported by the fact that palatal fusion is blocked by diazo-oxo-norleucine which is an inhibitor of glycosaminoglycan synthesis (Bulter and Juurlink., 1987)

This study has demonstrated a delay in disappearance of MES cells in the phenytoin-treated group as compared to the control group. The fusion of the bilateral palatal shelves to form definitive mammalian secondary palate is critically dependent on removed of the medial edge cells that constitute the midline epithelial seam. Conflicting views suggest that programmed apoptotic cell death or epithelial-mesenchymal transformation of these cells is predominantly involved (Sheehan and Hrapchak, 1980). A third view is that MEE cells migrate nasally and orally out of the seam and recruited into, and constitute the epithelial triangles on both the oral and nasal aspect of the palate (Han *et al*. 2003).

This study favors epithelial-mesenchymal transformation because of the observed increase in abundance of mesenchymal tissue which takes place along with the disruption and disintegration of MES. This process may be affected by phenytoin treatment since scanty mesenchymal tissue is seen in late stage palatal structure in the phenytoin-treated group. Regarding apoptosis in the MES, this issue requires further investigation of the process of apoptosis in the MEE using TUNEL techniques and apoptotic markers.

REFERENCES

Brent RL (2001). The cause and prevention of human birth defects: what have we learned in the past 50 years? *Congenit Anom* (Kyoto). 41: 3-21.

Brodie MJ, Dichter MA (1996). Antiepileptic Drugs. *New Eng J Med.* 334: 168–175.

Bromfield EB, Cavazos JE, Sirven JI (2006). An Introduction to Epilepsy. Am Epilepsy Society "Ed." Bookshelf ID: NBK2515

Brosh K, Matok I, Sheiner E, Koren G, Wiznitzer A, Gorodischer R, Levy A (2011). Teratogenic determinants of first- trimester exposure to antiepileptic medications. *J Popul Ther Clin Pharmacol*. 18: e89-e98.

Bulter H, Juurlink B(1987). An Atlas for staging Mammalian and Chick Embryos. *CRC Press, Inc., Boca Raton, Florida* .1987:110-138.

Carette M and Ferguson M (1992). Mouse embryonic palatal epithelial sheets in culture: an immunocytochemical study of proliferative activity using bromodeoxyuridine. *Epithelial Cell Biol*. 1: 119–127.

Chai Y, Maxson R (2006). Recent advances in craniofacial morphogenesis. Developmental dynamics. 235: 2353–2375.

Cuervo R, Covarrubias L (2004). Death is the major fate of medial edge epithelial cells and the cause of basal lamina degradation during palatogenesis. *Development.* 131: 15–24.

Danielsson B R , Danielson M, Rundqvist E, Reiland S(1992) *Teratology*. 41: 247–258.

Ferguson MWJ(1988). Palate development. *Development*. 103: 41-60.

Gilbert-Barness E (2010). Teratogenic Causes of Malformations. Ann Clin Lab Sci. 40 (2): 99-114.

Gu S, Wei N, Yu X, Jiang Y, Fei J, Chen Y (2008). Mice with an anterior cleft of the palate survive neonatal lethality. *Dev Dyn*. 237: 1509–1516.

Han M, Niwa K, Kasai M (2003). Rat embryos at various developmental stages *Theriogenology*. 59:1851-63.

Hansen D K, Dial SL, Terry KK, Grafton TF (1996). *Teratology*. 54, 45–51.

Harbison RD, Becker BA (1969). Relation of dosage and time of administration of diphenylhydantoin to its teratogenic effect in mice. *Teratology*.2: 305–311.

Harbison RD, Becker BA (1972). Diphenylhydantoin teratogenicity in rats. *Toxicol Appl Pharmacol*. 22:193–200.

Hill DS, Wlodarczyk BJ, Palacios AM, Finnell RH (2010). Teratogenic effects of antiepileptic drugs. *Expert Rev Neurother*. 10: 943–959.

Khera KS (1979). A teratogenicity study on hydroxyurea and diphenylhydantoin in cats. *Teratology*. 20: 447–452.

Letra A, Menezes R, Govil M , Fonseca R , McHenry T (2010). Association Studies of Chromosome Region 9q and Nonsyndromic Cleft Lip and Palate. *Am J Med Gene. Part A.* 152: 1701-1710.

Manent J, Jorquera I, Franco V, Ben-Ari Y, Perucca E, RepresaA (2008). Antiepileptic drugs and brain maturation: fetal exposure to lamotrigine generates cortical malformations in rats. *Epilepsy Res*. 78:131–139.

McClain RM, Langhoff L (1980). Teratogenicity of diphenylhydantoin in the New Zealand white rabbit. *Teratology*. 21: 371–379.

Meador K, Pennell P, Harden C, Gordon JC, Tomson T (2008). Pregnancy registries in epilepsy: a consensus statement on health outcomes. *Neurology.* 71:1109–1117.

Mima J, Koshino A, Oka K, Uchida H, Hieda Y, Nohara K, Kogo M, Chai Y, Sakai T(2013). Regulation of the Epithelial Adhesion Molecule Is Important for Palate Formation. *PLoS ONE*. 8: e61653.

Nanda A, Kaur S, Bhakoo ON, Kapoor MM, Kanwar AJ (1989). Foetal hydantoin syndrome: a case report. *Pediatr Dermatol*. 6:130-133.

Parker SE, Mai CT, Canfield MA, Rickard R, Wang Y, Meyer RE, Anderson P (2010). Updated national birth prevalence estimates for selected birth defects in the United States, 2004-2006. *Birth Defects Res A Clin Mol Teratol*. 88:1008–1006.

Paulson RB, George W, Paulo MD and Salim MS(1079). Phenytoin and carbamazepine in production of cleft palate in mice. *JAMA Neurology.* 36: 832-836.

Poswillo D (1988). The aetiology and pathogenesis of craniofacial deformity. *Development.* 103: 207-212.

Sadler TW (2012). Langman's Medical Embryology. 12th Ed. Lippincott William and Wilkins, USA.

Sharp P, Marie C and Suckow M (1998). The laboratory rat. 2nd Ed. *CRC Press.* Pp: 53-70.

Sheehan D and Hrapchak B (1980). Theory and Practice of Histotechnology. *Battelle Press, Columbus*. Pp 235–237.

Shkoukani MA, Chen M, Vong A (2013). Cleft lip Deformity– a comprehensive review. *Frontiers in Pediatrics*. Volume 1 "article 53":1-10. www.frontiersin.org

Shuler C, Halpern D, Guo Y, Sank AC (1992). Medial edge epithelium fate traced by cell lineage analysis during epithelial-mesenchymal transformation in vivo. *Develop Biol*. 154: 318–330.

Warrington A , Vieira A ,Christensen K , Orioli IM, Castilla EE (2006). Genetic evidence for the role of loci at 19q13 in cleft lip and palate. *J Med Genet*. 43: 1-17.

Yaari Y, Selzer M, Pincus J (1986). Phenytoin: mechanisms of its anticonvulsant action. *Ann Neurol*. 20:171-84.

Yau F-S, Fontes ML, Malhorta V (2012). Anesthesiology: Problem-Oriented Patient Management. *Lippincott William and Wilkins Philadelphia*, USA.

Yu W, Serrano M, Miguel SS, Ruest LB, Svoboda KKH (2009).Cleft lip and palate genetics and application in early embryological development. *Indian J Plast Surg*. 42: S35–S50.

Chronic Khat Consumption and Its Effect on Ovarian Structure in Mice and Their Offspring

Cinaria T. Albadri [1], Imad M. Alani [2], Hassan M. Hiba [3]

[1] *Department of Biology, Faculty of Science, Sana'a University, Sana'a, Yemen.*

[2] *Department of Basic Medical Science, Kulliyyah of Medicine, International Islamic University, Kuantan, Malaysia.*

[3] *Department of Biological Science, Faculty Of Science, King Abdul-Aziz University, P.O. Box 8023 Jeddah, KSA*

** Correspondance author: E-mail:cinariaalbadri@yahoo.com, Contact Number: 00353868842071*

ABSTRACT

Khat is considered a psychoactive drug and has many side effects on different parts of the body organs. In this study the effects of khat on ovarian structure in parental mice and their offspring were investigated. Twelve male and twelve female mice were given orally a dose of 50mg/kg body weight of khat extract by gastric gavage for 4 and 8 weeks. After four weeks of treatment, the male and female mice were allowed to mate. Khat treatment continued for the male mice and for the female mice during pregnancy and after giving birth to their offsprings up to 8 weeks. Adult offspring and their parent were killed at the 4th and 8th weeks of treatment. Histological examination of the ovaries showed many corpus luteum and developing Graafian follicles with mononuclear infiltration.

Keywords: Ovaries, khat, offspring, corpus luteum

INTRODUCTION

Khat is a stimulant drug derived from a shrub (*Catha edulis*) that is native to East Africa and Southern Arabia. The main psychoactive ingredients in khat are cathine and cathinone, chemicals that are structurally similar to, but less potent than, amphetamine; yet result in similar psychomotor stimulant effects (Kalix *et al*. 1985). The habit of khat chewing has prevailed for centuries among populations of Africa and the Arabian Peninsula including Yemen. Chewing khat leaves can induce a state of euphoria and elation as well as feelings of increased alertness and arousal (Kalix *et al*. 1985). Long term chronic users may develop personality disorders and mental deterioration (Granek *et al*. 1988). The user can also experience an increase in blood pressure and heart rate Brenneisen *et al*. 1990). The effects begin to subside after about 90 minutes to 3 hours, but can last 24 hours (Kennedy *et al*. 1983). At the end of khat session, the user may experience a depressive mode, irritability, anorexia and difficulty in sleeping (Nencini *et al*. 1989 and Al-Motarreb *et al*. 2002).

There are many adverse physical effects that have been associated with heavy or long-term use of khat, including tooth decay and periodontal disease, gastrointestinal disorders such as constipation, ulcers, inflammation of the stomach and increased risk of upper gastrointestinal tumors (Maitai CK., 1981, Heymann *et al*. 1995, Gunaid *et al*. 1999 and Gunaid *et al*. 1995).

The effects of khat on the male reproductive system are still unclear, as there are reports of increased sperm capacitation (Adeoya-Osiguwa SA. and Fraser LR., 2005) and reduced sperm motility (Mwenda *et al*. 2003). In chronic chewers, sperm count, sperm volume and sperm motility were decreased (Hakim 2002). In other studies, rabbits fed with khat for three months had an increased rate of spermatogenesis and the Leydig cells were in good condition (Al- Mamary *et al*. 2002). In a study involving humans (El Shoura *et al*. 1995), semen parameters in two groups of Yemeni males, khat 'addicts' and 'non-addicts', were compared; sperm concentration, morphology

and motility were reported to be significantly weaker in the 'addicts'. However, the age ranges in both groups were wide, there were no details on amounts of khat ingested by the addicts and there was no information on the men's intrinsic fertility, making it difficult to draw sound conclusions.

Detailed studies on the effects of khat on female reproduction are lacking. However, the limited available data reveal that chewing of khat has a negative impact on female reproductive health. Intrauterine growth retardation, low foetal birth weight and infant mortality are some of the most important reproductive health problems affecting most developing countries (Mwenda *et al*. 2003). Khat chewing during pregnancy is on the increase among women of reproductive age (Kennedy *et al*. 1980). Khat is reported to have genotoxic and has teratogenic effects on the foetus if regularly consumed by pregnant mothers (Mwenda *et al*. 2003). Lower mean birth weight have also been reported in khat-chewing mothers compared to non-chewing khat mothers, indicating an association between khat chewing and decreased birth weight (Abdul *et al*. 1987 and Dalu A., 2000).

Eriksson and co-workers found out that a khat-chewing mother produces less milk than non-users (Eriksson *et al*. 1991). Khat chewing in the third trimester of pregnancy was also found to significantly reduce the maternal weight gain (Jasson *et al*. 1988). The aim of this study was to investigate the effect of khat on ovarian structure in mice.

MATERIALS AND METHODS:

Animals

Forty eight mice of the balb c/strain were used in this study. They were randomly selected of twenty four virgin female and twenty four male (weighing 25-30 g and aged 6-8 weeks). The mice were kept under suitable environmental conditions such as a room temperature that was maintained at (20-24) °C and exposed to 12 hour/day light program. They received mouse food pellets and were allowed for free access of water *ad libitum*.

Khat Leaves

Leaves of khat were obtained from a crop in Haja (Sawty type) not sprayed with insecticides. The young leaves and shoots of khat were washed with distilled water and dried at room temperature of 24 ^{o}C in the laboratory. The dried leaves were powdered in an electrical grinder and the powder was kept in plastic bags in the freezer at -20 ^{o}C until its usage.

Experimental design

The animals were divided into two groups, (group 1) considered as the control group of twelve male and twelve virgin female and (group 2) was the khat group, also of twelve male and twelve virgin female. The khat group were administered daily with oral doses of (50 mg/kg) khat extract using gastric tube,[21] for 4 and 8 weeks respectively. Male animals were kept in separate cages from the virgin females. After 4 weeks of khat treatment, the males and females were allowed to mate. Khat treatment continued to males for another 4 weeks and for the females following diagnosis of pregnancy till the delivery of their offspring, up to another 4 weeks. After delivery, khat treatment was stopped. The offspring were weaned at 21 days of age and were allowed to reach maturity age of 6-8 weeks. Parent mice were sacrificed at the 4th and 8th weeks of treatment. Female offspring (of twelve mice each) were selected from group 1 and group 2 and sacrificed at maturity age.

Tissue preparation

Tissues of the ovaries were taken from female mothers after 8 weeks of treatment and from their female adult offspring, fixed with Bouin's solution for 24 hours, dehydrated by series of ethanol, cleared in xylene and embedded in paraffin wax. Paraffin sections of 5µm thickness were stained with haematoxylin and eosin.

RESULTS

Light microscopic examination of the ovaries of the control mice (mother and their female offspring) showed normal structural features of the ovaries revealing normal follicles and corpus luteum (Fig. 1, A&B).

After eight weeks of khat treatment, the ovaries of the female mother mice showed many primary and secondary follicles, developing and mature Graafian follicles and there were disintegrated zona granulosa cells with mononuclear infiltration. (Fig. 2, A&B). Ovarian tissues of

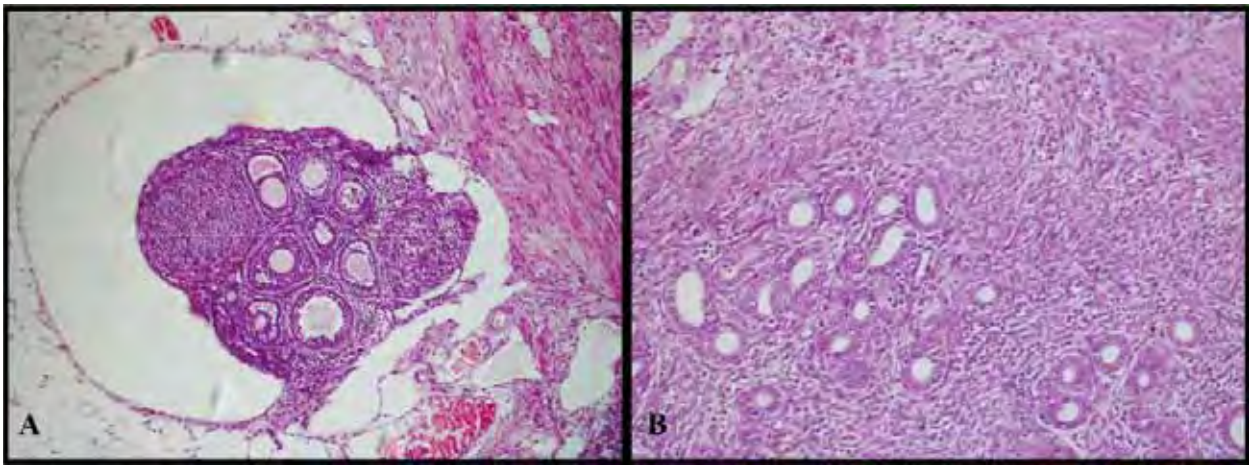

Fig. 1: Ovary tissue section of parent control group (A) and of their offspring (B), showing regular ovarian features with normal follicles and corpus luteum. (H&E. 50X).

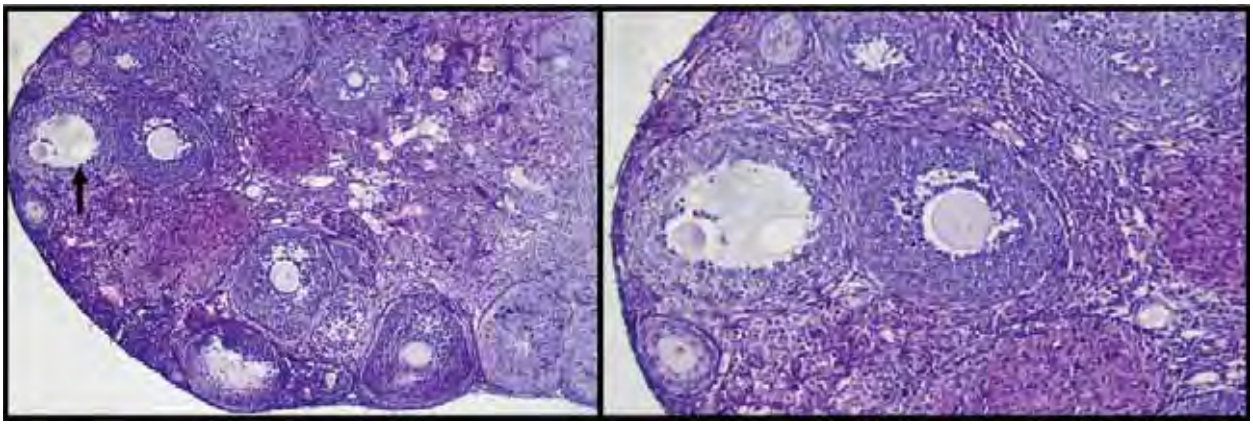

Fig. 2: Ovary tissue section of parent khat-treated group (A) showing many primary and secondary follicles, developing and mature Graafian follicles↑, some showing disintegrated zona granulosa cells with mononuclear infiltration. (H&E. 100X), (B) Magnified section of the same tissue. (H&E. 150X).

their offspring after 8 weeks of khat treatment revealed many corpora lutea, disintegrated oocytes within the developing follicles and congested blood vessels (Fig. 3). However, few sections showed normal Graafian follicles (Fig. 4).

DISCUSSION

The present findings showed the ability of the methanol extract of khat, *Catha edulis Forsk*, to present considerable changes of the ovarian structure in mother mice and their offspring. It has been previously concluded that the consumption of khat in pregnant women inhibits placental blood flow causing foetal growth defects (Goldenberg *et al*. 2004), and reduce birth weight (Abdul Ghani *et al*. 1987). Foetal mortality may be a result of placental insufficiency that has developed

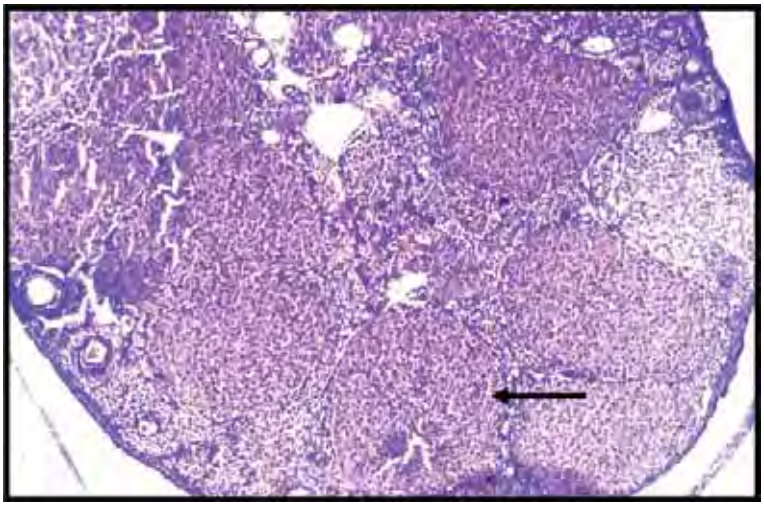

Fig. 3: Ovary tissue section of the offspring of parent khat-treated group showing many corpora lutea↑, disintegrated oocytes within the developing follicles and congested blood vessels. (H&E. 100X).

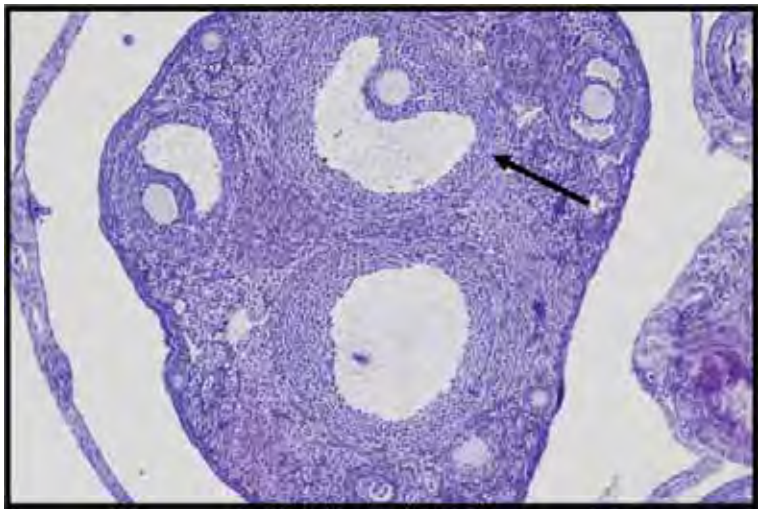

Fig. 4: Ovary tissue section of the offspring of parent khat-treated group showing normal Graafian follicles↑. (H&E. 100X).

from vasoconstriction caused by khat extract treatment (Jasson *et al*. 1988). In a previous study, no morphological changes were observed in ovaries of mice at all of the khat extract doses (100, 200 and 400 mg/kg), although khat has shown to be associated with antifertility and the possibility of sterility within higher dose treated animals (Asrade *et al*. 2013). However, results of the present study have shown no defects in foetal growth of the offspring of parent mice treated with the khat dose of 50mg/kg body weight which may be due to the lack of antifertility effect that is explained by the pharmacokinetic characteristics of khat components. Increasing dose treatments has shown to result in cathinone accumulation and thereby result in antiimplantation and antifertility effects (Cox G and Rampes H., 2003).

CONCLUSION

Khat extract at a dose of 50mg/kg body weight showed no deleterious effects on the ovarian structure in both female mice and their female offspring. Further research on higher doses and duration of khat treatment in parent mice and their offspring is recommended in future studies.

REFERENCES

Abdul Ghani N, Eriksson M, Kristiansson B, Qirbi A. (1987). The influence of chewing khat on birth-weight in full-term infants. Soc Sci Med, 24:625-627.

Adeoya-Osiguwa SA and Fraser LR. (2005). Cathine and norephedrine, both phenylpropanolamines, accelerate capacitation and then inhibit spontaneous acrosome loss. Human Reproduction, 20:268-276.

Al-Mamary M, Al-Habori M, Al-Aghbari A and Baker M. (2002). Investigation into the toxicological effects of Catha edulis leaves: a short term study in animals. Phytother Res, 16:127-132.

Al-Motarreb A, Baker K and Broadley K. (2002). Khat: pharmacological and medical aspects and its social use in Yemen. Phytother Res, 16:403-413.

Asrade S, Shibeshi W, Engidawork E. (2013). Evaluation of the reversibility and possible mechanisms of antifertility of Catha edulis F. (khat) extract following subacute administration in rodents. African J Pharm & Pharmacology, 7:2693-2700.

Brenneisen R, Fisch H, Koelbing U, Geisshusler S and Kalix P. (1990). Amphetamine-like effects in humans of the khat alkaloid cathinone. Br J Clin Pharmacol, 30:825-828.

Cox G, Rampes H. (2003). Adverse effects of Khat: a review. Adv Psychiatr Treat, 9:456-463.

Dalu A. (2000). Impact of long term consumption of khat on public health. The Sudama Concern, 21:475-477.

El Shoura S, Abdel A, Ali M, El Said M, Ali K, Kemeir M, Raoof A, Allam M and Elmalik E. (1995). Deleterious effects of khat addiction on semen parameters and sperm ultrastructure. Hum Reprod, 10:2295-2300.

Eriksson M, Ghani NA and Kristiansson B. (1991). Khat chewing during pregnancy-effect upon the offspring and some characteristics of the chewers. Afr Med J, 68:106-111.

Goldenberg D, Lee J, Koch WM, Kim MM, Trink B, Sidransky D, Moon CS. (2004). Habitual risk factors for head and neck cancer. Otolaryngol Head Neck Surg, 131:986-993.

Granek M, Shalev A and Weingarten A. (1988). Khat-induced hypnagogic hallucinations. Acta Psychiatr Scand, 78:458-461.

Gunaid AA, El Khally FMY, Hassan NAGM, Murray-Lyon IM. (1999). Chewing qat leaves slows the whole gut transit time. Saudi Med J, 20:444–447.

Gunaid AA, Sumairi AA, Shidrawi RG, Al-Hanaki A, Al-Haimi M, Al-Absi S, Al-Huribi MA, Qirbi AA, Al-Awlagi S, El-Guneid AM, Shousha S, Murray-Lyon IM. (1995). Oesophageal and gastric carcinoma in the Republic of Yemen. Brit J Cancer, 71:409–410.

Hakim LY. (2002). Influence of khat on seminal fluid among presumed infertile couples. East Afr Med J, 79:22-28.

Heymann TD, Bhupulan A, Zuriekat NEK, Bomanji J, Drinkwater C, Giles P. Murray-Lyon IM. (1995). Khat chewing delays gastric emptying of a semi-solid meal. Aliment Pharmacol Ther, 9:81–83.

Jasson T, Kristiansson B and Qirbi A. (1988). Effect of khat on uteroplacental blood flow in awake, chronically catheterized, late-pregnant guinea pigs. J Ethnopharmacol, 23:19-26.

Kalix P and Braeden O. (1985). Pharmacological aspects of the chewing of khat leaves. Pharmacol Rev, 37:149-164.

Kennedy JG, Teague J and Fairbanks L. (1980). Qat in North Yemen and the problem of addiction: A study in medical anthropology. Cul Med & Psychat, 4:311-344.

Kennedy JG, Teague J, Rokaw W and Conney E. (1983). A medical evaluation of the use of Qat in North Yemen. Soc Sci Med, 17:783-793.

Maitai CK. (1981). Effect of cathinone on chick embryo. Heart J Pharmac, 33:195.

Mwenda JM, Arimi MM, Kyama MC and Langat DK. (2003). Effects of khat (catha edulis) consumption on reproductive function: a review. East Afr Med J, 80:318-323.

Nencini P and Ahmed AM. (1989). Khat consumption: a pharmacological review. Drug Alcohol Depend, 23:19-29.

Tariq M, Qureshi S, Ageel AM and Al-Meshal IA. (1990). The induction of dominant lethal mutations upon chronic administration of khat (catha edulis) in albino mice. Toxicol Lett, 50:349-353.

INSTRUCTIONS TO CONTRIBUTORS

Official Journal of the Microscopy Society (Singapore)

Submission of a manuscript implies: (1) that the work described has not been published before (except in the form of an abstract or as part of a published lecture, review, or thesis); (2) that it is not under consideration for publication elsewhere; and (3) that its publication has been approved by all the authors as well as by the responsible authorities at the institute where the work has been carried out. Copyright: when any paper is accepted for publication, the authors agree to automatic transfer of the copyright to the publisher, and that the manuscript will not be published elsewhere in any language without the consent of the copyright holder.

Instructions to contributors

The journal publishes review articles, original research papers, short technical notes, letters to the Editors and short communications on the applications of microscopical techniques and specimen preparation procedures using all forms of microscopes and microanalysers.

Papers must be written in English and should be submitted electronically to the Editor- in-Chief:

Samuel SW Tay
Department of Anatomy, National University of Singapore
Blk MD10, 4 Medical Drive, Singapore 117597
Telephone (65) 6516 3210 Fax (65) 67787643
E-mail: anttaysw@nus.edu.sg

When an article is accepted for publication, the copyright on it passes immediately into the possession of the printer. The copyright covers the exclusive and unlimited rights to reproduce and distribute the article in any form of reproduction (printing, electronic media or any other form); it also covers translation rights for all languages and countries.

No manuscript processing fees, page charges or charges for halftone illustrations will be levied. Authors must prepare manuscripts in accordance with the journal's accepted practice. Authors submitting diskettes are requested to follow the technical instructions printed in each issue of the journal.

Manuscripts should be divided into the following sections: title page; **Abstract; Materials and Methods; Results; Discussion; Acknowledgements; References, Fig. legends and tables.** The original manuscript must be typed double spaced with wide margins and on one side of the paper only; duplicate copies must be photocopied on both sides of the paper to save on postage. In order to reduce mailing costs, when a manuscript is rejected only the original illustrations will be returned. Genus and species names should be marked with a single straight underline for italics. Words the author wishes to emphasize in the body of the text may also be set in italics and should be marked in the same way. The approximate desired positions of figures and tables should be marked in the margin of the manuscript. For literature citations in the text the name/year system should be used.

Brief accounts of particularly interesting results will be printed out of turn as "Short communications". These should not exceed two or at the most three printed pages.

1. The **title page** must give: first name(s) and surname(s) of author(s); title of the paper; initials(s) of given name(s) and last name(s) of author(s) with full addressees) of institute(s)- any footnotes referring to the title- address to which proofs should be sent and telephone and FAX numbers and e-mail address of the corresponding author.

2. **Abstract**. Each paper should be preceded by a summary not exceeding 200 words.

3. The list of **References** should include only works citied in the text. "Unpublished works" and "personal communications" may be referred to in the text but should not be included in the reference list. References should be listed at the end of the text as follows:
   a) Single author - list alphabetically and then chronologically.
   b) Author and one co-author - list alphabetically by first author and then by co-author and then chronologically.
   c) First author and more than one co-author - list alphabetically by first author and then chronologically, because only the first author's name and "*et al.*" followed by the year of publication will be used in the text.
   d) In the event that more than one paper by the same author or team of authors published in the same year

is cited, the letters a, b, c, etc., should follow the year - e.g., Williamson (1990a) - in both the text and the reference list.

Entries in the reference list should be set out as follows:

Journals: name(s) of author(s) followed by initials (do not use "and")- year of publication; complete title; journal as abbreviated in Index Medicus; volume number, first and last page numbers.

Example:

Andersson H, Bacchi T, Hoechl M, Richtel C (1998) Autofluorescence of living cells. J. Microsc. 119:1-7

Books: name(s) of author(s) followed by initials; year of publication; complete title (in English); edition and volume if appropriate; publisher; place of publication.

Examples:

Books: Klir G.J, Yuan B (1995) Fuzzy sets and fuzzy logic: Theory and application. Prentice Hall Englewood, New Jersey.

Book- chapters: Bach L, Mayer E (1987) Physics of water and ice: implications for cryofixation. In: Steinbrecht RA, Zierold K (eds). Cryotechniques in biological electron microscopy - Springer-Verlag, Berlin, pp 1-34.

4. **Figures**. The illustrations must be submitted in triplicate. Figures should be restricted in number to the minimum needed to clarify the text. Information given in the legends must not be repeated in the text, nor should the same data be presented in both graph and table form. Illustrations that have already been published elsewhere are not usually accepted. All figures, whether photographs, graphs or diagrams, must be numbered in a single continuous sequence in the order in which they are cited in the text. Each Fig. must be mounted on a separate sheet. The author's name, the number of the Fig. and the top of the illustration should be indicated on the back or on the sheet it is mounted on.

   Figures can be grouped into a plate with spaces of not more than I mm between the individual illustrations. All figures must he mounted on regular bond paper and not on cardboard. Layouts or single figures should either match the width of a single column (8.6cm) or the printing area (17.6 x 23.6cm). The publisher reserves the right to reduce or enlarge illustrations.
   a) Line drawings: Good-quality prints are needed. The inscriptions must be clearly legible. Letters 2mm high are recommended. Computer drawings are acceptable provided they are of comparable quality to line drawings.
   b) Halftone illustrations: Well-contrasted photographic prints, trimmed at right angles and in the desired final size must be submitted. Inscriptions should be about 3 mm high.
   c) Colour illustrations: There is a page charge if a manuscript contains colour illustrations.

5. **Legends**. Each Fig. should have a short title followed by a concise description. Magnification of micrographs should be given either in the legend of by a scale bar on the micrograph. Such remarks as: "For explanation, see text" should be avoided. Legends are part of the text and should be appended to it in a list starting on a separate page.

6. **Tables**. All tables must be numbered consecutively with arabic numerals. Each table must be typed on a separate sheet. The title of each table should provide a brief, self-sufficient explanation of its content.

7. **Proofs**. To accelerate publication only one set of proofs will be sent to authors. This will show the final form in which the paper will appear in the journal. Changes made in proof should be limited to the correction of typographical errors. Any others involve time-consuming and expensive work, and the costs will be charged to the author. If necessary, additions may be made at the end of the paper in a "Note added in proof'.

8. **Offprints** can be ordered at the time proofs are returned to the publisher.

Microscopy Society (Singapore)

c/o Department of Anatomy, National University of Singapore
4 Medical Drive, MD10, Singapore 117597
http://www.microscopy.org.sg/

Dear Colleagues & Friends,

The **Microscopy Society (Singapore)** is a non-profit think tank actively focused on the promotion of microscopy, organization of microscopy-related activities and facilitation of knowledge and information exchange among its members. With a membership of approximately 100, the society actively promotes and hosts scientific meetings and workshops, and provides scholarships for members to attend conferences.

The society always welcomes new members, and encourages members to actively participate and be involved in organizing microscopy-related activities and events.

Benefits of joining MS(S) include:

- Free subscription to the society's annual scientific journal - ***Annals of Microscopy***
- Free participation in the society's Annual General Meeting, scientific symposia and talks, education workshops, and other events
- Travel scholarships and discounted rates to attend international and regional microscopy-related scientific conferences
- Inclusion in mailing list for special events and forums on microscopy
- Many others

Dr Jeroen Anton van Kan
President

✂----------

MEMBERSHIP APPLICATION FORM

Mr/Ms/Mdm/Dr* _____

Female/Male*

Institution/Company: _____ Position: _____

Address: _____

Tel. No.: _____ (Office/HP) E-mail: _____

Type of Membership: Ordinary/ Corporate*
Membership fees per year: S$ 20.00 (Ordinary Member)
S$ 250.00 (Corporate Member)

Area of Interest: Life Sciences/ Physical Sciences*

Signature: _____ Date: _____
** Please delete where applicable*

Please submit the completed form together with the fees, and for cheque, please make payable to

MICROSCOPY SOCIETY (SINGAPORE) to:

Dr Wu Ya Jun (Hon. Secretary)
c/o Department of Anatomy, Yong Loo Lin School of Medicine, National University of Singapore.
4 Medical Drive,Singapore 117597.

Notes

JEOL
Solutions for Innovation

JEM-2800
Multi-Purpose Analytical Electron Microscope

JSM-7800F
Thermal field emission scanning electron microscope

JEM-ARM200F
Atomic resolution analytical electron microscope

Nano Technology

Meeting the needs of researchers and engineers to assist cutting-edge research, development and analysis

JEOL Electron Optics Instruments contribute to basic research and development of advanced materials as powerful analytical tools for nano-order areas and top-surface layers of substances.

For contact, please email: tstan@jeolasia.com.sg

JEOL ASIA PTE.LTD. | 2 Corporation Road #01-12 Corporation Place Singapore 618494
TEL : +65 6565 9989 http://www.jeol.com/

Solutions Beyond Expectation

Results with Confidence

Vis
UV
DUV
IR
X-ray
Lasers
Ultrasound
Electron
Ions
Probe

μm

nm

Å


Determination at die attach


SAM


3D Colour Metrology


Steep Flank of Micro-milling


DUV Multi Focus


IR Microscopy


Industrial Microscopy


Micro CT


Principal strain, Osteoporotic femur


Titanium implant


Fossilized bone: Ca-P-Si Elemental Map

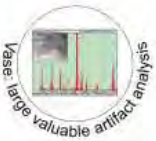
Vase: large valuable artifact analysis


Micro XRF


MIMS


Nitrogen isotope mapping


Malignant melanoma CN-


EDS multi-phase mapping


WDS map of Nb Lα


3D EBSD


EDS, WDS, EBSD


EPMA


In-situ dating of monazite


WDS Large Area Boron Map


WDS Spectrum of Monazite


UHR imaging (catalyst)

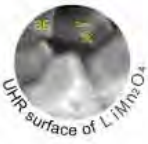
UHR surface of $LiMn_2O_4$


Ultra low voltage (CNT)


UHR FESEM / VP SEM


TableTop SEM


Print Circuit Board


Cloth


Baking Powder


Auto focus, human pancreas


Cryo-TEM


MWCNT


120kV / 300kV TEM


TOF SIMS


3D Al2+GaAl Distribution


Sodium, Lecithin and Serine maps


Surface Spectroscopy of Polystyrene

BF-STEM of catalyst Cell

Gate-oxide on Si substrate

C_s corrected STEM BF, GMR head

C_s corrected STEM

LEXES

B Dose Map

Dose Uniformity

Quantitative Dose Measurement

Carbon Isotope In Diamond

Geochronology - U/Pb Dating

Phosphorous Depth Profile

Sector SIMS

FIB

High quality TEM lamellas

High speed FIB milling

Micro-machining

3D Atomic structure of SiO_2

Atomic precipitation in Super-alloy

Tunnel Barriers Fe-MgO-Fe

TAP

LEIS

ALD Cycles of WNKCY

Mo-V-Te-O catalyst

Double Toroidal Energy Analyser

Laser Assisted Wide Angle 3D Tomographic Atom Probe

Quantitative Characterization of Top Atomic Layer

HI - TECH INSTRUMENTS

HI-TECH INSTRUMENTS SDN. BHD.
(Head Office)(388534-U)
19, Jalan BP4/8,
Bandar Bukit Puchong,
47120 Puchong, Selangor,
Malaysia.
Tel: +603 - 8061 2228
Fax: +603 - 8061 6668

(Penang Office)
2D-1, Tingkat Kenari 5,
11960 Sungai Ara,
Bayan Lepas,
Pulau Pinang, Malaysia.
Tel: +604 - 643 8668
Fax: +604 - 643 6226

(Kuching Office)
1295B, Lorong 6E
Jalan Keranji, Tabuan Jaya
93350 Kuching,
Sarawak, Malaysia.
Tel: +6082 - 369 203
Fax: +6082 - 369 204

General Email: sales@htimail.com.my, service@htimail.com.my Web Site: www.htiweb.com

HI-TECH INSTRUMENTS PTE. LTD.
(Singapore Office) (200103160-C)
3, Science Park Drive,
#04-15, The Franklin,
Science Park 1,
Singapore 118223.
Tel: +65 - 6899 9218
Fax: +65 - 6899 0989

HI-TECH INSTRUMENTS INC.
(Philippines Office)(A200110681)
Unit 112, Prince Reiji Building,
103 Gloria Diaz St cor L Bennet,
BF Resort Village,
Talon 2 Las Pinas City,
Manila, Philippines.
Tel: +632 - 873 3009
Fax: +632 - 873 3010

HI-TECH IMAGING CO. LTD.
(Thailand Office)(0105549128429)
125, Prasert-Manukit Rd.,
Jorakaebua, Ladprao,
Bangkok 10230,
Thailand.
Tel: +662 - 907 4515
Fax: +662 - 907 4516